

**CENTRO DE INVESTIGACIÓN Y DE ESTUDIOS AVANZADOS
DEL INSTITUTO POLITÉCNICO NACIONAL**

UNIDAD ZACATENCO

DEPARTAMENTO DE INGENIERÍA ELÉCTRICA

SECCIÓN DE BIOELECTRÓNICA

Análisis del estado transitorio en la señal EMG multicanal con fines de
identificación de movimientos de la mano

T E S I S

Que presenta

Michele Pla Mobarak

Para obtener el grado de

Maestra en Ciencias

En la Especialidad de

Ingeniería Eléctrica

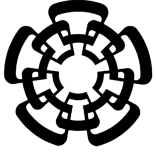
Directores de la Tesis:

Dr. Roberto Muñoz Guerrero

Dra. Valérie Louis Dorr

México, D.F.

Marzo 2014



**CENTRO DE INVESTIGACIÓN Y DE ESTUDIOS AVANZADOS
DEL INSTITUTO POLITÉCNICO NACIONAL**

UNIDAD ZACATENCO

DEPARTAMENT OF ELECTRICAL ENGINEERING

BIOELECTRONICS SECTION

Transient state analysis of the multichannel EMG signal for
identification of hand movements

T H E S I S

Presented by

Michele Pla Mobarak

To obtain the degree of

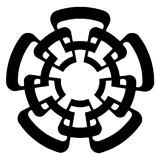
Master of Science

Specialized in

Electrical Engineering

Thesis Directors:

Dr. Roberto Muñoz Guerrero
Dr. Valérie Louis Dorr



**CENTRO DE INVESTIGACIÓN Y DE ESTUDIOS AVANZADOS
DEL INSTITUTO POLITÉCNICO NACIONAL**

UNIDAD ZACATENCO

DÉPARTEMENT D'INGÉNIERIE ÉLECTRONIQUE

SECTION BIOÉLECTRONIQUE

Analyse de l'état transitoire du signal EMG multivoie pour
l'identification des mouvements de la main

T H È S E

Présentée par

Michele Pla Mobarak

Pour obtenir le diplôme de

Master Scientifique

Spécialité

Ingénierie Électronique

Directeurs de thèse:

Dr. Roberto Muñoz Guerrero
Dr. Valérie Louis Dorr

Dedication

To my mom, my dad, and my little sister...

“For always being the constants
in this equation full of variables
that we call life.”

Acknowledgments

“Nobody can go back and start a new beginning, but anyone can start today and make a new ending.” – Maria Robinson

I would like to express my deepest gratitude to all the people that walked along with me this amazing journey that has now come to an end. In a way or another, you have been part of this, and I always keep you in my mind.

To Monica, Albert, and Nicole, who have given me unconditional love, trust, and support for pursuing my dreams and for never doubting I would be able to fulfill them. You are my eternal companions in the journey of life.

To my thesis supervisors, Dr. Roberto Muñoz and Dr. Valérie Louis Dorr, for giving me your time and support and for helping me in my professional growth.

To Dr. Juan Manuel, for your unconditional friendship and support, for your advice throughout this project, and for helping me believe in myself.

To the members of the jury, Dr. Lorenzo Leija, Dr. Pablo Rogelio Hernández, Dr. Juan Manuel Gutiérrez, and Dr. Roberto Muñoz for all your patience and advice.

To all my professors from the Bioelectronics section that influenced me somehow during this journey.

To my adoptive family from Lab. 11 and dear friends from the section, with whom I spent so many hours, so many lunches, so many laughs, and who had amazingly

figured out how to calm me down during stressful periods. I hope to be able to give back the same kind of friendship, care, and support I have received from you.

To Moisés León and Antonio Barraza, for your friendship and useful contributions in my thesis work.

To Ricardo Mejía, your friendship and endless talks gave me strength to continue at every step of the way.

To Carlos Sevy, for teaching me so much from life and from myself.

To Alejandro, Magdalena and Rosarop, for every late night sleep and early waking mornings.

To my friends in France, who helped making a foreign country feel like home.

To CONACYT, for providing the master's scholarship that made possible the completion of this project.

To Julien, who came into my life and changed in the most unexpected ways.

Abstract (*English, Spanish, and French*)

Chapter I. Introduction.....	1
1.1 Presentation.....	1
1.2 Problem Statement.....	3
1.3 Objectives.....	8
1.3.1 General Objective.....	8
1.3.2 Specific Objectives.....	9
1.4 Thesis Structure.....	9
Chapter II. Antecedents.....	11
2.1 Anatomy and Biomechanics of the Hand and the Forearm.....	11
2.2 Electromyography and Myoelectric Prosthesis Control.....	13
2.2.1 Electrical Noise and Factors Affecting the EMG Signal.....	18
2.3 Processing and Analysis Methods for Electrophysiological Signals.....	19
2.3.1 Electromyography Feature Extraction.....	20
2.3.2 Time-Frequency Representation.....	22
2.3.2.1 Discrete Wavelet Transform.....	23
2.3.3 Principal Component Analysis.....	28
2.3.4 Hjorth's Parameters.....	29
2.3.4.1 State of the Art in the Use of Hjorth's Descriptors.....	33
2.4 Artificial Neural Networks.....	37
2.5 K-Fold Cross-Validation.....	40
2.6 State of the Art in EMG Transient State Analysis for Myoelectric Control.	42
2.7 Advantages in the Use of Multichannel EMG.....	48
2.8 State of the Art in Our Laboratory.....	49

Chapter III. Method.....	53
3.1 Proposed Solution.....	53
3.2 Data Acquisition Protocol.....	54
3.2.1 Movements' Selection for Classification.....	55
3.2.2 EMG Database.....	55
3.2.3 Electrode Placement.....	57
3.2.4 Signal Acquisition and Conditioning System.....	58
3.3 Data Processing and Analysis.....	59
3.3.1 Pre-processing.....	59
3.3.1.1 EMG Signal Partition in Transient and Steady States.....	60
3.3.1.2 Window Selection.....	61
3.3.1.3 De-noising Algorithm and Mother Wavelet Selection.....	63
3.3.2 Feature Extraction.....	66
3.3.2.1 Hjorth's Parameters.....	66
3.3.2.2 DWT's Variance.....	67
3.3.2.3 DWT Using PCA.....	69
3.3.3 Artificial Neural Network Model.....	70
3.3.3.1 K-Fold Cross-Validation.....	71
3.3.4 Algorithm's Tolerance to Additive White Gaussian Noise.....	71
3.3.5 Virtual Hand Model.....	73
Chapter IV. Results.....	75
4.1 Overview.....	75
4.2 Hjorth's Parameters.....	78
4.2.1 Selection of Window Parameters.....	79
4.2.1.1 Window Type.....	79
4.2.1.2 Window Length.....	81
4.2.2 Neuron Number Selection.....	83
4.2.3 Hjorth's Parameters Selection.....	85
4.2.4 Transient Vs. Steady State Analysis.....	87
4.3 DWT's Variance.....	94

4.3.1 Transient Vs. Steady State Analysis.....	94
4.4 Models' Tolerance to Additive White Gaussian Noise.....	98
4.5 DWT Using PCA.....	101
4.5.1 Transient State Analysis.....	101
4.6 Transient State Analysis: Comparison in Performance Between Methods.....	104
4.7 Proposed Control Algorithm.....	105
 Chapter V. Discussion.....	 107
 Chapter VI. Conclusions and Future Work.....	 117
5.1 Future Work.....	119
 References.....	 123
 ANNEX A. Submitted Papers.....	 139

List of Figures

Figure 1.1	Imaging of raw differential EMG in a two dimensional array.....	4
Figure 1.2	Multichannel EMG seen as a movie.....	5
Figure 1.3	Importance of EMG electrode placement.....	6
Figure 2.1	Wrist and hand movements.....	12
Figure 2.2	Hand pronation and supination.....	13
Figure 2.3	Frequency content of surface and needle EMG signals.....	14
Figure 2.4	Raw sEMG signal and its power spectrum.....	15
Figure 2.5	Time-frequency plane for different discrete, linear TFRs.....	23
Figure 2.6	DWT decomposition tree.....	25
Figure 2.7	Discrete wavelet packet (DWP) decomposition tree.....	26
Figure 2.8	Use of different mother wavelets for EMG signal analysis.....	26
Figure 2.9	Identification of time of EMG bursts using wavelet coefficients.....	27
Figure 2.10	Time-frequency relationship given by Hjorth's parameters.....	31
Figure 2.11	Multivariate approach using Hjorth's descriptors.....	33
Figure 2.12	Typical three-layer artificial neural network.....	37
Figure 2.13	K-fold cross-validation for $k = 4$	41
Figure 2.14	Patterns of transient MES activity.....	43
Figure 3.1	General diagram describing the proposed solution.....	54
Figure 3.2	Representation of three classes of antagonist movements.....	55
Figure 3.3	Electrode placement for EMG signal recording.....	58
Figure 3.4	Signal acquisition and conditioning system.....	59
Figure 3.5	Two main states found in muscle contraction.....	61
Figure 3.6	Diagram of the method using Hjorth's parameters.....	67
Figure 3.7	Diagram of the method using the variance of wavelet coefficients.....	68

Figure 3.8	Diagram of the method of DWT using PCA.....	69
Figure 3.9	Different hand motions represented in the virtual hand model.....	74
Figure 4.1	Multichannel raw EMG signal of wrist extension.....	76
Figure 4.2	Raw multichannel EMG signal of wrist extension and its FFT.....	77
Figure 4.3	De-noised EMG segment and corresponding frequency components.....	78
Figure 4.4	Mean classification percentage depending on window type.....	80
Figure 4.5	Mean error percentage for window type selection.....	80
Figure 4.6	Mean classification percentage of the transient EMG state depending on window length.....	81
Figure 4.7	Mean classification percentage of the steady EMG state depending on window length.....	82
Figure 4.8	Mean error percentage in classification performance depending on window length for transient and steady EMG states.....	83
Figure 4.9	Classification performance according to the number of neurons in the hidden layer of the ANN.....	84
Figure 4.10	Mean classification percentage according to the combination of Hjorth's parameters used to build the feature matrix.....	85
Figure 4.11	Mean error percentage according to the combination of Hjorth's parameters used to build the feature matrix.....	86
Figure 4.12	Classification performance by subject for the transient and steady states using Hjorth's parameters and a window length of 256 ms..	88
Figure 4.13	Mean classification performance by movement for the transient and steady states using Hjorth's parameters and a window length of 256 ms.....	88
Figure 4.14	Classification performance by subject for the transient and steady states using Hjorth's parameters and a window length of 128 ms.	90
Figure 4.15	Mean classification performance by movement for the transient and steady states using Hjorth's parameters and a window length of 128 ms.....	90

Figure 4.16	Summary of transient and steady EMG states classification using window lengths of both 256 ms and 128 ms.....	93
Figure 4.17	Classification performance for the transient and steady states using the DWT's variance.....	95
Figure 4.18	Mean classification performance by movement for the transient and steady states using the DWT's variance method.....	95
Figure 4.19	New signal generated by averaging previous recorded EMG signals.....	98
Figure 4.20	EMG segment contaminated with different levels of additive white Gaussian noise.....	99
Figure 4.21	Models' responses to AWGN.....	100
Figure 4.22	Classification performance for the transient EMG state using DWT reduced by PCA.....	102
Figure 4.23	Mean classification performance by movement for the transient EMG state using DWT reduced by PCA.....	102
Figure 4.24	Comparison in the mean classification percentage of the transient EMG state for each movement type using the three methods.....	104
Figure 4.25	Comparison in the standard deviation of the whole test population for each movement type using the three methods.....	105
Figure 4.26	Flow diagram of the proposed control algorithm.....	106
Figure 5.1	Confusion matrix of the training and testing stages of the ANN from one of the subjects using Hjorth's parameters and a window length of 128 ms.....	114

List of Tables

Table 2.1	Decomposition level and corresponding frequency range of sEMG signals.....	28
Table 3.1	Movements' selection for classification.....	55
Table 3.2	Forearm muscles recorded by each EMG differential channel.....	57
Table 3.3	Time and frequency representations of tested windows.....	62
Table 3.4	Final ANNs' architecture.....	70
Table 4.1	Mean classification percentage and SD according to window type	81
Table 4.2	Mean classification percentage and SD for transient EMG according to window length.....	82
Table 4.3	Mean classification percentage and SD for steady EMG according to window length.....	82
Table 4.4	Comparison of mean error percentage and SD for transient and steady EMG states according to window length.....	83
Table 4.5	Classification performance related to the number of neurons in the hidden layer of the ANN.....	84
Table 4.6	Mean classification percentage using Hjorth's parameters arranged in different feature matrix schemes.....	86
Table 4.7	Transient vs. steady EMG classification percentage using Hjorth's parameters extraction from a 256 ms Hamming window.....	89
Table 4.8	Transient vs. steady EMG classification percentage using Hjorth's parameters extraction from a 128 ms Hamming window.....	91
Table 4.9	Mean classification and SD percentage per subject for transient and steady EMG states using Hjorth's parameters.....	92
Table 4.10	Summarized results from transient vs. steady EMG state classification using Hjorth's parameters.....	93

Table 4.11	Transient vs. steady EMG classification percentage using DWT's variance extraction from a 256 ms Hamming window.....	96
Table 4.12	Mean classification and SD percentage per subject for transient and steady EMG states using DWT's variance	97
Table 4.13	Summarized results from transient vs. steady state classification using DWT's variance.....	97
Table 4.14	Mean classification accuracy of the trained models when testing with averaged transient state recordings contaminated with different noise levels.....	100
Table 4.15	Transient EMG classification percentage using DWT reduced by PCA.....	103
Table 4.16	Summarized results of the comparison of the mean classification and SD percentages for each movement type using the three methods.....	105

Myoelectric control has most often being based on the analysis of the steady state of the muscle contraction; however, it has as main drawback the impossibility of identifying the movement from the beginning of the contraction; therefore, this causes a delay that can result on the user's frustration. The proposal for controlling myoelectric devices by analyzing the transient state of the muscle contraction had been previously raised; however, the analysis methods that have been applied had only been able to achieve classification percentages significantly lower than those obtained for the steady state analysis.

In this work, a new proposal is made for the classification of upper limb movements by analyzing the transient state of the muscle contraction using Hjorth's parameters.

With the proposed method, it was possible to carry out the identification of movements with classification accuracy higher than 95%. The obtained results suggest the existence of highly relevant information in the dynamic part of the muscle contraction as to be able to propose myoelectric control schemes from its analysis.

El control de dispositivos mioeléctricos se ha basado en el análisis del estado estable de la contracción muscular; sin embargo, esto presenta como principal desventaja que no sea posible identificar el movimiento desde el inicio de la contracción y por lo tanto, genera un retardo que puede resultar frustrante para el usuario. La propuesta de control de dispositivos mioeléctricos a partir del análisis del estado transitorio de la contracción muscular había sido planteada anteriormente; sin embargo, los métodos de análisis empleados sólo habían logrado porcentajes de clasificación significativamente menores que los obtenidos para el análisis del estado estable.

En este trabajo se hace una nueva propuesta para la clasificación de movimientos de la extremidad superior analizando el estado transitorio de la contracción muscular por medio de los parámetros de Hjorth.

Con el método propuesto fue posible llevar a cabo la identificación de movimientos con un porcentaje de clasificación superior al 95%. Los resultados obtenidos sugieren que existe información suficientemente relevante en la parte dinámica de la contracción muscular como para poder plantear esquemas de control mioeléctrico a partir de su análisis.

La commande des dispositifs de control myoélectrique a été basée sur l'analyse de l'état stable de la contraction musculaire; cependant, ceci a pour principal inconvénient qu'il ne soit pas possible d'identifier le mouvement à partir du début de la contraction. La commande introduit ainsi un retard qui peut être frustrant pour l'utilisateur. La proposition de commande des dispositifs myoélectriques à partir de l'analyse de l'état transitoire de la contraction musculaire a déjà été abordée. Néanmoins les méthodes d'analyse utilisées donnaient des pourcentages de classification significativement faibles comparés à ceux obtenus par l'analyse de l'état stable.

Ce travail propose une nouvelle méthode de classification de mouvements des membres supérieurs, en analysant l'état transitoire de la contraction musculaire avec les paramètres de Hjorth.

Avec la méthode proposée, il est possible de faire l'identification de mouvements avec un pourcentage de classification supérieur à 95%. Les résultats obtenus suggèrent qu'il existe suffisamment d'informations pertinentes dans la partie dynamique de la contraction musculaire pour concevoir des systèmes de contrôle myoélectrique à partir de son analyse.

Introduction

1.1 Presentation

It is a real ambitious challenge the attempt to replicate the sensory-motor function of the human hand, which is capable of delicate and precise manipulation, and of power grasping of heavy objects. In order to approximate the hand's functions, it is necessary to develop a system with a large number of degrees of freedom, proprioceptive and exteroceptive sensors, and a complex hierarchical control. Commercially available prosthetic devices do not provide the manipulation capabilities of the human hand and require a great amount of training and concentration in order to be used effectively. Moreover, most of them do not have more than two active degrees of freedom [1].

There are many signal-processing methods that have been applied to achieve prosthesis control, but the question of which one has the most advantages still remains. It is true that the problem can be solved through different approaches, but none of the approaches that already exist have been able to sufficiently approximate the functions that can be executed by a human limb, the time of reaction, and the naturalness of the movements. Because of this, there is still a long path to travel and new techniques that should be explored and applied.

Surface electromyographic signals (sEMG) constitute a source of information for assistive devices control such as prostheses. These signals have been broadly studied and used in different applications because of the relative simplicity that implies collecting samples, the possibility to generate non-invasive devices that respect the integrity of the

user, the reusability of the device between different users, and the easiness to remove the device for maintenance and calibration [2].

An electromyographic (EMG) signal can be recorded using only one acquisition channel. This allows making predictions about the muscle activation and force; nonetheless, it is necessary to reduce unwanted variability in order to improve the quality of the signal. The use of multichannel EMG, which consists in multiple bipolar electrodes spatially distributed over the muscle belly, decreases EMG variability and allows a more reliable control, constituting one of the main reasons that have awakened interest in multichannel systems [3].

The area of prosthetics and orthotics continues to make significant technological innovations. Prostheses and orthoses give patients the possibility to compensate partially or regain some of the functions that were lost through limb amputation, but at the same time, it is important not to forget all the psychological implications involved in the amputation itself and in the acceptance of the prosthetic device as a new part of the individual's body that may affect physical rehabilitation. Based on this, in order to explore the potential of technological innovations in prostheses, development should be closely related with the understanding of the psychological complexities of the therapeutic context [4]. It is important not to forget that the objective does not consist in creating the most complicated device, but in creating something that adjusts to the patient's needs and that has the best compromise between functionality, naturalness in movement's execution, price accessibility, cosmetics, and every aspect that affects the patient's daily life and inclusion in society.

1.2 Problem Statement

Patients with amputations and disabilities face a great loss of functionality. This has motivated numerous efforts throughout history to develop devices that allow replacing the loss or that can at least assist in daily life activities in which the patient struggles because of the amputation.

Myoelectric controlled prostheses for hand, wrist, and arm amputations are commercially available. Some of the most commonly used control methods for these systems consist in generating a control signal based on the mean absolute value (MAV) of the myoelectric signal (MES), and most often, they use a reduced number of EMG channels. When the signal is collected by only one EMG channel, its amplitude is used to select one of three possible operation states (systems based on the EMG contraction's force level). The signal can also be collected using two EMG channels. The channel with the maximum amplitude determines the device's state; once this is selected, the prosthetic device can work at a constant speed, or it can have a variable speed that changes proportionally with the EMG signal's level. Even if there are functional prostheses that have been controlled through these methods, they still face a great number of limitations, and patients need long training periods without always obtaining the desired results [5,6].

Due to the present limitations in myoelectric controlled prostheses that employ a limited number of EMG channels, the use of multichannel EMG has been proposed as a promising alternative; however, processing and analyzing multichannel registers imply a greater use of resources, an increased computational cost, and a longer processing time. Thus, it is necessary to find the appropriate analysis tools in order to select the ideal number of channels that represent a good compromise between the amount of information to be processed and the reliability of the generated control signal.

Multichannel EMG registers are accomplished by placing electrodes over the muscles involved in the movement's execution [7]. This allows identifying the participation that each muscle has in the movement. The electrodes detect the spatial distribution of potential on the skin producing not a picture, but a sort of movie that shows that potentials on the surface are continuously changing because the sources in the muscles are moving. This movie is both sampled in time (frames per second) and space (electrodes per meter). Fig. 1.1 illustrates the theoretical scheme of this movie formation [8].

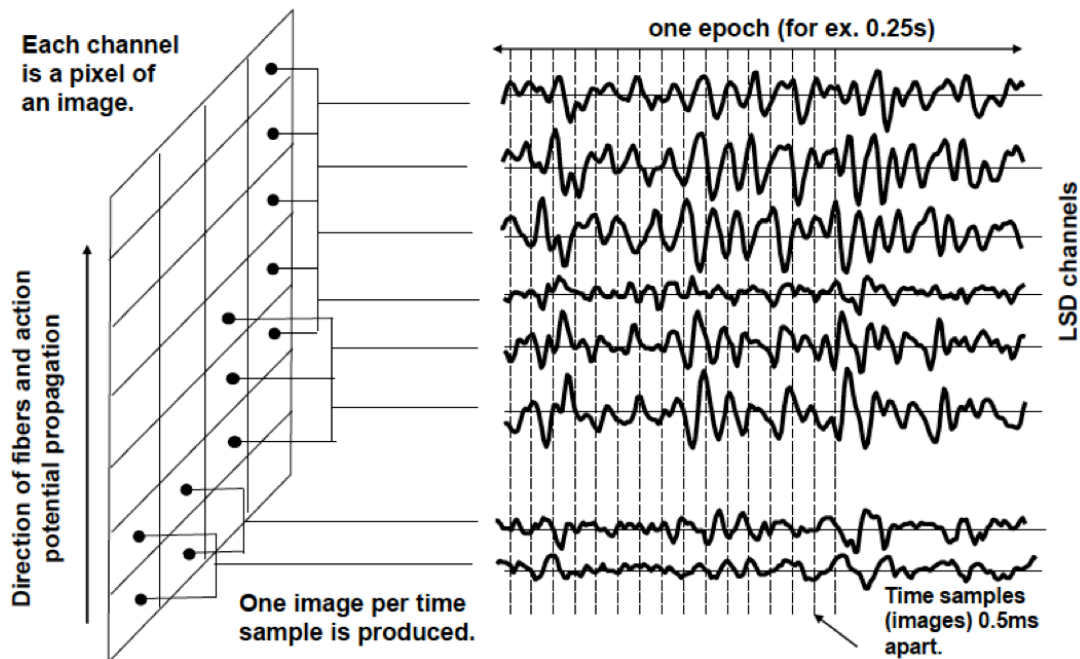


Fig. 1.1. Imaging of raw differential EMG in a two dimensional array. It reflects the spatial distribution of potential in the skin surface. A movie is obtained in time by gathering a series of images showing potential distribution at a given moment that will eventually allow seeing how this potential distribution changes in time as the sources in the muscles are moving. Voltage levels may be represented by colors [8].

A real example of this movie formation can be observed on the change in the surface potential of the biceps brachii during an elbow flexion-extension movement as shown in Fig. 1.2 where different color intensities represent different voltage levels.

smallest details are important to draw final conclusions because they can mark the difference between two similar things.

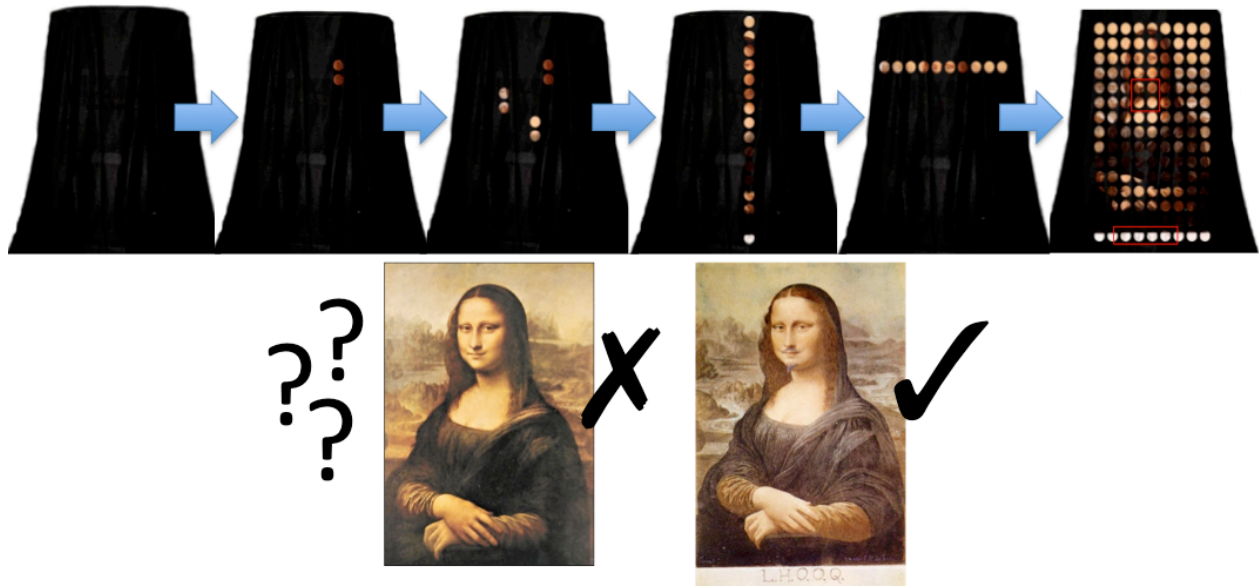


Fig. 1.3. Importance of EMG electrode placement. This figure compares electrode placement to a painting guessing game. The sixth frame seems to have enough holes as to guess the painting, but it is possible to get confused between the Mona Lisa from Leonardo Da Vinci and the Mona Lisa with Mustaches from Marcel Duchamp. This example helps understanding that well located electrodes and paying attention to small details are important elements for drawing final conclusions [8].

Two main states can be identified in the EMG signal during muscle contraction. The first one is known as the transient state, and it is described as the burst of myoelectric activity that accompanies sudden muscular effort. The second one is known as the steady state¹ and corresponds to the muscular effort during a sustained contraction when the movement's final position is reached and the muscle length is no longer modified. It consists of a constant firing rate [2]. The steady state analysis of the muscle contraction for EMG classification simplified prosthetic devices' control and is the most frequently used technique; however, the steady state has very little temporal structure of

¹ Throughout this work, the term 'EMG steady state' is constantly alluded. It is known that the characteristics of the EMG signal are non-stationary and stochastic; therefore, the aforementioned term will be used to refer the myoelectric signal produced by a stable muscle contraction.

the active modification of recruitment and firing patterns that are needed to sustain a contraction. This information is contained in the transient state of the signal, which could give more precision about the movement while the muscle contraction is being generated and could provide useful information for EMG classification [1,6]. The aforementioned reasons motivate the study and analysis of the transient state in the EMG signal.

The main advantage of using the transient state of the EMG signal for myoelectric control consists in reducing the time required to obtain a response from the device. It is generally agreed that 300 ms is the longest acceptable delay in a prosthetic control system. A 200 to 300 ms interval is a clinically recognized maximum delay that users find acceptable before they get frustrated with the slow response of the prosthesis [6,9,10].

The performance of a myoelectric control system is evaluated with regards to three important aspects of controllability [11]:

- *The accuracy of movement selection*, which is essential for obtaining a precise execution of a user's intent.
- *The intuitiveness of actuating control*, which relieves the user from focalizing all his attention in the device's control and allows him to do it in a more natural way.
- *The response time of the control system*, which should not introduce a delay that is perceivable by the user. This places a real-time constraint on the control system's task of acquiring and processing myoelectric data [6,9-11].

The first 100 ms of the transient burst of the EMG signal appear to have enough information as to differentiate between motions and therefore suggest a promising means of MES classification [6,9]. The movements could be classified since the beginning of the muscle contraction reducing considerably the user perceived lag introduced by the systems that wait until the steady state is reached to generate a control command.

In addition to the problems that have already been discussed, there is also an evident need to find an optimal number of EMG channels that represent a good compromise between computational cost and decreasing EMG variability [3]. Multichannel systems have the advantage that the positions of the electrodes can become less critical as compared to those systems that use a reduced number of channels [12,13]. It is also important to determine the best electrode placement and better processing and analysis techniques that will permit obtaining more reliable and less delayed control signals. This should eventually allow myoelectric prostheses control in real time and with shorter training periods due to the fact that control would be based in the activation of several muscles and not in the change of contraction intensity of a single muscle.

1.3 Objectives

1.3.1 General Objective

Perform signal processing and analysis on the transient state of multichannel EMG signals acquired from several forearm muscles in order to classify a set of simple hand movements and create an algorithm that will allow reproducing normally limbed subjects' hand movements in a virtual hand model.

1.3.2 Specific Objectives

- Reduce the delay produced by the acquisition and processing of the EMG signal that is present when the control system has to wait until the steady state of the contraction to generate a control signal.
- Selection of a multichannel EMG processing and analysis tool that will allow obtaining useful characteristic sets to create robust control algorithms using forearm EMG signals extracted from a database of normally limbed subjects.
- Testing of Hjorth's parameters, which are normally applied to EEG analysis, in EMG classification performance.
- Selection of an appropriate classifier to discriminate signals based on characteristic extraction.
- Generation of control algorithms based on the EMG signals' transient state to reproduce the movements from a healthy subject over a virtual hand model.
- Comparison between classification performance while using the transient and the steady states of the muscle contraction.

1.4 Thesis Structure

The present thesis is divided into six chapters. The first one provides with a general scope of this work. It presents some of the problems and limitations that exist in EMG signal analysis and processing when used for prosthesis control and the need to explore new EMG acquisition and processing techniques in order to achieve a more reliable and natural control of these devices. It also contains the explanation of the problem that motivated this thesis and the general and specific objectives that were pursued.

The second chapter explains general concepts related to the hand's biomechanics, the EMG signal, and some of the signal-processing techniques that were employed for analysis and discrimination of the executed movements. It also presents the state of the art in prosthesis control and some of the previous works that have been done in our laboratory related to this subject. Additionally, it introduces Hjorth's parameters and their use in biomedical signals.

The third chapter consists in the methodology that was followed to solve the stated problem. It mentions the characteristics of the used database, and it gives a detailed description of the protocol for EMG processing and feature extraction in order to classify different hand movements. The algorithms that were created to reproduce the movements on a virtual hand model are also explained in this chapter.

The fourth chapter presents the results obtained from classification and a description of the virtual model's performance. These results are further discussed in the fifth chapter.

Finally, the sixth chapter contains conclusions, some of the problems that were encountered during the execution of this thesis, and the future work that can be done in relation to this thesis in order to improve results on EMG classification and control.

Antecedents

2.1 Anatomy and Biomechanics of the Hand and the Forearm

The human hand is a complex system that includes a large number of degrees of freedom, sensorial elements, actuators, tendons, and a hierarchical control that relates them all, but despite all of this, the effort required to make different movements is small. On the contrary, a prosthetic hand is an essay to replicate the natural hand. This has a drastic reduction in grasping capabilities and in the sensory feedback received by the user [1].

Muscle activation is controlled by the central and peripheral nervous systems by means of the types and activation frequencies of the recruited motor units [14]. The hand is the most distal element of the upper limbs. It has both motor and sensitive abilities. The movements executed by the shoulder, elbow, and wrist allow hand positioning, orientation, and stability to perform an activity [15].

The muscles of the hand and the wrist are mainly located in the forearm. They narrow into tendons and traverse the wrist to insert in the bony or ligamentous components of the hand. The flexors act in part as supinators of the forearm, and the extensors assist in pronation. The hand is able to execute a wide range of movements including fixation movements; movements that can change from slow to fast with direction, intensity and rate control; and ballistic movements. In all types of prehension movements, the hand assumes a fixed position. If the object is unyielding, it affords reaction to the flexion forces of the hand's muscles, and if it is fragile or the hand is empty, contractions of the

opposing muscle groups allow the hand to maintain any prehensile posture. For movements ranging from slow to rapid, there is always some degree of contraction that ensures control and that allows changes in force and velocity. Ballistic movements are rapid motions, usually repetitive, that are begun by active muscle contractions that give momentum, and that are subsequently ceased or diminished during the latter part of the motion [16]. Flexion and extension movements are produced with respect to a transverse axis as shown in Fig. 2.1. During flexion, the hand moves towards the anterior part of the forearm, and during extension, it moves towards the dorsal part. Abduction and adduction are also known as radial and ulnar deviations. Abduction pulls the hand away from the midline part of the body and adduction pulls it towards it as shown in Fig. 2.1. Pronation of the hand consists in rotating the forearm and moving the palm from an anterior-facing position to a posterior-facing one (the palm faces downwards). Supination consists in the opposite rotation (the palm ends facing upwards) as it is shown for both movements in Fig. 2.2 [17].

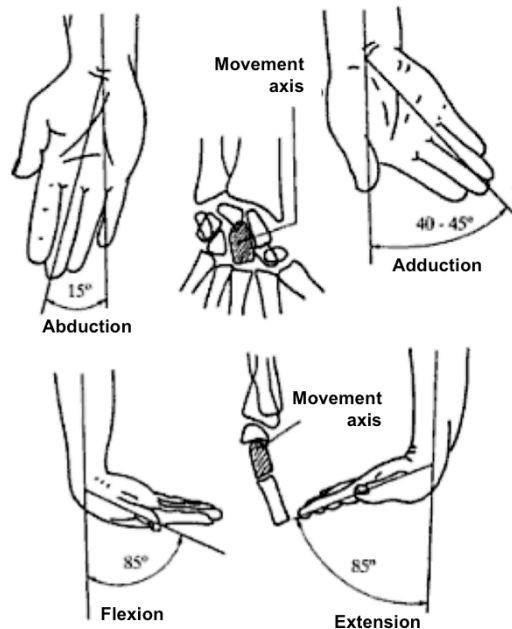


Fig. 2.1. Wrist and hand movements. This figure shows hand abduction, adduction, flexion, and extension. It presents the range of motion for each of the movements [17].

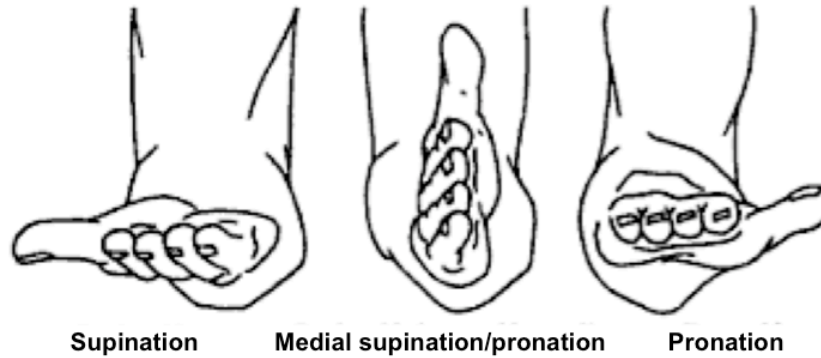


Fig. 2.2. Hand pronation and supination. The palm faces upwards after the forearm rotation during supination and it faces downwards for pronation [17].

2.2 Electromyography and Myoelectric Prosthesis Control

Electrophysiological signals are electrical signals generated by any organ representing a variable of interest. They are usually a function of time, so they can be described in terms of their amplitude, frequency and phase. Electromyography (EMG) is a type of electrophysiological signal that measures electric currents generated during muscle activity (contraction/relaxation) and that are controlled by the nervous system. Even if the EMG signal origin is nervous, it depends on the anatomical and physiological properties of muscles, which make these types of signals subject dependent and create a problem for selection of electrode location on the forearm. The complexity of EMG signal analysis also lies in its non-stationary characteristics. There are several factors that may affect these signals such as the motor unit action potential (MUAP), muscle fatigue, and force. Variability in the signals due to subject dependency when using the same electrode disposition is one of the toughest problems encountered for EMG signal classification [18,19].

EMG signal analysis provides important information in clinical diagnosis and biomedical applications. Neuromuscular disorders can be diagnosed based on the shapes and firing rates of MUAPs. Surface electromyography (sEMG), which consists of EMG signals

collected by electrodes placed on the skin surface, can be used in different applications such as prosthetic devices control [18,20].

The typical amplitude of sEMG signals is 0-10 mV. The information channel of the sEMG signal goes from 10-500 Hz, but the main concentration of energy is located within the frequency band of 50-150 Hz [2,18] as shown in Fig. 2.3 and Fig. 2.4. The frequency content in the two main types of EMG studies (needle and surface EMG) can be seen in Fig. 2.3.

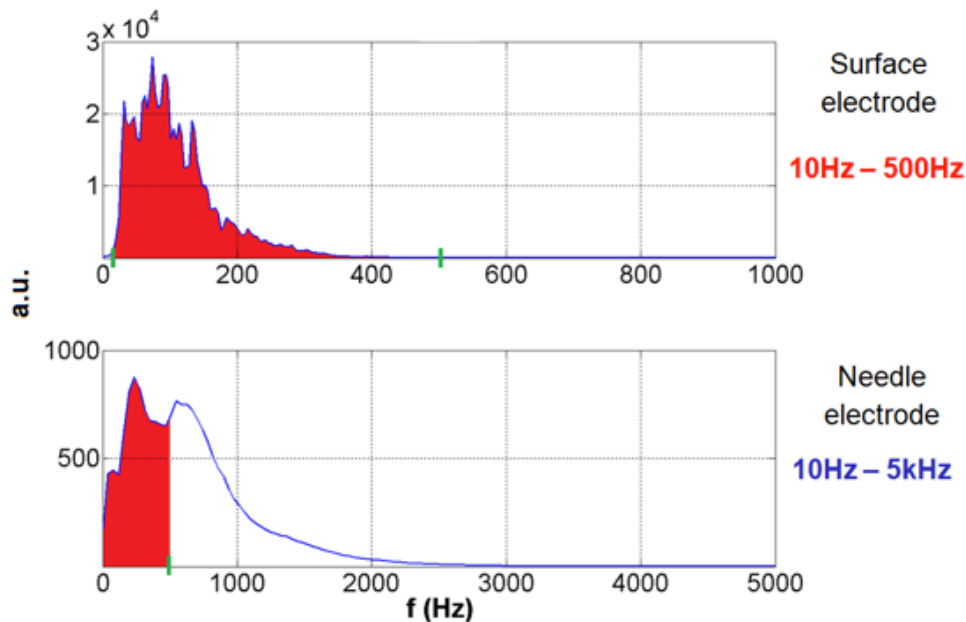


Fig. 2.3. Frequency content of surface and needle EMG signals. The upper panel shows the frequency content of the EMG power spectrum collected using surface electrodes, and the lower panel illustrates the equivalent for needle EMG. The x-axis measures frequency content in Hz, and the y-axis is represented in arbitrary units (a.u.). The shadowed area on the lower panel corresponds to the cut-off frequencies used for sEMG and demonstrates that using the same frequency range for needle EMG would result in a considerable information loss [21].

Commonly, in sEMG, electrodes are located on the skin above the belly of the muscle of interest, in a region between the tendon and the innervation zone; therefore, the electric

currents generated by depolarization of the muscle fibers must travel through connective tissues, fat, vessels, and skin to reach the region underneath the electrodes. Jointly, these elements have the properties of a low-pass filter, so the signals reach the electrodes with a slower time course and decreased amplitude. In needle EMG, the electrodes are closer to the source of electric activity, and the signals do not suffer the same amplitude attenuation as described for sEMG; as a result, needle EMG has better signal-to-noise ratios and their power spectra have components at higher frequencies (see lower panel of Fig. 2.4). Nonetheless, while needle EMG has a higher selectivity, it is hard to evaluate a larger number of motor units (MUs) to obtain a better scheme of muscle activation. For this purpose, sEMG is more indicated [21].

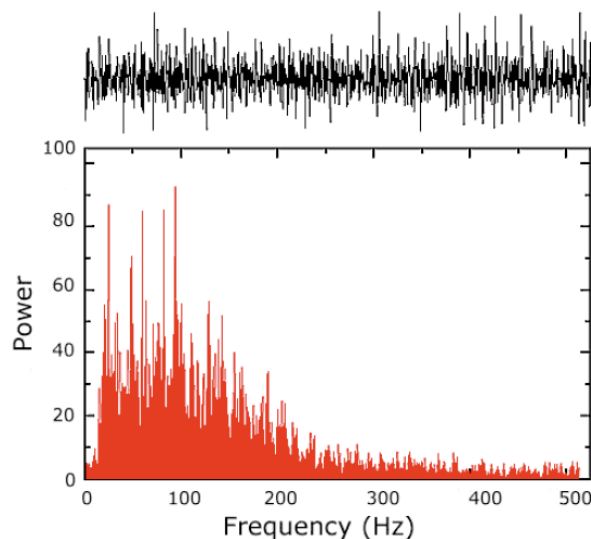


Fig. 2.4. Raw sEMG signal and its power spectrum. The raw sEMG signal was obtained from the tibialis anterior muscle during an isometric contraction with constant force at 50% of the maximum. The lower panel shows its power spectrum [22].

The EMG signal consists in the summation in time and space of MUAP trains. The shape of a generic MUAP detected on the skin surface can be approximated by a function $f(t)$. This allows the description of a MUAP train (MUAPT) as stated in (2.1) where j indicates a specific MU, k_j is an amplitude factor, θ_{ij} are the times in which the MUAPs of the MU occur, and α_j is a scaling factor [23].

$$MUAPT_j(t) = \sum_i k_j \cdot f\left(\frac{t - \theta_{ij}}{\alpha_j}\right) \quad (2.1)$$

The EMG signal $s(t)$ can be expressed as shown in (2.2). The $n(t)$ represents the additive noise. The amplitude and scaling factor depend mainly on the depth and size of the MU [23].

$$s(t) = \sum_j MUAPT_j(t) + n(t) = \sum_j \sum_i k_j \cdot f\left(\frac{t - \theta_{ij}}{\alpha_j}\right) + n(t) \quad (2.2)$$

The sEMG signal recorded during voluntary dynamic contractions can be considered as a zero-mean Gaussian process modulated by the muscle activity and corrupted by a zero-mean Gaussian additive noise [18].

Myoelectric systems have been widely used for prosthetic control in individuals with amputations. These systems extract the control signals from an estimate of the amplitude or the rate of change of the MES. A myoelectric prosthesis is a system actuated by servomotors that are controlled by the electromyographic (EMG) signals collected from the patient's stump. These signals can be either intramuscular and are collected through needles, or they can be superficial in which surface electrodes are used instead. When only a single EMG channel is used to generate the control signal, the amplitude of the signal allows choosing the state of operation for the device [2,6].

The sEMG signal is stochastic due to the random nature of the joint activity of the motor units within the capturing region of the electrodes; therefore, myoelectric control systems are based on the assumption that there is no useful information in the instantaneous value of the MES. When several motor units become active, the firing rate increases and

their pooled activity approaches a Gaussian process, which means that the instantaneous amplitude of the MES is a random variable with zero mean and its variance is a function of the contraction level [6].

Different attempts to implement EMG controlled prosthetic devices have been started since the 1970s decade. In the beginning, EMG control was implemented by coding the EMG amplitude level; however, in order to get a precise response, the patient must be able to control correctly the level of muscle contraction. This requires a great amount of training, and the desired repeatability of the system is not always achieved. Researchers started using more rigorous statistical analysis methods in order to classify the EMG signal, which included autoregression models as well as autoregressive-moving-average (ARMA) models. In an ideal scenario, classification of the EMG signal by extracting features and using pure statistical analysis could be able to give good results; anyways, in a real situation, the performance would decline due to a variable and increasing amount of noise during the acquisition portion of the system. Other factors that may directly affect the signal are the skin-electrode interface, which becomes sensitive to the movements of the patient, and muscle fatigue. In order to minimize the effect produced by all these factors, the concept of pattern recognition should be included in the system, allowing it to recognize slight generalizations of the pattern [5]. The implementation of pattern recognition was not suggested until 1972, but because of limited processing power and algorithm complexity, it was only until 1993 that Hudgins *et al.* [6] used it successfully to classify EMG signals. In their work, they suggested that in order to develop an EMG controlled multifunctional prosthesis, it was necessary to extract more information from each EMG channel or assign a control function to a specific combination of signals in a multichannel system. In this way, the number of control outputs is greater than the number of channels and allows a more specific control [6]. Classification of EMG signals has been recently possible through the use of artificial neural networks and support vector machines allowing the development of more natural and advanced control systems [5].

2.2.1 Electrical Noise and Factors Affecting the EMG Signal

There are several factors that may affect the integrity of the EMG signals such as electrical noise, which is acquired while the signal travels through different tissues. The different categories of electrical noise affecting EMG signals as classified by Raez *et al.* in [18] are described below:

- *Inherent noise in electronics equipment*, which is reduced by the use of high quality electronic components, but that always remains to some degree while acquiring the EMG signal.
- *Ambient noise*, which is generated by electromagnetic radiation that is also constantly present on the body surface. This type of noise may have amplitude that is one to three orders of magnitude greater than the EMG signal.
- *Motion artifacts*, which cause irregularities in the data and can be generated in the electrode interface and in the electrode's cable.
- *Inherent instability of the signal*. This refers to how the EMG signal is affected by the firing rate of the motor units, which generally fire in the frequency region of 0 to 20 Hz and cause random amplitudes in result.

In addition to electrical noise, there are other factors that affect EMG signals and that can be summarized into three main categories as stated in [18]:

- *Causative factors*: They affect signals directly. They can be divided into:
 - *Extrinsic*, which are caused by characteristics of the electrode structure and placement, such as the location of the electrodes with respect to the motor points in the muscles.

- *Intrinsic*, which are the physiological, anatomical, and biochemical factors that take place due to the number of active motor units, the fiber type composition, the amount of tissue between the surface of the muscle and the electrode (quantity of fat tissue), among others.
- *Intermediate factors*: They are physical and physiological phenomena influenced by causative factors. Examples of this are superposition of action potentials in the detected EMG signal, crosstalk from nearby muscles, conduction velocity of the action potential along the muscle fiber membrane, among others.
- *Deterministic factors*: They are influenced by intermediate factors. The amount of active motor units, the firing rate, and the mechanical interaction between muscle fibers have a direct influence on the information contained in the EMG signal and its recorded force.

2.3 Processing and Analysis Methods for Electrophysiological Signals

An electrophysiological signal is the result of a collection of electrical signals generated as a function of time, which allows describing it in terms of amplitude, frequency and phase [18]. Due to this reason, analysis methods are generally based in extracting time and frequency features from the signal.

Raw information from electrophysiological signals is only useful after signal processing when it becomes quantifiable. Different signal-processing methods are applied to eliminate noise and undesired artifacts in order to obtain more accurate information from the features extracted from the signals [18]. Some of the current signal-processing methods for electrophysiological signal analysis are explained below.

2.3.1 Electromyography Feature Extraction

Feature extraction permits obtaining the most relevant information from the signal and discriminating noise and irrelevant data. Features can be extracted in either the time or the frequency domain, or they can be extracted in the time-frequency domain.

Features in the time domain are quickly calculated because they do not require a transformation. They continue being frequently used due to the fact that they allow faster algorithms, and they normally require less computational resources. Some of the most commonly used in EMG signal analysis are described by Zecca *et al.* in [1] and are briefly enounced below:

- *Mean Absolute Value (MAV)* of the signal as described by (2.3), where x_i is the signal in a segment i which length is N samples.

$$\bar{X}_i = \frac{1}{N} \sum_{k=1}^N |x_k|, \quad \text{for } i = 1, \dots, I - 1 \quad (2.3)$$

- *Mean Absolute Value Slope (MAVSLP)* represents the difference between sums in adjacent segments as shown in (2.4).

$$\Delta \bar{X}_i = \bar{X}_{i+1} - \bar{X}_i, \quad \text{for } i = 1, \dots, I - 1 \quad (2.4)$$

- *Willison Amplitude (WAMP)* is a unit indicator of firing MUAP. It is the number of counts for each change of the EMG signal amplitude that exceeds a defined threshold as indicated in (2.5).

$$WAMP = \sum_{k=1}^N f(|x_k - x_{k+1}|) \quad \text{with} \quad f(x) = \begin{cases} 1, & x > \text{threshold} \\ 0, & \text{otherwise} \end{cases} \quad (2.5)$$

- *Variance of the EMG* is related to the force developed by the muscle, therefore, it is a measure of its power. It is described by (2.6).

$$VAR = \sigma^2 = \frac{1}{N-1} \sum_{k=1}^N x(k)^2 \quad (2.6)$$

- *Zero Crossing (ZC)* corresponds to the number of times that the signal crosses zero. It provides a rough estimate of the properties in the frequency domain.
- *Slope Sign Changes (SSC)* is a parameter that provides a bit of information about frequency properties of the waveform.
- *Waveform Length (WL)* measures the cumulative length of the waveform over the time segment. It provides a measure of waveform amplitude, frequency, and duration. It is calculated as shown in (2.7).

$$l_0 = \sum_{k=1}^N |\Delta x_k|, \quad \text{where} \quad \Delta x_k = x_k - \Delta x_{k-1} \quad (2.7)$$

Frequency Ratio (FR) was proposed with the objective of distinguishing between muscle contraction and relaxation in frequency domain. It is necessary to apply the Fast Fourier Transform (FFT) to the EMG in time domain to find the frequency ratio of the j^{th} channel as described by (2.8). A threshold determined through experimentation divides between

low and high frequencies. A high FR corresponds to a high muscle contraction and a low FR means the opposite.

$$FR_j = \frac{|F(\cdot)|_{j \text{ low freq}}}{|F(\cdot)|_{j \text{ high freq}}} \quad (2.8)$$

The features mentioned above are just a few examples of many that can be extracted from the EMG signal. The success obtained from their use often relies on the number of features and the combination selected to create the set of characteristics that will feed the classifier. Quickly calculated features allow the implementation of faster algorithms, which also represents a major advantage for their use.

2.3.2 Time-Frequency Representation

A time-frequency representation (TFR) localizes the signal energy both in time and frequency, which provides a more accurate description of the signal, but requires a transformation that generally implies a higher computational cost. Some of the most commonly used TFRs are discrete and linear ones because they are computationally less heavy and make more feasible the implementation of real-time applications. Some of these are the short-time Fourier transform (STFT), the discrete wavelet transform (DWT), and the wavelet packet transform (WPT). They differ one from the other in the way in which they partition the time-frequency plane as it can be compared in Fig. 2.5. The STFT has a fixed tiling that after being specified generates each cell with an identical aspect ratio. The DWT has a variable tiling, which means that the aspect ratio of cells varies in order to have a frequency resolution that is proportional to the center frequency. Finally, the WPT provides an adaptive tiling and according to the desired application, the most convenient one is chosen. The variable tiling from the DWT has been proved to be more efficient for physiological signals; nevertheless, the partition is

still fixed. This is one of the main reasons that have widened the application of WPT for EMG signal classification [1].

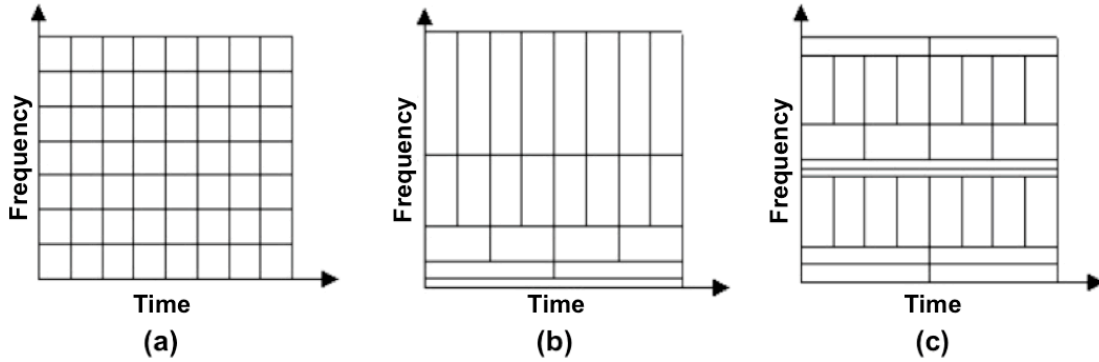


Fig. 2.5. Time-frequency plane for different discrete, linear time-frequency representations. The first part (a) represents the time-frequency plane of the STFT, which has a fixed tiling and cells with an identical aspect ratio. The second part (b) shows the variable tiling of the DWT. Finally, the third part (c), illustrates the adaptive tiling of the WPT [1].

2.3.2.1 Discrete Wavelet Transform

The wavelet transform is broadly used for biosignal processing. It can be used in either its continuous or its discrete form, but the continuous one requires more computational resources and a longer processing time. The continuous wavelet transform (CWT) of a signal $s(t)$ is defined as the integral of the product between the signal $s(t)$ and the daughter wavelets, which are the time translation and scale expansion/compression versions of a mother wavelet function $\psi(t)$. This generates wavelet coefficients $CWC(a,b)$, that allow determining the similarity between the signal and the daughter wavelets located at position b (time shifting factor) and positive scale a as denoted in (2.9) [19].

$$CWC(a, b) = \int_{-\infty}^{+\infty} s(t) \frac{1}{\sqrt{a}} \psi^* \left(\frac{t-b}{a} \right) dt, \quad (2.9)$$

where * stands for complex conjugation.

A discrete signal can be approximated as defined below in (2.10).

$$f[n] = \frac{1}{\sqrt{M}} \sum_k W_\phi[j_0, k] \phi_{j_0, k}[n] + \frac{1}{\sqrt{M}} \sum_{j=j_0}^{\infty} \sum_k W_\psi[j, k] \psi_{j, k}[n], \quad (2.10)$$

where $f[n]$, $\phi_{j_0, k}[n]$ and $\psi_{j, k}[n]$ are discrete functions defined in $[0, M-1]$, totally M points. The wavelet coefficients can be obtained from the inner product in (2.11) and (2.12) because the sets $\{\phi_{j_0, k}[n]\}_{k \in \mathbb{Z}}$ and $\{\psi_{j, k}[n]\}_{(j, k) \in \mathbb{Z}^2, j \geq j_0}$ are orthogonal to each other [24].

$$W_\phi[j_0, k] = \frac{1}{\sqrt{M}} \sum_n f[n] \phi_{j_0, k}[n] \quad (2.11)$$

$$W_\psi[j, k] = \frac{1}{\sqrt{M}} \sum_k f[n] \psi_{j, k}[n] \quad j \geq j_0 \quad (2.12)$$

A mother wavelet function is actually a band-pass filter in the frequency domain. The obtained coefficients allow identifying the local features of the signal. The selection of the mother wavelet is thus, essential for feature extraction. The discrete wavelet transform (DWT) projects a signal into a set of basis functions that are scaled and delayed versions of the chosen mother wavelet; therefore, it is the mother wavelet who determines the projection space, and it is expected that with the use of different types, feature extraction will vary [7, 19].

The DWT implies downsampling the signals, which can lead to significant information loss, and is though not convenient for signals with low signal to noise ratio (SNR). There are two basic types of DWT decompositions: pyramid and packet decompositions. In any of these forms, signals are divided into approximation (low frequencies) and detail (high frequencies). In the pyramid decomposition, after the first level, only

approximations are decomposed through higher levels as shown in Fig. 2.6, whereas for the packet decomposition, both approximation and detail are decomposed into further levels providing more information of the signals [19]. This can be seen in Fig. 2.7.

Wavelets have been widely used as basis functions for EMG feature extraction because surface EMG signals are the summation of motor unit action potential trains, which are compact support waveforms repeating with similar shape over time [7]. There is a large set of mother wavelets that can be used for reconstruction of a signal. The Daubechies wavelet family seems to resemble motor unit potentials the most. The simplest wavelet of this family is Daubechies 2 (db2) because db1 is actually the Haar wavelet. The db4 wavelet is smoother than db2 and has more zero-crossings. Fig. 2.8 presents the continuous wavelet transformation of a 200 ms biceps EMG segment using three different mother wavelets (Gaussian, Haar, and Daubechies 4) and the correlations between the wavelet shape and the EMG shape [25]. The fourth order Coiflet mother wavelet has also proved to have a good performance when classifying EMG signals. According to Englehart *et al.* [9], it yields better accuracy than other wavelet families.

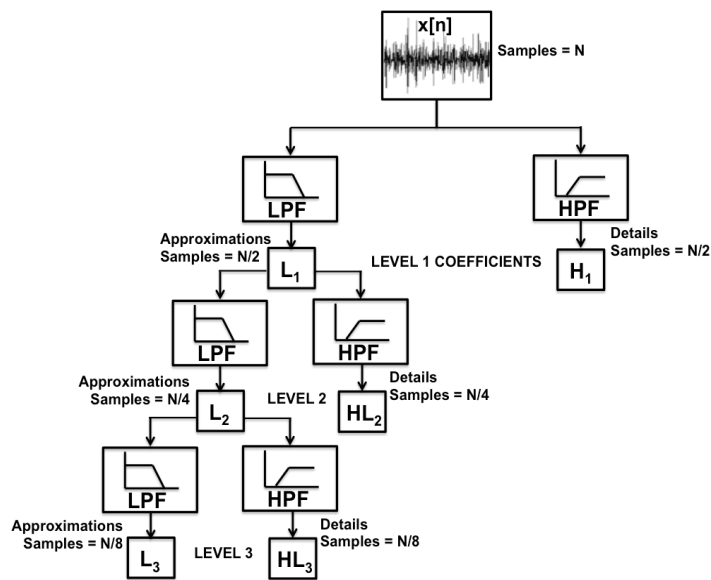


Fig. 2.6. Filter bank representation of the DWT. Approximation coefficients are obtained from the low-pass filters (LPF) and the detail coefficients from the high-pass filters (HPF). In every level, the signal is downsampled by 2 [26].

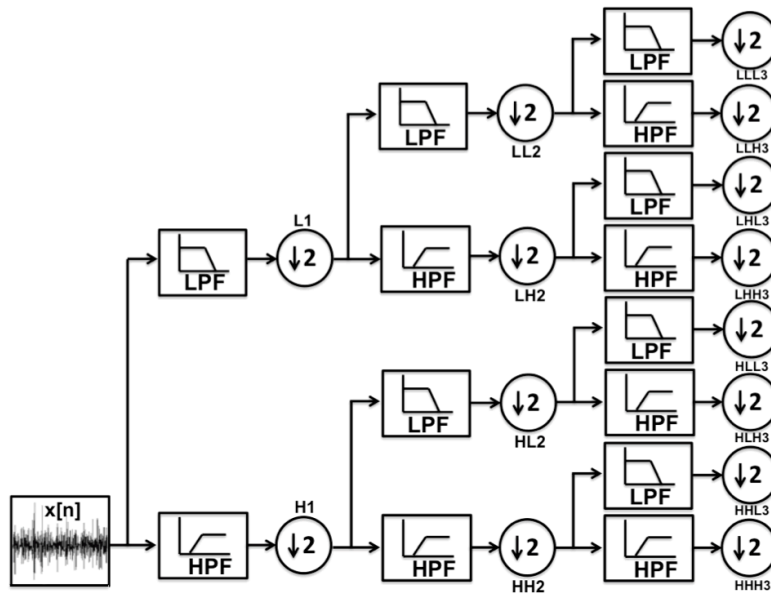


Fig. 2.7. Discrete wavelet packet (DWP) decomposition tree [26].

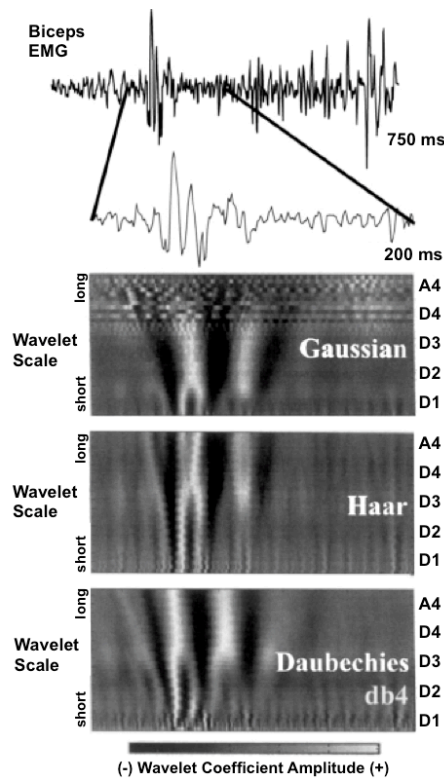


Fig. 2.8. Use of different mother wavelets for EMG signal analysis. Three different mother wavelets (Gaussian, Haar, and db4) were used for the continuous wavelet transform of a 200 ms biceps segment. The wavelet coefficients are plotted in gray scale. Whiter colors represent strong positive correlations between the wavelet shape and the EMG shape, and black represents the largest negative values. The Gaussian curve did not provide a good fit for low frequency components [25].

Wavelet analysis can also be used for identifying time of occurrence of EMG bursts. A wavelet is a waveform of finite length and average value of zero. When the shape of a wavelet that is being convolved with an EMG trace is highly correlated with the rapid fluctuations occurring at the center of the EMG burst, the peak-to-peak amplitude of the coefficient trace is very high as represented on the example in Fig. 2.9. Wavelet transformation, as described above, represents a filtering process in which a discrete series of paired filters are applied to repeatedly split the signal into high and low frequency bands. In order to avoid doubling the number of data points at each stage, the signal is progressively downsampled [25].

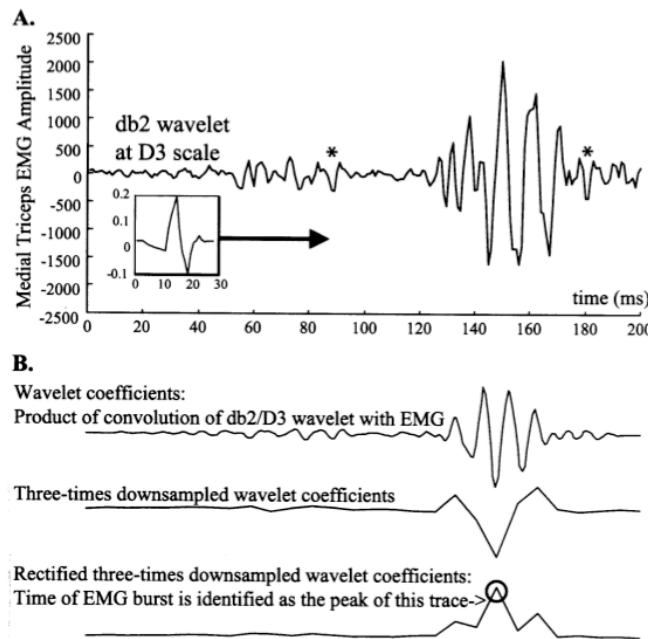


Fig. 2.9. Identification of time of EMG bursts using wavelet coefficients. In section A, a db2 wavelet was convolved with an EMG signal from medial triceps at a medium scale (details at level 3). Section B shows the resulting wavelet coefficients and their downsampled versions that allow identifying the time of occurrence of the EMG burst by taking the peak of the absolute value of the downsampled signal [25].

The DWT has advantages over other techniques for representing functions with discontinuities and sharp peaks. In addition, a multiresolution analysis allows accurate deconstruction and reconstruction of finite, non-periodic, and non-stationary signals. The

statistics calculated over the wavelet coefficients provide information regarding the tendencies, abnormalities, and energy of the sEMG signal [27].

Another important aspect for using wavelet analysis is defining the decomposition level. Each level is related to a frequency range as shown in TABLE 2.1 for an EMG signal sampled at a sampling rate of 1024 Hz as it was defined for the present study. The dominant energy of the EMG signal is located within the 50-150 Hz frequency band, matching mainly the second and third decomposition levels [27].

TABLE 2.1
DECOMPOSITION LEVEL AND CORRESPONDING FREQUENCY RANGE OF SEMG SIGNALS

DECOMPOSITION LEVEL	FREQUENCY RANGE [HZ]
1 st Level	256 to 512
2 nd Level	128 to 256
3 rd Level	64 to 128
4 th Level	32 to 64
5 th Level	16 to 32

2.3.3 Principal Component Analysis

Principal components analysis (PCA) is a technique from linear algebra that allows reducing complex data sets into lower dimension sets often revealing simpler structures. PCA allows identifying patterns in data and highlights their similarities and differences, which makes it a powerful tool for data compression and analysis [28,29].

PCA is a simple, non-parametric analysis tool widely used in diverse fields from neuroscience to computer graphics because it allows extracting relevant information

from confusing data sets [28]. It provides a linear map from the original set of variables $v \in V \subseteq \mathcal{R}^M$ into a reduced-dimension set of uncorrelated variables $z \in Z \subseteq \mathcal{R}^L$ (the principal components), minimizing the mean square error (MSE) between the original feature set and the projected one. The transformed variables are ranked according to their variance, so they reflect a decreasing effectiveness in representing the original set of variables [1,27].

2.3.4 Hjorth's Descriptors

The possibility to control a system dynamically by making adjustments in a timely manner increases when changes within the process can be quickly detected; however, temporal variations in a process are often complex and non-stationary.

In 1970, Hjorth [30] introduced three parameters based on time domain properties intended to describe the graphical characteristics of an electroencephalography (EEG) trace in terms of amplitude, slope, and slope spread, which is why they also receive the name of normalized slope descriptors (NSDs). They allow characterizing any signal and its derivatives in the frequency and time domains. These parameters receive the name of “activity”, “mobility”, and “complexity” [31-33]. Their computation is made over the segment of interest in the nonlinear time series $f(t)$ as shown in (2.13) – (2.15).

$$Activity = m_0 = \sigma_a^2, \quad (2.13)$$

$$Mobility = \sqrt{\frac{m_2}{m_0}} = \frac{\sigma_d}{\sigma_a}, \quad (2.14)$$

$$Complexity = \sqrt{\frac{m_4}{m_2} - \frac{m_2}{m_0}} = \frac{\sigma_{dd}/\sigma_d}{\sigma_d/\sigma_a}, \quad (2.15)$$

where σ_a^2 is the variance of the nonlinear time series $f(t)$, and σ_d and σ_{dd} are the standard deviations (SDs) of the first and second derivatives of $f(t)$ respectively. The variable m_n , calculated using (2.17), represents the spectral moment at order n . In order to have a better understanding of Hjorth's parameters, it is helpful defining the relationship between the time and frequency domains. The frequency description from the Fourier transform is always symmetrical with respect to zero frequency; hence, in a statistical approach to the shape of the frequency distribution, all odd moments will become zero, and all the information will be found in the even moments. The computation of m_0 , m_2 , and m_4 , which contain the useful information for Hjorth's parameters calculation, is further explained in (2.18) - (2.20). The nonlinear time series can also be expressed as a function of frequency $F(\omega)$ by means of the Fourier transform. The power spectrum $S(\omega)$ is obtained by multiplying $F(\omega)$ by its conjugate $F^*(\omega)$ as shown in equation (2.16).

$$F(\omega) \cdot F^*(\omega) = S(\omega) \quad (2.16)$$

$$m_n = \int_{-\infty}^{+\infty} S(\omega) d\omega \quad (2.17)$$

The parameters can be transformed between the time and frequency domains based on the energy equality within the actual epoch, where the total power in the frequency domain is identical to the mean power in the time domain. Hjorth's parameters serve as a bridge between a physical time domain interpretation and the conventional frequency domain description [30-33]. This time-frequency parametric connection is illustrated in Fig. 2.10.

$$m_0 = \int_{-\pi}^{\pi} S(\omega) d\omega = \frac{1}{T} \int_{t-T}^t f^2(t) dt \quad (2.18)$$

$$m_2 = \int_{-\pi}^{\pi} \omega^2 S(\omega) d\omega = \frac{1}{T} \int_{t-T}^t \left(\frac{df(t)}{dt} \right)^2 dt \quad (2.19)$$

$$m_4 = \int_{-\pi}^{\pi} \omega^4 S(\omega) d\omega = \frac{1}{T} \int_{t-T}^t \left(\frac{d^2f(t)}{dt^2} \right)^2 dt \quad (2.20)$$

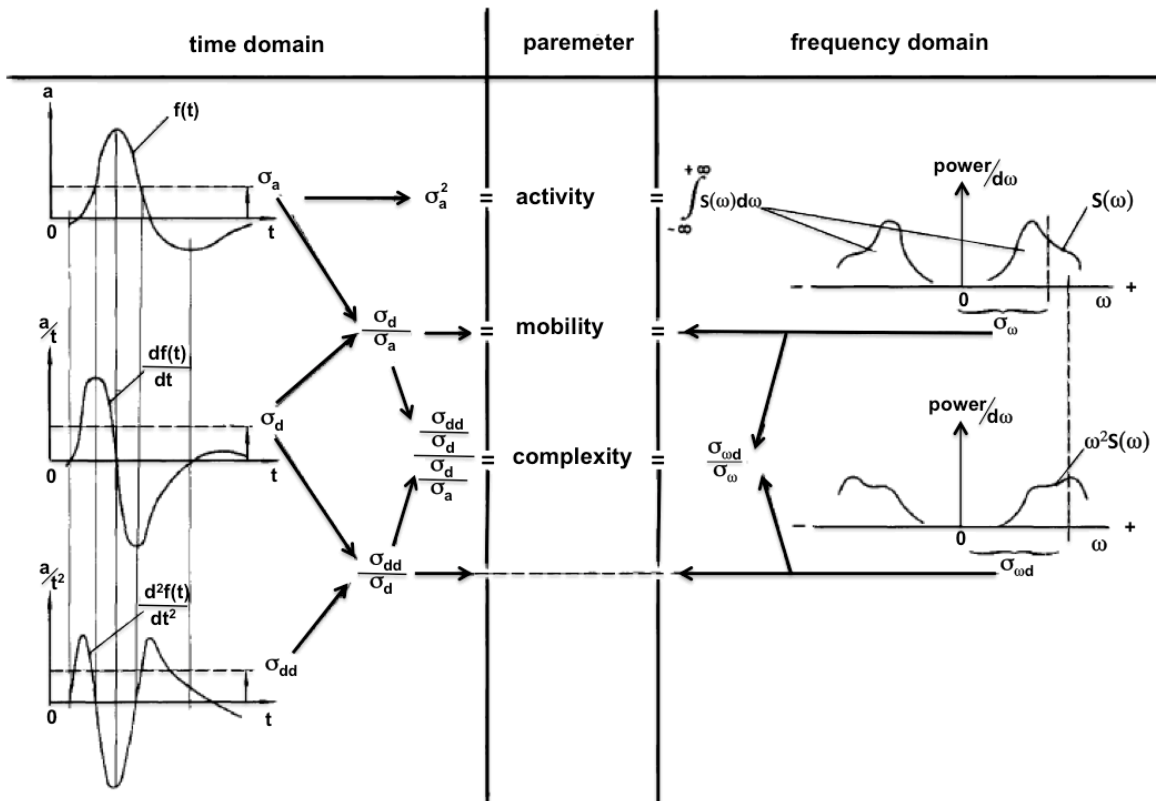


Fig. 2.10. Time-frequency relationship given by Hjorth's parameters. This figure shows the path between the time domain properties and the spectral characteristics of an arbitrary signal [32].

The characteristics of each of the aforementioned parameters allow understanding their significance in both the time and frequency domains [31,32,34]. These features are explained below:

- **Activity:** The mathematical definition of this parameter can be found in equation (2.13). In the frequency domain, it is interpreted as the surface of the

power spectrum (see Fig. 2.10). In time, it reflects the variance in the amplitude of the signal. It has an additive property that allows integrating different observations during the epoch.

- *Mobility*: Equation (2.14) gives the mathematical definition of this parameter. The ratio between the standard deviations that characterize it is given per time unit; hence, it represents the dominant frequency. This ratio will depend on the curve shape in such a way that it measures the relative average slope.
- *Complexity*: This parameter is defined by equation (2.15). It is dimensionless and relates the mobility of the first derivative of the nonlinear time series with the mobility of the nonlinear time series itself. It indicates the deviation of the slope and can be interpreted as a measure of change in frequency of the input signal; i.e., a measure of the signal's bandwidth. This parameter quantifies any deviation from the sine shape as an increase from unity.

A multivariate approach consists of extracting several features from a nonlinear time series and submitting them to a multivariate control chart that will allow determining the moment in which a change point is detected. When variables are correlated, multivariate control charts allow detecting shifts in the mean or the relationship (covariance) between these parameters and help monitoring if the process has gone out of statistical control. Fig. 2.11 is a graphical representation of a multivariate approach where Hjorth's descriptors have been extracted as correlated features to detect the dynamic changes in the nonlinear time series [31]. The Hotelling control chart [35] that appears on this figure is a widely used multivariate procedure to control changes in the mean vector of several correlated quality characteristics.

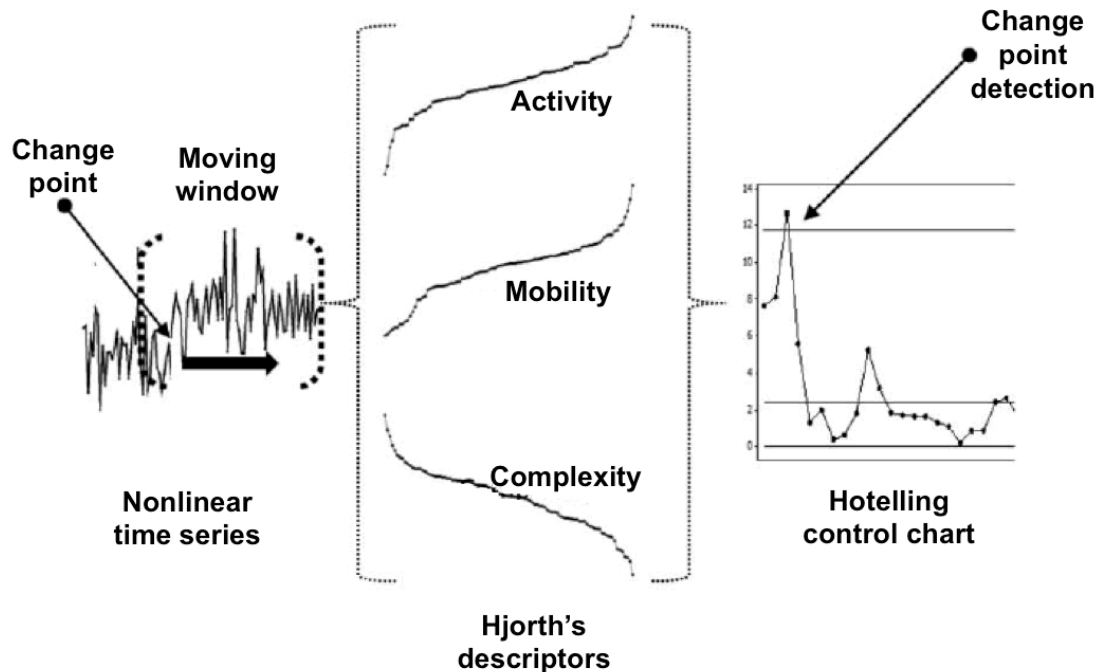


Fig. 2.11. Multivariate approach using Hjorth's descriptors. The three parameters (Mobility, Activity, and Complexity) constitute the extracted features from a given nonlinear time series. The Hotelling control chart allows detecting change points within the signal [31].

One of the main advantages of using Hjorth's descriptors is that though they are based on spectral moments, they are calculated by time variances, which reduces considerably the computational cost and the processing time as compared to other methods. This is one of the main reasons why they can be considered as a feasible alternative for real-time implementations [30-33].

2.3.4.1 State of the Art in the Use of Hjorth's Descriptors

Hjorth originally formulated his parameters in 1970 to describe the EEG signal [30,32]. Since then, these descriptors have been mainly used in sleep EEG processing for data reduction and automatic sleep stage scoring, as well as in several other applications associated to EEG data analysis. However, some studies within the biomedical field have explored the use of Hjorth's parameters for novel purposes.

In 1977, Spehr *et al.* [36] applied spectral analysis and Hjorth's descriptors to quantify the EEG signals obtained from 20 patients with renal failure before and after hemodialysis (HD). They also applied statistical procedures to find the relationship between EEG, blood variables, and psychological performance. Their results showed significant EEG changes after HD. Concerning Hjorth's parameters, these changes were reflected on an increase of Hjorth's mobility and a decrease of Hjorth's complexity, concluding that computerized EEG gives predictive information in monitoring HD.

Neurophysiologists are able to visualize on the scalp the distribution and intensity of a localized EEG abnormality; however, it is difficult to convey the information in a verbal report to the referring clinician. Based on this idea, Persson and Hjorth (1983) [37] found a creative application of the aforementioned parameters. They used them to analyze the EEG signals and converted the obtained values into ink density topograms to reflect EEG changes.

In 1985, Kanno and Clarenbach [38] investigated the effect that two drugs (clonidine and yohimbine) have on sleep. For this purpose, six healthy subjects were submitted to all-night polygraphic sleep studies under the effect of clonidine, yohimbine, a combination of both, or placebo at random order. The conventional scoring of sleep stages was extended by an on-line analysis of the EEG according to Hjorth. The results showed a decrease on REM sleep and a reduction of the parameters mobility and complexity during non-REM sleep when subjects were under the effect of clonidine. This signified synchronization of the EEG. Contrary, yohimbine increased REM sleep. Increases of mobility during both REM and non-REM sleep signified desynchronization of the EEG for this part of the experiment. The combined treatment did not alter the parameters significantly. On that same year, Spehr and Stemmler [39] evaluated the EEG analysis of patients with sequels of chronic alcoholism using Hjorth's descriptors. They were able to determine different types of EEG reactions in postalcoholic stages.

Depoortere *et al.* (1993) [40] evaluated the micro- and macrostructural elements of sleep in different experimental conditions in rats using the NSDs proposed by Hjorth. They were able to discriminate the various stages of the sleep-wakefulness cycle in rats. Even if this method corresponds to a condensed presentation of the spectral analysis, it has the advantage of being faster and easier to apply. They also reported the usefulness of Hjorth's parameters in psychotropic drug research and sleep quality assessment in both animals and humans. In 1995, Ziller *et al.* [41] classified sleep stages by using only Hjorth's mobility and complexity. They compared their results to those of a dimensionality analysis obtaining a superior classification with Hjorth's parameters. They found as well a very high statistical correlation between the estimator of fractal dimension and Hjorth's mobility.

Mouzé-Amady and Horwat (1996) [34] analyzed EMG signals with NSDs in order to clear some doubts that existed about general applications of these parameters. They concluded that Hjorth's descriptors, previously reserved to EEG analysis, can also be used to explore the spectral content in sEMG signals. Their results showed that during repetitive movements, Hjorth's mobility can be significantly correlated with FFT-estimated mean frequency. They obtained high correlation coefficients, ranging from 0.81 to 0.93. The degree of correlation depended highly on data segmentation. Finally, based on the use that these parameters have in data reduction, they proposed the possibility of applying them for monitoring muscular fatigue in real time during long periods.

Ansari-Asl *et al.* [42] proposed in 2007, a channel reduction method for EEG classification in emotion assessment using a synchronization likelihood approach. They achieved a reduction in the number of EEG channels from 64 to 5 with a global loss mean for all classes and features of only 1.6% and a considerable reduction in computation time. They used Hjorth's parameters to evaluate the performance of the

method. When extracting Hjorth's features, time was reduced from an average of 397 seconds while using every channel to 35 seconds after channel reduction.

More recently, Cecchin *et al.* (2010) [33] described a semi-automatic method for temporal lobe seizures lateralization using raw scalp EEG signals intended to help neurologists in clinical evaluation. They used the first two Hjorth's descriptors, namely activity and mobility, to estimate quadratic mean and dominant frequency of signals and characterized the seizure by a point in a frequency/amplitude plane.

The EEG signal is often contaminated by various artifacts that difficult analysis but that can also serve to control an electronic device when they are correctly classified. Pourzare *et al.* (2012) [43] developed a novel approach to classify various facial movement artifacts in EEG signals using root mean square, polynomial fitting and Hjorth's parameters. They obtained an average classification accuracy of 94% in 3 subjects when discriminating between 5 classes.

Hjorth's parameters have also been applied successfully in non-biomedical fields. For example, Balestrassi *et al.* [31] present a case study that describes the use of NSDs to model and forecast variations in electricity load, which is of great importance for industrial consumers. This method can be applied to detect dynamic changes in nonlinear time series.

For multichannel EEG interpretation, Wackermann proposed three global descriptors Ω , Σ , and Φ that allow analyzing EEG activity from all channels at a given time interval. These descriptors are similar to Hjorth's parameters in the sense that Σ and Φ can be considered multichannel equivalents of Hjorth's activity and mobility. The descriptor Σ is a measure of a total power, and Φ is a descriptor of generalized frequency. Ω is new. It

is a global measure of complexity or synchronization not related to Hjorth's measure of complexity. These descriptors have been used for multichannel EEG sleep analysis representing an alternative approach [44]. It could also be worthy considering them for multichannel EMG analysis.

2.4 Artificial Neural Networks

An Artificial Neural Network (ANN) is a relatively new computational modeling tool intended to emulate the information processors that are found in biology; however, its objective is not to replicate the operation of the biological systems but to make use of what is known about their functionality for solving complex problems [45,46]. ANNs may be defined as structures comprised of densely interconnected adaptive simple processing elements (called artificial neurons or nodes) that are capable of performing massively parallel computations for data processing and knowledge representation [46]. A typical three-layer artificial neural network structure is shown in Fig. 2.12. Some of the main areas in which ANNs have proven good performances are: pattern completion, classification, optimization, feature detection, data compression, approximation, association, prediction, and control [45].

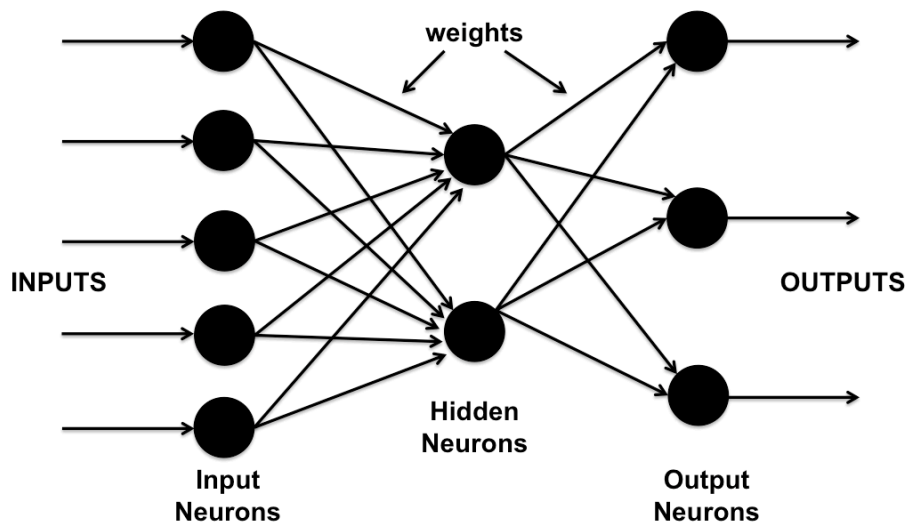


Fig. 2.12. Typical three-layer artificial neural network [45].

ANNs have become very attractive algorithms because they integrate the following characteristics [46,47]:

- *Nonlinearity*, which allows better fitting of the data.
- *High parallelism*, which implies fast processing and hardware failure-tolerance.
- *Learning and adaptability*, which allow the system to modify (update) its internal structure in response to a changing environment.
- *Generalization*, which enables the application of the model to unlearned data and provides the system with the ability to handle imprecise and fuzzy information. This increases the system's tolerance to noise.

An artificial processing neuron receives inputs in the form of stimuli from the environment. The net input (ξ) is computed as the inner product of the input signals (x) and the weights (w). The net input passes through a linear threshold gate, and the output (y) is transmitted to another neuron or to the environment. The neuron becomes activated only when ξ exceeds the neuron's threshold (also called bias, b). For n signals, the perceptron neuron operation is expressed as shown in (2.21) where 1 indicates 'on' and 0 indicates 'off', or class A and B, respectively, in classification problems. .

$$y = \begin{cases} 1, & \text{if } \sum_{i=1}^n w_i x_i \geq b \\ 0, & \text{if } \sum_{i=1}^n w_i x_i < b \end{cases} \quad (2.21)$$

If weight connections are positive ($w_i > 0$), the link is called excitatory and the neuron gets activated, whereas negative weights reduce ξ and inhibit the neuron's activity, generating inhibitory links. Weights change in proportion to the difference (error)

between the target output (Y) and the perceptron solution (y). The learning process consists in obtaining the set of weights that corresponds to the global minimum. In order to deal with nonlinearly separable problems, additional layer(s) of neurons, called hidden layers, can be placed between the input and output layers generating a multilayer perceptron (MLP) architecture [46].

Two classes of learning procedures exist. In unsupervised learning, network models are first presented with an input vector from the set of possible network inputs. The network is required to self-organize, and the learning rule adjusts the weights so that input examples are grouped into classes based on their statistical properties. Supervised learning consists in providing the network with both input data and its targets. Outputs are calculated based on current inputs and later compared with a desired output (target). The error between the two is used to modify the weights in order to reduce the error, and it makes the network more likely to give a correct answer when similar input data is presented. Learning is performed iteratively as the network is provided with training examples. It is possible to evaluate if a system has learned based on its ability to handle imprecise, fuzzy, noisy, and probabilistic information without affecting the response quality, and its ability to generalize when unknown data is presented [45,46,48].

Back-propagation (BP) networks are the most widely used type of networks. They are MLPs consisting of an input layer with nodes that represent the input variables, an output layer with nodes that represent the dependent variables, and one or more hidden layers containing nodes to help capturing nonlinearity in the data. The BP, which is a very common supervised learning algorithm, is a gradient descent method that establishes the weights in a multi-layer, feed-forward adaptive neural network. The system is initialized using small arbitrary weights, and learning is accomplished by successively adjusting the weights based on a set of input patterns and the corresponding set of desired output patterns. The error computed at the output side is propagated backwards from the output layer all the way to the input layer in order to

adjust the weights. Once the net effect at one hidden node is determined, the activation at that node is calculated using a transfer function [46,49].

Bayesian networks are useful for representing statistical dependencies. A Bayesian network is a graph-based model of joint multivariate probability that captures properties of conditional independence between variables. These models are attractive for their ability to describe complex stochastic processes and because they provide a clear methodology for learning from noisy observations [49].

There are many different kinds of networks and learning algorithms that can be used according to the problem that wants to be solved. Some of them combine characteristics and methods that allow dealing with the problem using a better and more focused approach.

Artificial neural networks have been widely applied to EMG classification problems. A few examples can be seen in Hudgins *et al.* [6], Englehart *et al.* [51,52], Liu *et al.* [53], Gazzoni *et al.* [54], Chan *et al.* [10], among many others. ANNs are continuing to gain popularity and are being applied in many areas of the biomedical field as well as in non-related fields.

2.5 K-Fold Cross-Validation

Cross-Validation (CV) is a popular method for algorithm selection. The main idea behind it is to split data, once or several times, for estimating the risk of each algorithm. Part of the data is used for training, and the remaining part is used for estimating the risk; then, CV selects the algorithm with the smallest estimated risk. This method avoids overfitting because the training sample is independent from the validation sample [55].

There are different types of CV; all of them form part of a family of re-sampling methods. Even if these methods require a higher computational cost, they compensate the drawbacks from the holdout method, which are the difficulty of setting aside a portion of the dataset for testing when there is a sparse dataset, and since it is a single train-and-test experiment, the holdout estimate of error rate can be misleading when the data split is not adequate. Some of these methods are: random sub-sampling, k-fold cross-validation, and leave-one-out cross-validation [56].

The k-fold cross-validation, sometimes called rotation estimation, is a general procedure for estimating the prediction error of any supervised classifier. In order to implement this method, at the beginning of the process, the training set must be divided into k equally populated folds. The system will be trained on $k - 1$ folds and evaluated on the remaining fold. The process will be repeated k times, leaving subsequently all the folds out and using them for error estimation [56-60]. This procedure is illustrated in Fig. 2.13.

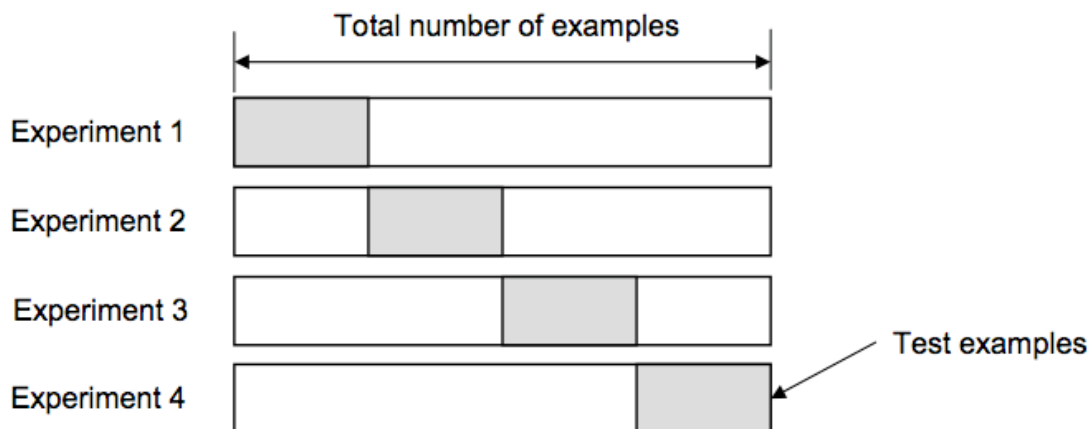


Fig. 2.13. K-fold cross-validation for $k = 4$ [56].

The true error is estimated as the average value of the errors committed in each fold as shown in (2.22). The error estimator depends on two factors: the training set and the partition into folds [56,61]. The bias of an error estimator is defined as the real error

value minus the expected estimated error value. According to [61], when the goal is to measure the error, a less biased error estimator should be used. For that purpose, they recommend the use of $k = 5$ or $k = 10$, which are less biased than $k = 2$ and have less computational cost than $k = n$. They also advise the use of repeated cross validation when it is computationally feasible.

$$E = \frac{1}{K} \sum_{i=1}^K E_i \quad (2.22)$$

The advantage of k-fold cross-validation is that every fold from the dataset is eventually used for both training and testing.

2.6 State of the Art in EMG Transient State Analysis for Myoelectric Control

Surface EMG analysis has been widely studied over the years for prosthesis control using many different signal-processing techniques; however, there are just a few works reported on the use of the transient state of the EMG signal.

This section will give a general perspective on EMG signal-processing techniques for myoelectric controlled devices; nonetheless, it will mostly concentrate in explaining the few works reported for transient EMG analysis.

Research on the use of EMG for upper limb prosthesis control has been conducted since the 1940s. Reiter (1948) was the first one to use the EMG signal to control a simple prosthetic device [1,62,63]. There was significant international progress in the 1960's, but it was in the 1970's that myoelectric prostheses began to make a significant clinical impact [11,64]. In 1975, Graupe and Cline [65] used four parameters of an

autoregressive-moving-average (ARMA) model of steady state signal to classify four upper-limb functions with a performance over 95%. Several groups continued studying and making improvements on myoelectric control based on the steady state of the EMG signal. However, it was until 1993, that Hudgins *et al.* [6] proposed a new control strategy considering the transient state of the signal. They based their work on the observation that there is considerable structure in the MES during the onset of a contraction and in the fact that it is different for distinct limb movements, which could make it useful for classification as shown in Fig. 2.14. They were able to discriminate between four movements (elbow flexion and extension and medial and lateral humeral rotations) using a single bipolar electrode pair. The features that were extracted from the EMG signal were MAV, MAVSLP, ZC, SSC, and WL. They later used a two-layer ANN as the classifier obtaining a correct average classification range of 91.2% (SD 5.6%) for 9 normally limbed subjects and an average of 85.5% (SD 9.8%) for 6 amputee subjects. This work introduced the idea that the MES is not random during the initial phase of the muscle contraction, thus, finding deterministic components in the instantaneous myoelectric signal. Basha *et al.* [66] and Yamazaki *et al.* [67] found further evidence of deterministic components in the MES.

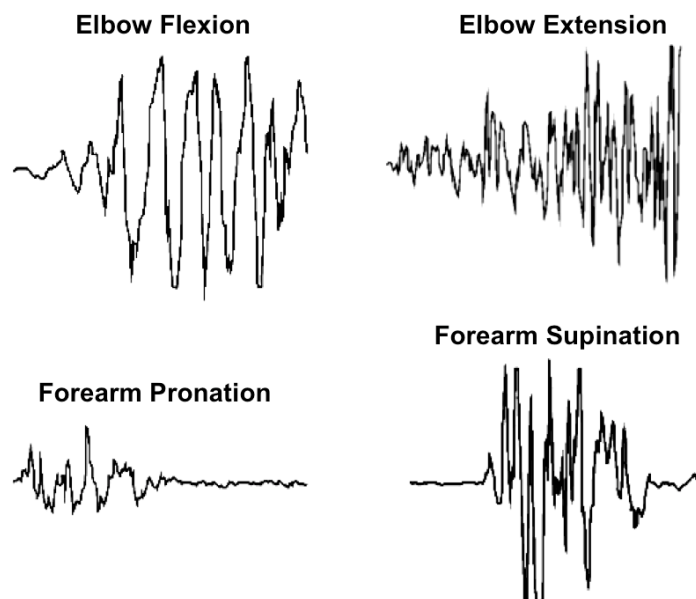


Fig. 2.14. Patterns of transient MES activity. They were recorded using a single bipolar electrode pair placed over the biceps and triceps [68].

Kuruganti *et al.* [13] suggested, in 1995, a similar protocol to the one followed in [6], but used a two-channel acquisition system. The classification accuracy obtained by the two-channel system was significantly better than that of the one-channel system. They obtained an average classification accuracy of 93.7%, however, their classification accuracy for the one-channel data was lower than the one reported in [6]. They attributed this to changes in the instrumentation and slight differences in the electrodes' location.

In 1995, Englehart *et al.* [51,52] proposed the use of a dynamic feedforward neural network for classification of myoelectric signal patterns with the objective of integrating more efficiently the temporal information in transient signals. A few years later, they presented another study [9,69,70] in which they demonstrated that four channels of myoelectric data greatly improve the classification accuracy, as compared to one or two channels. They discriminated between six different classes of motion (flexion/extension of the wrist, ulnar/radial deviation of the wrist, and hand opening/closing). The first data set was produced comprising transient bursts by generating quick, moderately strong contractions, and the second data set consisted of steady state signals produced by holding each contraction with constant effort. They found that PCA dimensionality reduction was imperative to the success of the time-frequency based feature sets. Moreover, they demonstrated that the performance improves in the procession: time domain feature set (TD) → short-time Fourier transform (STFT) → wavelet transform (WT) → wavelet packet transform (WPT). Their results indicated a better classification accuracy using steady state data as compared to transient data. Based on this, they concluded that steady state data contains greater discriminating information. The performance was better for the four-class problem than for the six-class problem. The four-channel system, using a WPT feature set for steady state analysis, yielded 0.5% error when discriminating between four classes and 2% error with 6 classes. Another tested parameter was classification performance according to the record length. They found that classification performance has less degradation when decreasing the size of the window for feature extraction of steady state data, whereas degradation is more

evident using smaller windows with transient data. This could allow using shorter records and obtaining a faster system response from the steady state of the EMG signal. After their analysis, they proposed a continuous classifier that could produce classification results using the WPT on a continuous stream of steady state data [11].

A control system based on Hudgin's work was designed at the University of New Brunswick (UNB) in Canada [68,71]. The UNB myo-controller identified four types of muscular contraction from the signals measured in the biceps and triceps with a single EMG channel. It used a simple MLP artificial neural network as a classifier of a TD set, originally described in [6], that was extracted from the first 200 ms of myoelectric activity following the initiation of a contraction to determine the intent of the amputee. This system was capable of providing multifunction control from a single site and had the advantage that the control signals could be derived from natural contractions, thereby minimizing the conscious effort of the user. The UNB controller has been tested in the clinical setting and has been demonstrated to be highly reliable. After a short period of training, users were able to produce a correct function selection rate of over 90%.

Chan *et al.* [72] proposed a fuzzy approach to classify single-site EMG signals for multifunctional prosthesis control and employed the same database as [6]. They obtained a slight improvement in classification.

Liu *et al.* [53] developed a real-time learning method for motion discrimination using the MES. They applied wavelet transform and an ANN for classification of five different types of movements using a four-channel system in order to control a prosthetic device. They used both the steady and transient states of the EMG signal.

Ajiboye and Weir [73] presented a heuristic fuzzy logic approach to multiple EMG pattern recognition for multifunctional prosthesis control in 2005. They discriminated between four EMG patterns for subjects with intact limbs and between 3 patterns for limb-deficient subjects. Overall classification rates ranged from 94% to 99%. Their algorithm demonstrated success in real-time classification, both during steady state motions and motion state transitioning. The system's update rate was of 47.5 ms. The onset for each contraction was automatically determined as the point when the active rms signal was greater than the rms quiescent signal mean plus three standard deviations and later verified through visual inspection.

Karlsson *et al.* [74] introduced non-stationary signal analysis methods to analyze the EMG signals during dynamic contractions by estimating the time-dependent spectral moments. They obtained the best results using the continuous wavelet transform (CWT). They concluded that during dynamic contractions, spectral analysis must be handled with great care because the number of active motor units changes, the position of the electrodes with respect to the active muscle fibers varies as the contraction evolves, the muscle fiber length is modified, etc. All these factors, in addition to changes in muscle fiber conduction velocity due to muscle fatigue, tend to greatly increase the non-stationarity of the EMG signal.

Several works have proposed real-time control methods, such as the research presented by Nishiwaka *et al.* [75-77] that contemplates the use of the Gabor transform and the MAV for a real-time learning method capable of discriminating ten forearm motions (4 wrist and 6 hand motions) using two EMG channels. Learning was achieved between 4 and 25 minutes. They obtained an average discriminating rate in an 8 forearm motions experiment with 5 subjects of 85.1%. Chu *et al.* [78] proposed a real-time pattern-recognition system implemented for a multifunction myoelectric hand. They attempted to recognize nine kinds of hand motions and achieved up to 97.4% of classification range, but results were stable only for steady state motions and

classification decreased during transient state motions, even if they used a fixed movement velocity. They concluded that this made it difficult to apply the proposed method to the tasks of daily living for a limb-deficient individual, and they stated that future work should look into using the method to recognize motions from EMG signals related to dynamic contractions and various movements velocities. Other methods, such as the use of Gaussian mixture models (GMMs) for classification using continuous myoelectric signals and four EMG channels for six classes of limb motions [79], have also been tested with good results and low computational load.

Pattern recognition based myoelectric control systems have been widely researched; however, just a few of them have been implemented in a clinical environment. Hangrove *et al.* [80] made evident the fact that classification accuracy is the metric most often reported to describe how well control systems perform, but works mostly never relate this measure to the usability of the system. In their study, MES data corresponding to seven classes of motion (elbow flexion/extension, wrist flexion/extension, hand open, hand close, and rest) were collected from healthy subjects using an assistive brace described in [81] for performing isometric contractions. They used four MES channels placed around the circumference of the forearm and four additional channels placed around the circumference of the humerus. Initially they recorded steady contractions. Each subject held the contraction during 4 seconds until it reached a steady state. Afterwards, they included recordings that integrated the transient portion of the contraction. Subjects performed an additional four repetitions of the seven types of contractions initiating from the rest state. The first two repetitions of each type of contraction were used as training data, and the remaining two were used for testing. They extracted TD features from each window frame of 125 ms and used them as inputs to a linear discriminant analysis (LDA) classifier. Periodic misclassifications were found to occur during the transient portions of the EMG signals. Their results showed that including transient data along with steady state data for classifier training increases the classification error, but it also increases system usability. The authors suggest that classification error should not be the sole measure of a

system's usability and performance. The importance of including transient state analysis is that it is easier to include transitions in the training data than to constrain the subject to be in a steady state position prior to data collection; the subject is simply prompted to perform a contraction in a natural manner.

2.7 Advantages in the Use of Multichannel EMG

As previously mentioned in the first chapter, multichannel EMG recordings are performed with electrodes placed on the involved muscles that can be used to identify the movement based on the fact that each movement corresponds to a specific pattern of activation of several muscles. The use of multichannel EMG helps reducing unwanted variability and allows a better representation of the real muscle activity in the collected signal [3,7]. Each channel includes the muscle group, the volume conductor between each muscle of the group and the electrode, and the summing electrode [64].

Performance improvements in classification can be obtained through an increase in the number of EMG channels. Davidge [82] investigated the increase in classification performance while increasing the number of channels. The results showed that the classification performance for discrimination of 10 functions using a linear discriminant (LD) classifier increased with the number of channels, reaching 94% at 16 channels. However, the performances at eight and four channels drop to only 93% and 87%, respectively [64].

One of the main advantages found in multichannel EMG recordings is that even if using less channels results in a lower computational load, with multichannel EMG, the positions of the electrodes can become less critical and the classification accuracy can be increased [12]. Several studies have proven increases in classification accuracy for

both steady and transient EMG states while increasing the number of channels [9,13,69,70].

In order to increase the number of devices under the control of the MES more information must be extracted from it about the active muscle state. One of the main approaches to achieve this consists in the use of multiple EMG channels, which would provide localized information at a higher number of muscle sites [11,78].

2.8 State of the Art in Our Laboratory

There have been several projects developed in our laboratory with the objective of analyzing and processing the EMG signal in order to find useful techniques to control prosthetic devices and virtual interfaces. Some of the most recent ones are described in this section.

In 2003, a system that allowed identification of seven hand movements from an EMG signal registered on the forearm using only two EMG channels was developed. The classifier consisted on an ANN that identified EMG patterns generated during isometric contractions; in other words, it searched the relationship between the EMG signal and the final position of the hand [83].

In November 2010, an experimental training system was developed in order to allow an amputee to become familiar with a myoelectric control prosthesis through a virtual environment. This computer interface simulates an upper limb prosthesis for an above-elbow amputee. It was developed in MATLAB® (version r2009a), and the control algorithm was generated from a single differential EMG channel (two register electrodes located on the muscle of interest and one reference electrode) from which three levels of

force were defined. The user was able to practice and identify each of the force levels generated by the contraction of the remaining muscle in his stump by receiving a visual feedback from the interface [84]. In this same year, there was another ongoing project that consisted in the design and implementation of a movement control system using a microcontroller for a transhumeral prosthesis with four degrees of freedom and parallel linear actuators [85].

In 2011, a student developed an automatic system to decompose myoelectric signals using wavelet analysis and a support vector machine for the classification process. The objective was to isolate and classify the motor unit action potential from characteristics such as firing rate, form, and duration. The system was able as well to identify and classify the signals when a simulated noise was added [86]. There was another project that intended to execute different routines in an upper limb prosthetic device using as reference the movement patterns extracted from a healthy subject. The objective was to achieve the execution in a more continuous and anthropomorphic way. The implemented routines consisted of the necessary movements to achieve the following activities: drinking water, waving the hand, answering the phone, opening a door, and serving a glass of water from a jar. The algorithms were created by relating the prosthesis's actuators with a set of angles measured during each activity. An artificial neural network allowed this classification [87,88].

In 2012, there was a project that consisted in the creation of an electronic system for algorithm evaluation that allows the design and implementation of parallel control algorithms for the robotic limb developed previously in the laboratory. This allows a finer control and improves consequently the performance of the executed routines [89].

Leon's work [90] served as antecedent for this study. The goal of his research was to develop a system capable of identifying 27 movements of the upper limb for the

simultaneous control of 3 degrees of freedom on a virtual anthropomorphic robotic arm. The system was based on the off-line analysis of the steady state of the EMG signal. Two databases were created. The first one consisted in the acquisition of 9 simple movements using 4 EMG channels and 12 healthy subjects. The second one, which is the one used in this study, was acquired using 8 EMG channels placed on the forearm of 20 healthy subjects to identify 27 motions (rest, 6 simple movements, 12 combinations of two simple movements, and 8 combinations of three simple movements). Features from both the time and frequency domains were extracted and three different classifiers (LDA, ANN, and support vector machines (SVM)) were used. For the experiment with the first database, a 98.8% classification was obtained for the best case, and it was concluded that ANNs and SVMs outperformed LDA classifiers. From the experiment with the second database, conclusions showed that classification performance of the ANN and SVM systems increased using frequency domain features over TD features. The increase in the amount of data to identify all the classes decreased the accuracy of the classifiers. A 96.25% average classification was achieved, and it was proved that when using the information from just 6 of the 8 EMG channels, classification accuracy could remain over 95%.

In [91], Leon *et al.* proposed the use of LDA, ANN, and SVM for classification of 9 forearm motions (inactive, hand opening/closing, wrist pronation/supination, wrist flexion/extension and radial and ulnar deviations) from 12 healthy subjects using 4 EMG channels and extracting frequency features from the steady state of the signals. They obtained the best performance employing frequency features and a SVM classifier with an average misclassification rate of 1.53% (SD 1.08%).

Based on the whole previous revision about the state of the art in EMG control, it is clear the importance of having a reliable method for predicting the final position of a limb while the muscle fibers are contracting. This gives the possibility to action the prosthetic device while the subject initiates the contraction with no perceivable delay, and it also decreases the degree of concentration that would be needed to sustain a movement in a final position. This, together with the use of a multichannel technique that makes less critical the positions of the electrodes and increases classification accuracy [12], could result in a more robust and reliable control and could represent a promising alternative.

Method

3.1 Proposed Solution

The general method proposed as a solution for the analysis of the EMG transient state is described in Fig. 3.1. Several methods were tested and will be explained below; however, the novel method, which has yet not been reported in literature, consists in using Hjorth's parameters, originally intended as EEG descriptors, in the analysis of the EMG signal. The intention is to investigate their possible application for EMG analysis based on the fact that the definitions of Activity, Mobility, and Complexity seem to be particularly suitable to adapt to the nature of myoelectric signals.

For this study, the system's inputs consist on multichannel EMG signals taken from a database that will be subsequently described. The intention in the future is to be able to use the multichannel EMG signals directly recorded from the patient's forearm muscles as inputs to achieve an on-line analysis.

The transient EMG state was extracted from the whole EMG recording in order to be analyzed, and Hjorth's parameters were extracted from it using a sliding window. The resulting feature matrix was used to feed an ANN that allows classifying the different hand motions. The performance of this method was tested using a virtual model where motions are reproduced as identified by the classifier.

The following points will be discussed in this section:

- *Data acquisition protocol*, in which the movements that were selected for classification, the EMG database, the electrode placement used for this study, and the acquisition and conditioning system will be described.
- *Data processing*, including the pre-processing technique, a detailed description of the different types of feature extraction, and information about the ANN model and the validation method.
- *Validation of the model*, describing how tolerance to noise was tested and a description of the virtual hand model.

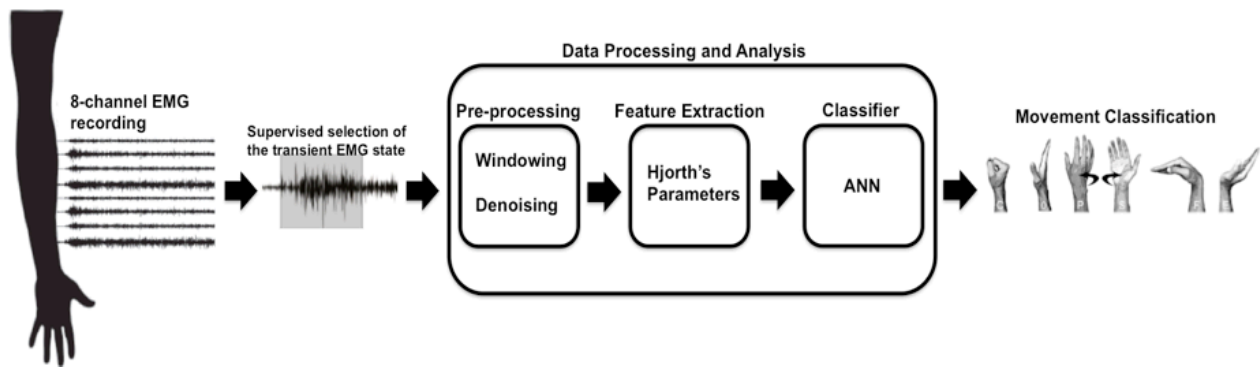


Fig. 3.1. General diagram describing the proposed solution.

3.2 Data Acquisition Protocol

The EMG data used for this study is taken from the second database described in [90]. Some details will be provided on how this database was created and on the information that was selected for the present study.

3.2.1 Movements' Selection for Classification

Six different motions were selected for classification. This corresponds to three different classes, each class containing an agonist and an antagonist movement in which the action of antagonist muscle groups are involved. The movements are enlisted in TABLE 3.1 shown below and represented by Fig. 3.2.

TABLE 3.1
MOVEMENTS' SELECTION FOR CLASSIFICATION

CLASS	MOVEMENT 1	MOVEMENT 2
I	Hand Closing (C)	Hand Opening (O)
II	Wrist Pronation (P)	Wrist Supination (S)
III	Wrist Flexion (F)	Wrist Extension (E)

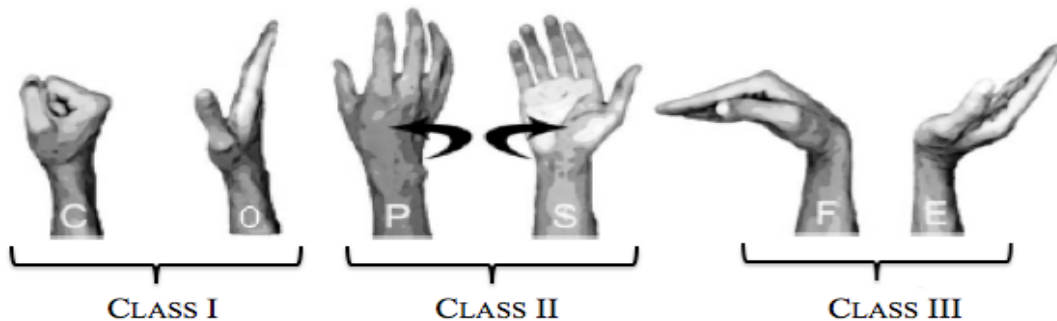


Fig. 3.2. Representation of three classes of antagonist movements. Class I consists of hand closing and opening; class II stands for wrist pronation and supination, and class III includes wrist flexion and extension [90].

3.2.2 EMG Database

The original database was created pursuing the objective of searching and analyzing the steady state of the EMG signal, which makes it not ideal for the transient state analysis,

but allows proving the capacity of adaptation and robustness of the model according to the provided signals.

The database consists on the EMG signals collected from the dominant forearm of 21 normally limbed subjects (19 males and 2 females) aged between 23 and 50 and with no register of neuromuscular disorders. During the creation of the aforementioned database, each subject was asked to repeatedly close and open the hand until the desired muscles for each of the EMG channels were identified. The skin was carefully cleaned before electrode placement. Afterwards, eight pairs of electrodes (one pair for each channel) were located in the designated areas. The reference electrode was subsequently placed on the elbow.

Written consent was obtained from every subject before starting the study. A test session previous to the actual recording of the signals was made, and it consisted of explaining the participants how to execute each of the movements and allowed amplification gain calibration of the eight differential EMG channels to a common maximum value.

The whole database contains 27 different movements of the forearm that were repeated five times each creating a total of 135 EMG recordings per subject. The objective of the study for which the database was initially created consisted on the analysis of the steady state during isometric sustained contraction; therefore, there was no regulation on the movements' speed and acceleration. The subjects were asked to execute the movement until reaching a specified position (the portion between initiation of the movement and the final position comprises the transient state of the EMG signal) and to sustain it until the end of the recording with a relative medium force level (steady state of the signal). Each recording is 20 seconds in length. After each six recordings, a one-minute rest period was given to avoid muscle fatigue.

Only 6 types of movements (see TABLE 3.1) were analyzed for the present study, having a total of 30 recordings per subject (5 recordings per movement). The position of the subjects was standardized in order to reduce variability. They were all asked to perform the study in a standing position. Previous to each recording, their dominant arm was extended to the front and the hand rested in a relaxed position.

3.2.3 Electrode Placement

The EMG signals were recorded from eight differential channels placed on the forearm of the subject. Each channel consists of a pair of Ag-AgCl surface electrodes (model VERMED NeuroPlus A10043) with an interelectrode distance of 1.5 cm and a common reference electrode located on the subject's elbow. The forearm muscles that were selected for each of the EMG channels are named in TABLE 3.2 and their anatomical position is shown in Fig. 3.3 (posterior and anterior views respectively).

TABLE 3.2
FOREARM MUSCLES RECORDED BY EACH EMG DIFFERENTIAL CHANNEL

EMG CHANNEL	FOREARM MUSCLE
1	Extensor digitorum communis
2	Extensor carpi ulnaris
3	Differential measure between extensor digitorum communis and extensor carpi ulnaris
4	Extensor carpi radialis longus
5	Brachioradial
6	Flexor carpi radialis
7	Palmaris longus
8	Flexor carpi ulnaris

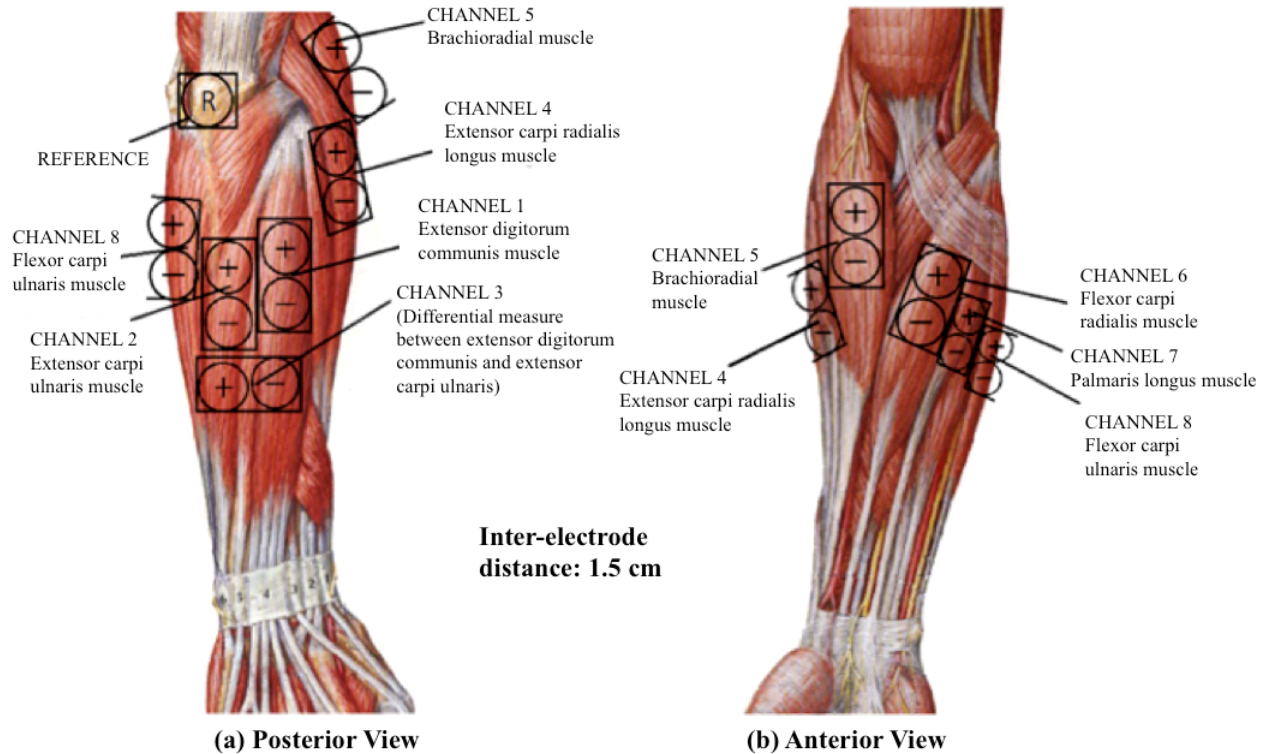


Fig. 3.3. Electrode placement for EMG signal recording. The left side (a) presents the posterior view of the forearm, and the right side (b) corresponds to the anterior view. They both show the location of each differential EMG channel used for this study.

3.2.4 Signal Acquisition and Conditioning System

The acquisition system consisted of 8 differential channels with an adjustable amplification gain that could vary between a range of 1000 and 7000 with a common mode rejection ratio (CMRR) superior to 96 dB. Each channel contained a first order analog band-pass filter with a low cut-off frequency of 20 Hz and a high cut-off frequency of 400 Hz. An image of this system is shown in Fig. 3.4.

The analog outputs from each channel were connected by a shielded cable to a National Instruments acquisition card (model DAQ-Card 6024E) for 12-bit A/D conversion. The sampling rate used for the acquisition was 1024 Hz.

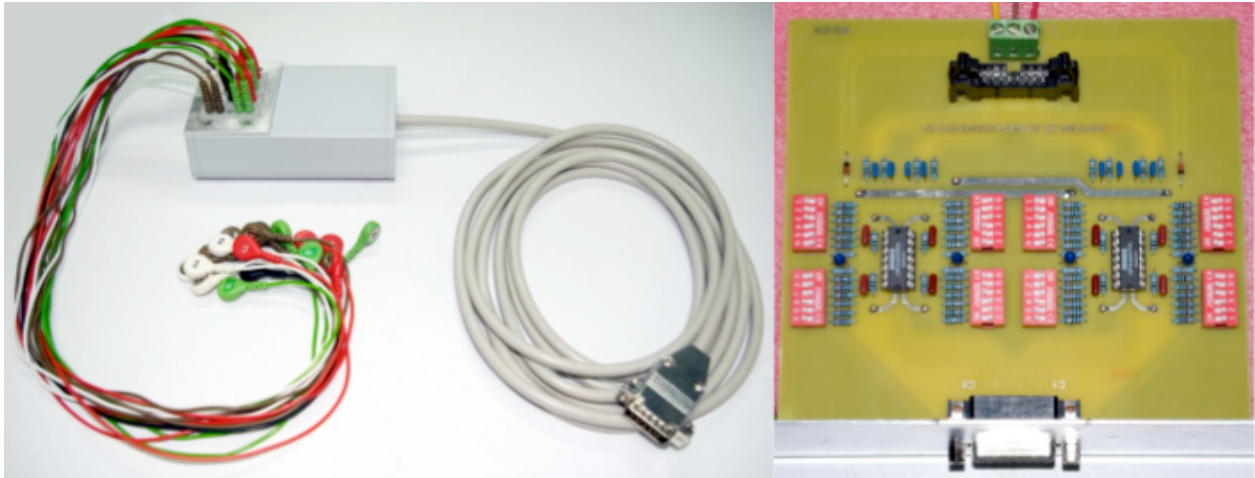


Fig. 3.4. Signal acquisition and conditioning system. The first section of the image shows the cables that attach to the electrodes corresponding to each of the channels and the shielded cable that connects the output of the system to the National Instruments acquisition card for 12-bit A/D conversion. The second section of the image shows the electric circuits for filtering and amplification of each channel [90].

The software for EMG acquisition was developed in our laboratory using LabVIEW 8.5. It allowed visualization of the signal in order to avoid possible errors before starting data recording.

3.3 Data Processing and Analysis

The EMG data was processed and analyzed using MATLAB® (version R2012b). All the steps that were followed in order to define the parameters for pre-processing and classification are described below.

3.3.1 Pre-processing

In order to start analyzing the EMG data, the transient state was identified in the signal. It was also necessary to define the type and size of window that gave the best

classification performance and to propose a de-noising algorithm to extract information from the frequency bands of interest.

3.3.1.1 EMG Signal Partition in Transient and Steady States

Each recording was divided by supervision in transient and steady states as shown in Fig. 3.5. An attempt to make automatic selection of the transient state was made based on the change of the signal's energy level and detection of its maximum; however, some difficulties were encountered because the database was not originally created with the intension of analyzing the transient segment. Therefore, the variability on where the movements started to be recorded and the noise level in the inactive segment of the signal decreased precision in the detection. The equation used for energy calculation is presented in (3.1). The decision of using a supervised method was taken to obtain a more reliable selection of the EMG transient state for every channel and every movement and to ensure that the analysis was done over the portion of interest of the signal.

$$E = \sum_{n=1}^N |x(n)|^2, \quad (3.1)$$

where $x(n)$ is the vector of the EMG signal considered within a window of length N .

A visual inspection was made in order to determine where the transient state started for each of the recordings; afterwards, a fixed number of samples (1048 samples that correspond to 1.023 s) were selected for analysis. For the steady state, the same amount of samples was extracted from the corresponding segment of the signal.

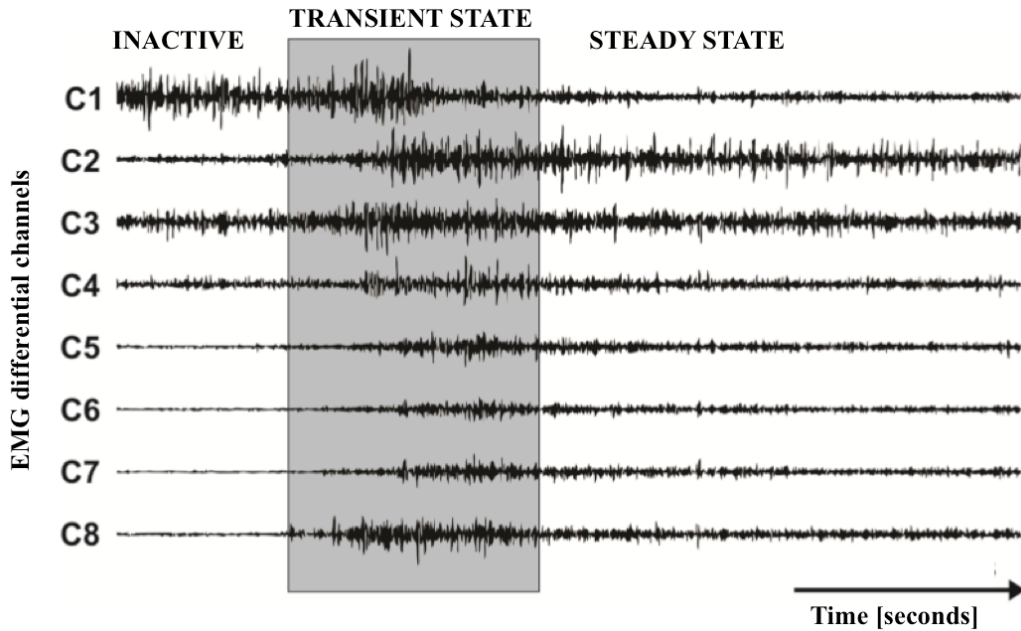


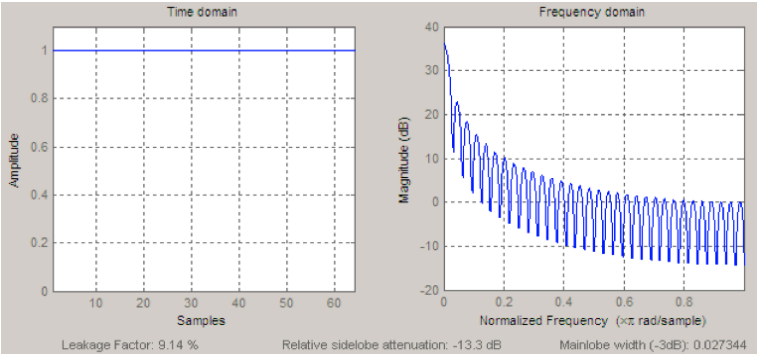
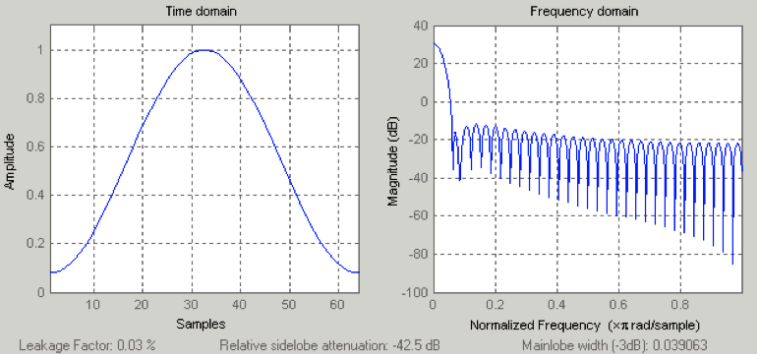
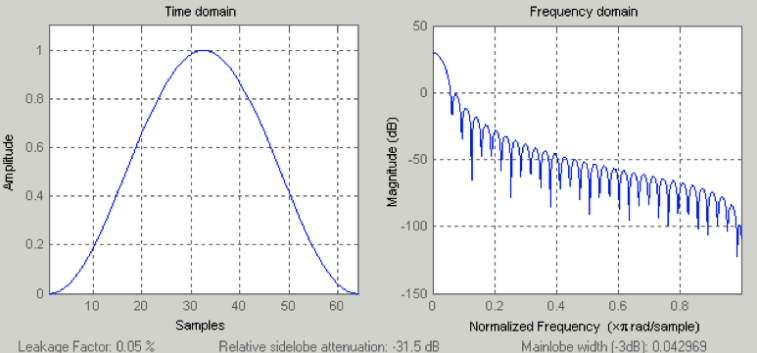
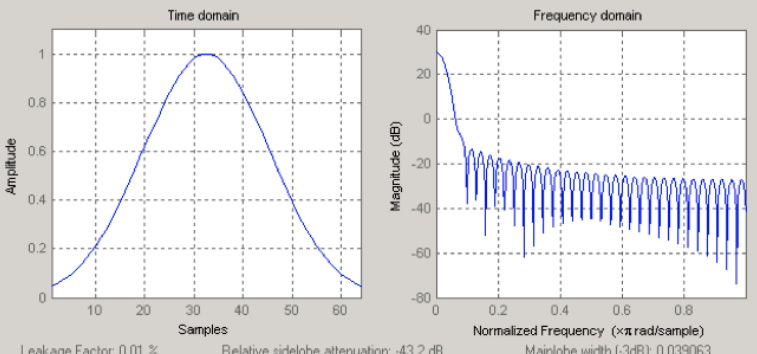
Fig. 3.5. Two main states found in muscle contraction. They appear identified in an 8-channel EMG record of hand closure [90]

3.3.1.2 Window Selection

As previously mentioned in chapter I, the longest acceptable delay in a prosthetic control system has generally been established as 300 ms [6,9,10]; therefore, the window length for feature extraction in a real-time application cannot overpass 300 ms. Moreover, it is also necessary to consider the processing time together with the length of the window in order to calculate the total delay.

Several types of windows were tested, namely rectangular, Hamming, Hanning, and Gaussian windows, in order to determine the one that provided best classification accuracy. The time and frequency representations of these windows can be seen in TABLE 3.3.

TABLE 3.3
TIME AND FREQUENCY REPRESENTATION OF TESTED WINDOWS

Window Type	Time and Frequency Representations
Rectangular	 <p>Time domain: Amplitude vs. Samples (0 to 60). Amplitude is constant at 1.0.</p> <p>Frequency domain: Magnitude (dB) vs. Normalized Frequency ($\times\pi$ rad/sample) (0 to 1.0). Mainlobe width (-3dB): 0.027344. Relative sidelobe attenuation: -13.3 dB. Leakage Factor: 9.14 %.</p>
Hamming	 <p>Time domain: Amplitude vs. Samples (0 to 60). Amplitude follows a smooth bell-shaped curve peaking at 1.0.</p> <p>Frequency domain: Magnitude (dB) vs. Normalized Frequency ($\times\pi$ rad/sample) (0 to 1.0). Mainlobe width (-3dB): 0.039063. Relative sidelobe attenuation: -42.5 dB. Leakage Factor: 0.03 %.</p>
Hanning	 <p>Time domain: Amplitude vs. Samples (0 to 60). Amplitude follows a smooth bell-shaped curve peaking at 1.0.</p> <p>Frequency domain: Magnitude (dB) vs. Normalized Frequency ($\times\pi$ rad/sample) (0 to 1.0). Mainlobe width (-3dB): 0.042969. Relative sidelobe attenuation: -31.5 dB. Leakage Factor: 0.05 %.</p>
Gaussian	 <p>Time domain: Amplitude vs. Samples (0 to 60). Amplitude follows a smooth bell-shaped curve peaking at 1.0.</p> <p>Frequency domain: Magnitude (dB) vs. Normalized Frequency ($\times\pi$ rad/sample) (0 to 1.0). Mainlobe width (-3dB): 0.039063. Relative sidelobe attenuation: -43.2 dB. Leakage Factor: 0.01 %.</p>

After determining the type of window that yielded the best performance, several window lengths were tested (32 ms, 64 ms, 128 ms, and 256 ms) [9,70] all of them with an overlap of 50% of the samples.

3.3.1.3 De-noising Algorithm and Mother Wavelet Selection

For de-noising applications, it is often necessary to search for the optimal minimum mean squared error (MSE). In this study, a multisignal de-noising algorithm, consisting of a wavelet shrinkage method using Stein's unbiased risk estimate (SURE) [92], was applied to each of the EMG windowed segments before feature extraction. This algorithm uses wavelet decomposition and attempts to reject noise by damping or thresholding in the wavelet domain. Reconstruction of the signal is made by selecting only a subset of the wavelet coefficients [93,94].

The wavelet shrinkage method relies on the basic idea that the energy of a function will often be concentrated in a few wavelet coefficients while the energy of noise is spread among all the coefficients; therefore, in the wavelet domain, the nonlinear thresholding function will tend to keep coefficients representing the function, and noise coefficients will tend to reduce to zero. By assumption, the noise is regarded as a random variable. The scalar product between the noise and the wavelet functions generate weak wavelet coefficients because the noise is uncorrelated to the wavelet. On the other hand, the scalar product between the EMG signals and the wavelet functions must generate greater wavelet coefficients because of the correlation that exists between them. The difficulty relies on determining the value of the threshold to apply between low and strong coefficients. The basic steps in wavelet shrinkage methods consist in first applying the DWT to the signal and obtaining the wavelet coefficients; afterwards, a threshold value that minimizes the mean-squared error (MSE) is obtained with simulated signal, and the nonlinear soft-threshold function is applied to the wavelet coefficients at each scale in order to remove those coefficients that are smaller than the threshold.

Finally, the inverse DWT is applied on the thresholded wavelet coefficients to obtain the estimate of the function [95-97].

As a consequence of the orthogonality of the DWT, white noise is transformed into white noise in the wavelet domain. Hence, the wavelet coefficients of a noisy sample are just noisy versions of the noiseless wavelet coefficients [98].

Wavelet shrinkage has proved to be an efficient noise cancelling technique. Applied to EMG, it has enabled to extract the bursting and sustained activity by reconstructing signals with few non-zero coefficients according to a predetermined threshold [96]. A basic model for compound EMG signal [96] can be defined as shown in (3.2), where f is the signal of rhythmic bursting activity and z is a Gaussian white noise. The objective is to recover f by suppressing the noise, which can be achieved by optimizing the MSE in (3.3) between the estimated \hat{f} and the true f .

$$EMG = f + z \quad (3.2)$$

$$E\|\hat{f} - f\|^2 \quad (3.3)$$

The Stein's unbiased risk estimate is an adaptive threshold selection rule that minimizes the mean squared risk by determining a threshold level for the detail coefficients at each scale. For a model of white noise with a variance different to 1, the thresholds need to be rescaled by the SD of the noise estimated from the first level of decomposition. However, if the noise is unlikely to be white noise and distributes unevenly across scales, the SD of noise is estimated level by level, and thus the threshold is adaptively rescaled [96]. Based on the fact that sEMG signals contain crosstalk from nearby muscles, motion artifacts, inherent noise from the electronic equipment, noise from the skin-electrode interface, among other interferences previously explained in chapter II,

the noise was not assumed as pure white Gaussian noise. Therefore, rescaling of the threshold values in the de-noising algorithm implemented for this study was made based on a level dependent estimation of noise. The de-noising is applied scale by scale if the noise power spectral density is not constant; i.e., white noise. Wang *et al.* concluded in [96] that the optimal performance for separating the bursting and sustained activity from the compound sEMG is obtained by combining the SURE principle with non-white noise model.

Certain wavelet functions closely resemble the motor unit action potentials that constitute the MES [25]; therefore, they have been widely applied for EMG analysis. In order to choose the mother wavelet that yielded the best performance for the wavelet shrinkage de-noising algorithm, both a fourth order Coiflet (coif4) and a fourth order Daubechies (db4) mother wavelets were tested. This was made calculating the correlation coefficients between the original signals and the ones reconstructed from the coefficients extracted at each level of decomposition. These two wavelets have been previously applied for EMG classification by different authors [2,9,19,25,27,53,96]. The coif4 mother wavelet yielded better results and was therefore selected.

Coiflets have properties of (1) orthogonal transform, (2) compact support, and (3) highest number of vanishing moments. They have near zero phase properties. This avoids significant phase shift between the raw and decomposed signals. One of the reasons why they outperform Daubechies wavelet filters is that the latter have non-linear phase properties [96].

Since the information channel of the sEMG signal goes from 10-500 Hz, but the main concentration of energy is located within the frequency band of 50-150 Hz [2,18], the signal was decomposed until the third level. The corresponding frequency components are shown in TABLE 2.1.

3.3.2 Feature Extraction

Features were extracted in both the time and frequency domains using different methods that will be explained in this section. The present study is focused on the transient state analysis of the EMG signal; however, some of the latter explained methods were tested as well on the steady state for comparison purposes.

The use of Hjorth's descriptors for multichannel sEMG classification is a novel proposal; therefore, the signals were analyzed using other methods based on the DWT in order to compare performance. The DWT has been widely applied to EMG analysis and classification; nonetheless, the method concerning extraction of the variance from the wavelet coefficients is also a new proposal.

3.3.2.1 Hjorth's Parameters

The three Hjorth's parameters, namely 'Activity', 'Mobility', and 'Complexity', were calculated along the eight EMG channels for each window of the previously de-noised signals.

The performance of the algorithm for classification of the sEMG signals was initially tested using the three parameters, and later on using the three possible combinations of two parameters 'Activity + Mobility', 'Activity + Complexity', and 'Mobility + Complexity'.

Fig. 3.6 explains the way in which the feature matrix was created to feed the classifier. This was made for each subject individually. Every extracted parameter was normalized for each of the movements. This method was tested for both the transient and steady states of the EMG signals.

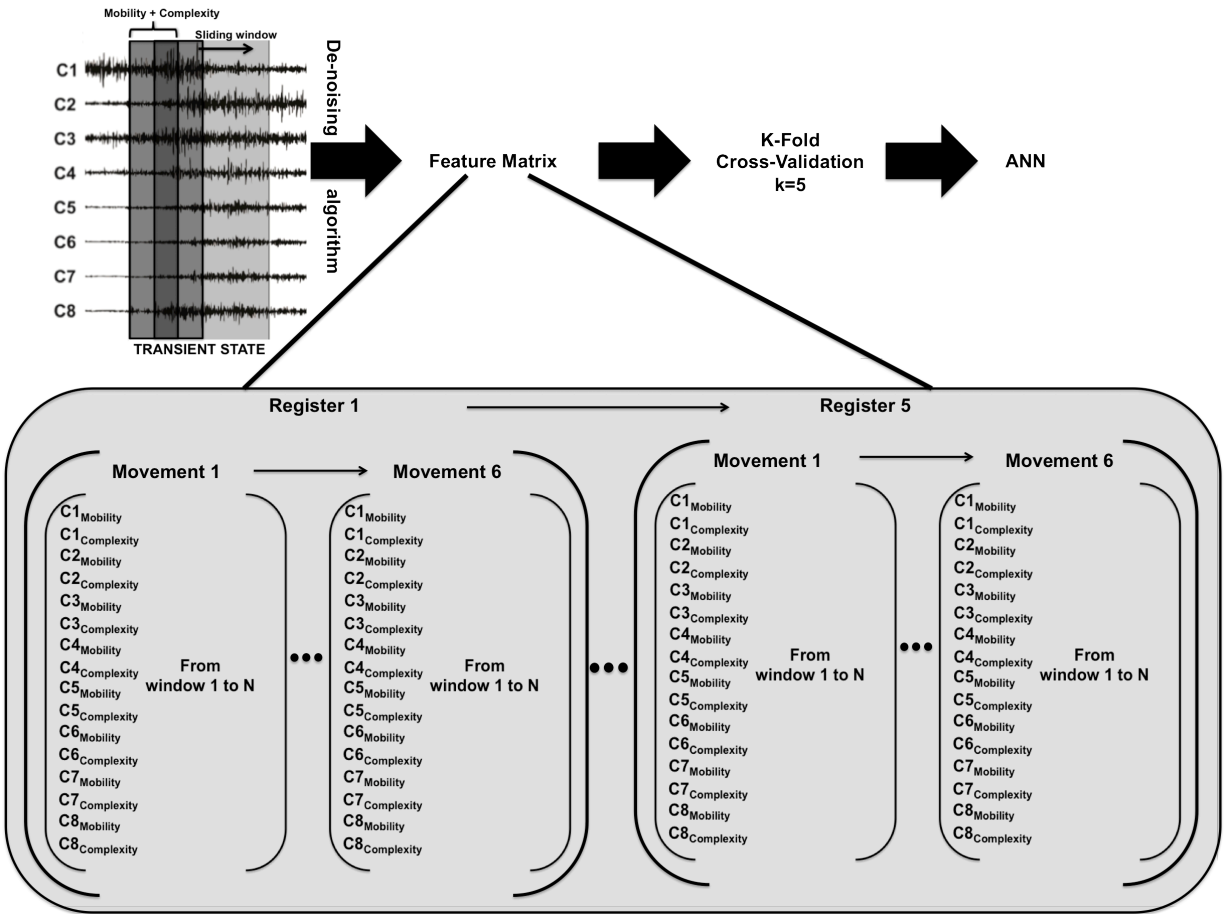


Fig. 3.6. Diagram of the method using Hjorth's parameters. In the initial part of the image, a sliding window is applied to the transient state of the EMG signal. This part of the signal is de-noised and the corresponding parameters are calculated afterwards. The feature matrix in the middle shows the way in which the extracted parameters from each of the windows are arranged to feed the classifier. 'Mobility' and 'Complexity' parameters from each channel are arranged by rows. K-fold cross-validation with $k=5$ is applied to the feature matrix, and the result is fed into the ANN classifier.

3.3.2.2 DWT's Variance

This method consisted in feeding the ANN classifier using a feature matrix created from the variance of the wavelet coefficients. Once the signal was windowed and the wavelet shrinkage algorithm at level 3 of decomposition using a fourth order Coiflet mother wavelet was applied to each of the windows, the variance was calculated from the detail coefficients of the second and third levels of decomposition. The values of the variance

for both decomposition levels were normalized for each of the movements and were used to build the feature matrix. This was made individually per subject. The previously explained method was tested in both the transient and steady states of the EMG signal.

The variance was used as an approach to preserve the tendency of the wavelet coefficients but reducing the size of the feature matrix. The general diagram describing this method can be seen in Fig. 3.7.

In order to decide from which coefficients extract the variance to create the feature matrix, several combinations were tested. These combinations included the variances from the detail coefficients of the first three levels of decomposition and the approximation coefficients of the third level; however, the aforementioned combination (variance of detail coefficients from second and third levels of decomposition) proved to have a better performance than every other tested combination.

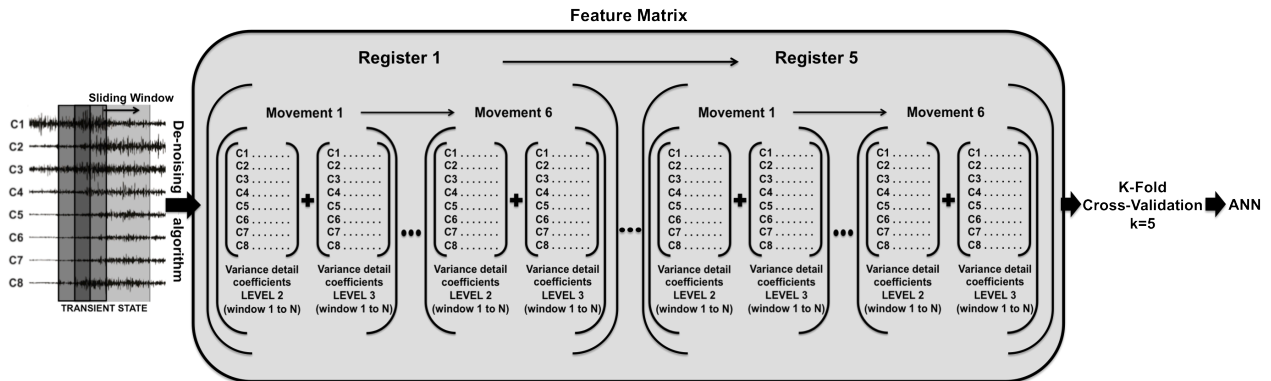


Fig. 3.7. Diagram of the method using the variance of wavelet coefficients. In the initial part of the image, a sliding window is applied to the transient state of the EMG signal. This part of the signal is de-noised using a wavelet shrinkage algorithm and the wavelet coefficients are extracted. The feature matrix in the middle is created by calculating the variance of the detail coefficients at level 2 and 3 of decomposition for each channel. K-fold cross-validation with $k=5$ is applied to this feature matrix, and the result is fed into the ANN classifier.

3.3.2.3 DWT Using PCA

This third method was only tested on the transient state of the EMG signals. The procedure that was followed is described in Fig. 3.8, and it is similar to the one proposed in [9,27,69,70].

In order to create the feature matrix, the wavelet coefficients from the first three levels of decomposition (details from the first to the third levels and approximations from the third level) were extracted for each of the movements after the de-noising algorithm was applied to the windowed segment of the signal. PCA was applied afterwards to reduce the dimension of the data, and the resulting matrix was used to feed the ANN classifier. K-fold cross-validation with $k=5$ allowed dividing the data in training and testing sets.

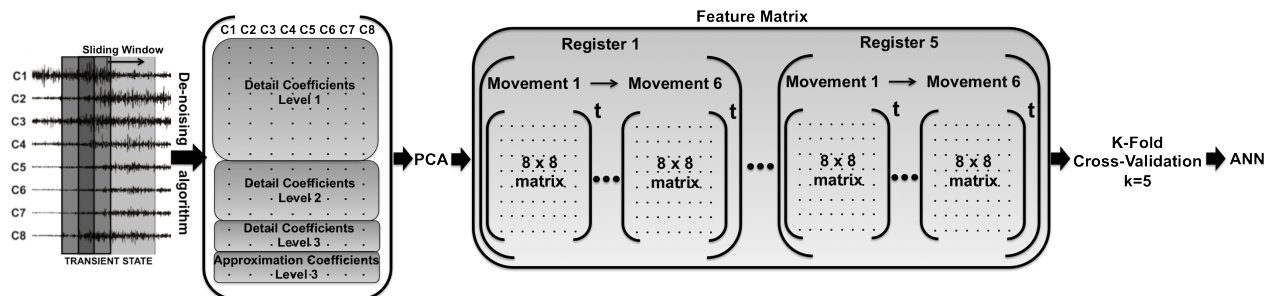


Fig. 3.8. Diagram of the method of DWT using PCA. In the initial part of the image, a sliding window is applied to the transient state of the EMG signal. This part of the signal is de-noised using a wavelet shrinkage algorithm, and the wavelet coefficients are extracted from detail levels 1 to 3 and approximation level 3 for each of the movements. PCA is applied in order to reduce data dimensionality, and the resulting matrix of principal components is transposed and joined with those from the other movements creating the feature matrix in the middle. K-fold cross-validation with $k=5$ is applied to this feature matrix, and the result is fed into the ANN classifier.

3.3.3 Artificial Neural Network Model

To build the classifier models, different ANNs were constructed according to the EMG state under analysis and the method selected for feature extraction. Final architecture depended on the available feature matrix. The number of neurons in the hidden layer established for each of the models was determined based on experimental testing. The characteristics for each model are presented in TABLE 3.4.

TABLE 3.4
FINAL ANNS' ARCHITECTURE

Model Type	EMG State	Neurons on the Hidden Layer	Output	Training Algorithm
Hjorth's Parameters	Transient	9	Binary codified	'trainbr**
	Steady	9	Binary codified	'trainbr**
DWT's Variance	Transient	10	Binary codified	'trainbr**
	Steady	10	Binary codified	'trainbr**
DWT using PCA	Transient	15	Binary codified	'trainbr**

**TRAINBR' is Bayesian Regulation Backpropagation Algorithm

The models were trained individually for each of the subjects based on the fact that the exact form and execution of the contraction types is subject dependent. Previous works, such as the one in [6], have not attempted to compare data across subjects. As a means to validate this, an essay to classify subjects' data using a model trained with the recordings obtained from another one was made. The performance was low for most of the subjects; therefore, this effort was abandoned, and the models were trained individually. However, some movements were indeed correctly classified which suggests that a similar structure exists.

Every ANN model in this study was trained using a Bayesian regulation backpropagation algorithm ('TRAINBR'), which is a useful algorithm when there is not a big amount of

information available because only two data sets are needed: training and testing sets. Other training algorithms were evaluated, but the best performance was achieved with the one previously mentioned.

The network's output was binary codified. Three neurons were used in order to generate the necessary combinations to codify the six different movements.

3.3.3.1 K-Fold Cross-Validation

In order to evaluate the ANN's performance, k-fold cross-validation ($k=5$) process was carried out. This assures the randomness of the windows selected for training and testing, which helps proving the robustness of the classifier and avoids overfitting of the model.

The size of the training set n_t is determined as shown in (3.4), where n is the number of samples in the complete data set [55]. The remaining samples are used for testing. The process is repeated k times. This procedure is useful when data sets are not very large.

$$n_t = n \left(\frac{(k-1)}{k} \right) \quad (3.4)$$

The data sets obtained from these partitions were used to feed the ANN classifier.

3.3.4 Algorithm's Tolerance to Additive White Gaussian Noise

In order to test the algorithm's robustness, the tolerance of the classifier to additive white Gaussian noise (AWGN) was tested. White Gaussian noise has uniform power across

the frequency band; thus, it allows simulating the effect of many random processes that occur in nature. In the time domain, it presents a normal distribution and an average value of zero.

Due to the fact that there was not a big amount of information available per subject for each of the movements, new registers were created by averaging the available ones. These registers were contaminated with AWGN by the procedure subsequently described:

- The signal power (P_s) was calculated as indicated in (3.5), where N is the total number of samples. The value was converted to dB using equation (3.6).

$$P_s = \frac{1}{N} \sum_{n=1}^N |x(n)|^2 \quad (3.5)$$

$$P_{s_{dB}} = 10 \log_{10} P_s \quad (3.6)$$

- The SNR was calculated according to the desired percentage of noise, n_p , as shown in equation (3.7). The value of n_p is given in decimals.

$$SNR_{dB} = 10 \log_{10} \left(\frac{1}{n_p} \right) \quad (3.7)$$

- The noise power (P_n) was later calculated by subtracting the SNR from the signal power as it appears in equation (3.8).

$$Pn_{dB} = Ps_{dB} - SNR_{dB} \quad (3.8)$$

- Finally, the white Gaussian noise was calculated according to the noise power obtained from (3.8) using the MATLAB® function 'wgn'. This was added to the signal created from the averaged registers in order to create a new contaminated register that allowed testing the classifier's robustness.

The noise calculation and signal contamination were made for each window considering that in an on-line application, contamination affects the recorded segment over which the analysis is being made, and the rest of the signal does not exist at that instant of time. The signal's power was calculated per channel; therefore noise was calculated proportionally to each channel's power and added to achieve the desired percentage in all of them.

3.3.5 Virtual Hand Model

The virtual hand model used for testing the algorithm is shown in Fig. 3.9. This model was developed by Barraza [84,99,100] and later used by Leon in [90].

The model was created using the MATLAB® virtual reality tool (V-Realm Builder 2.0). The general functioning of the algorithm is based in calculating the angular displacement needed to reach from an actual position to an objective one.

A table was built with the values of the angles for the wrist and the finger's phalanges that the model had to take in order to reach the desired positions as seen in Fig. 3.9. These values were determined experimentally by manipulating the model.

The virtual model changes from one position to another in a fixed number of steps that can be changed by software in order to give a more paused or rapid appearance to the movement.

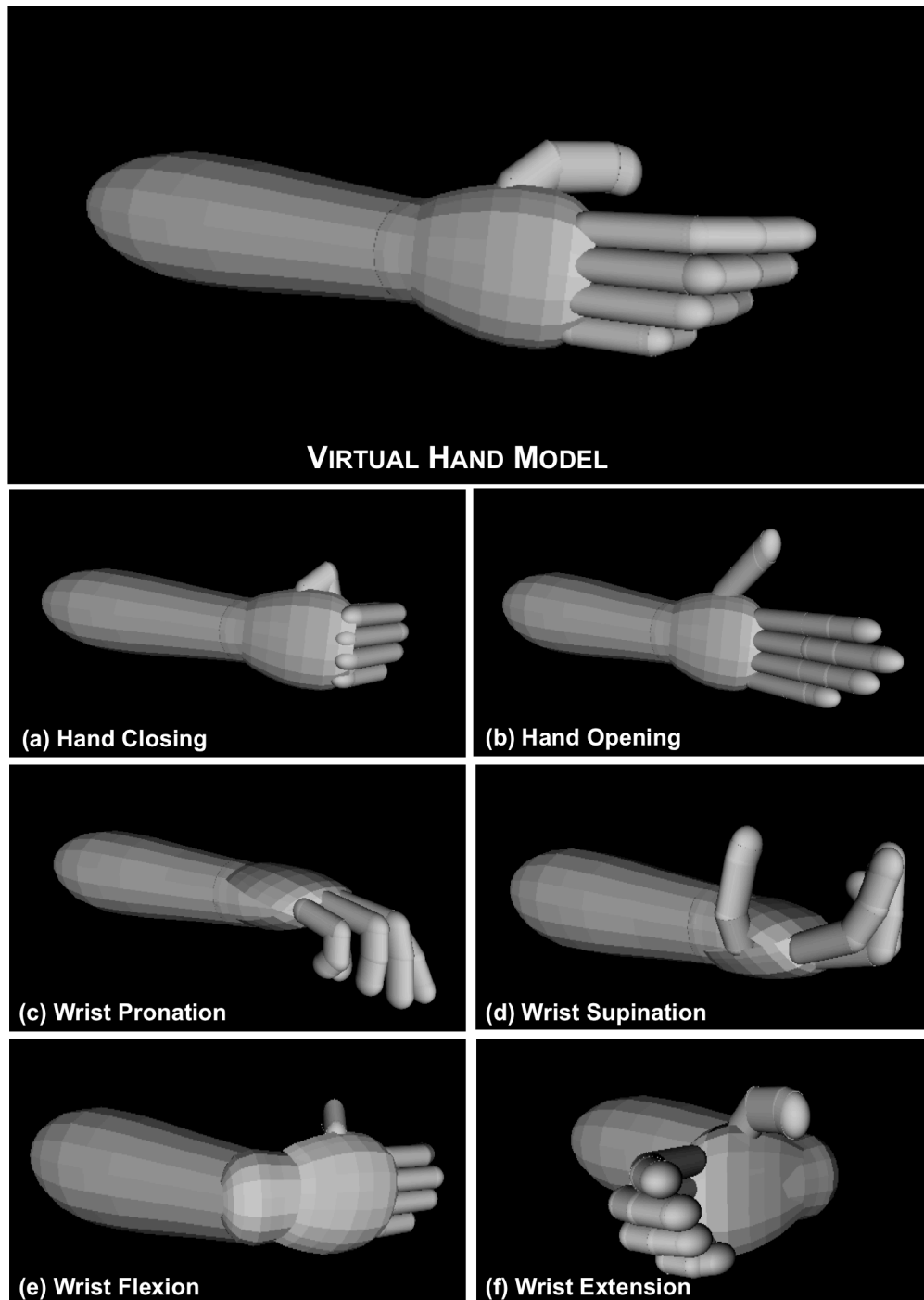


Fig. 3.9. Different hand motions represented in the virtual hand model.

Results

4.1 Overview

The results obtained for the methods described in the previous chapter will be presented in this section and will be later discussed on Chapter V.

The general definition of the system's variables was based on the method consisting of the transient state analysis using Hjorth's parameters. All the variables are essential to the system's performance and assigning a hierarchy of how they should be defined is complicated. Therefore, every time that one of them was established, the joint system was tested.

The parameters that were defined for the method using Hjorth's descriptors were later evaluated for every other method (DWT's variance and DWT using PCA) in order to ensure as much as possible similar conditions between processing time, model complexity, and classification accuracy. Some individual elements, such as the number of neurons in the hidden layer as will be later mentioned, were adjusted individually for each method.

In order to start processing the signals, it was essential to study their properties in both time and frequency domains to be able to decide which techniques were more suitable for their analysis. The following information gives a general idea of the basic properties of these signals.

Fig. 4.1 gives an example of a segment of the multichannel raw EMG signal recorded from one of the subjects during an extension and indicates how the segments were separated in order to be processed as transient and steady states, respectively. The first shadowed region covers the transient state of the signal and corresponds to the dynamic part of the contraction in which the fiber lengths are modified while the subject is executing the movement. The second shadowed region is placed over a portion of the steady state. In this part of the signal, the subject has already reached the final position and holds the contraction. Here, the fiber lengths remain constant. Before the contraction was initiated, the subject maintained the limb in an inactive position; however, it is possible to appreciate the presence of noise, specially, in channels 4 to 8, which complicates processing. A set of signals as the one presented in this example constitutes the database used for the study.

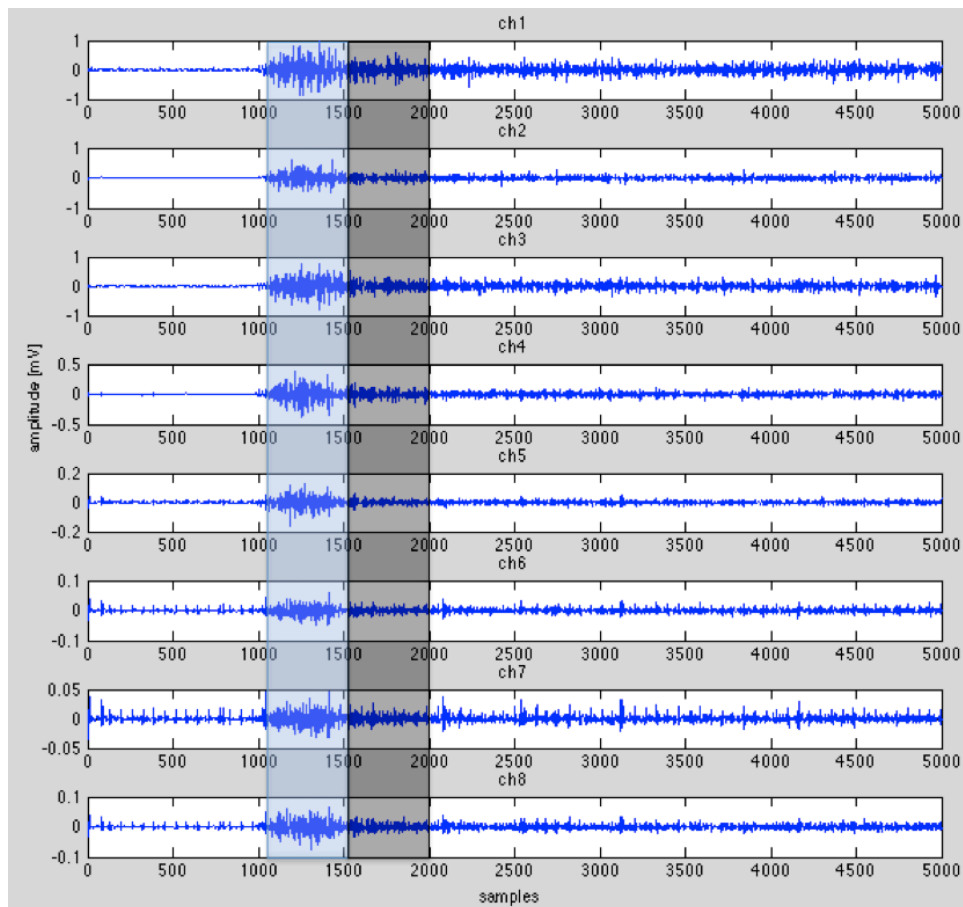


Fig. 4.1. Multichannel raw EMG signal of wrist extension. The first shadowed region covers the transient state of the signal, and the second one corresponds to the steady state.

The same movement for the same subject is again shown in Fig. 4.2; however, in this figure, the FFT for each channel was calculated and presented next to the original signal. The first four channels have higher amplitude values than the last four. In the same way, the magnitude of the frequency spectrum of these channels is significantly weaker than that of the first four, which are all associated to extensor muscles as previously shown in TABLE 3.2 and Fig. 3.3. The shadowed portion of the FFT shows the frequency components comprised within the first three levels of wavelet decomposition as denoted in TABLE 2.1.

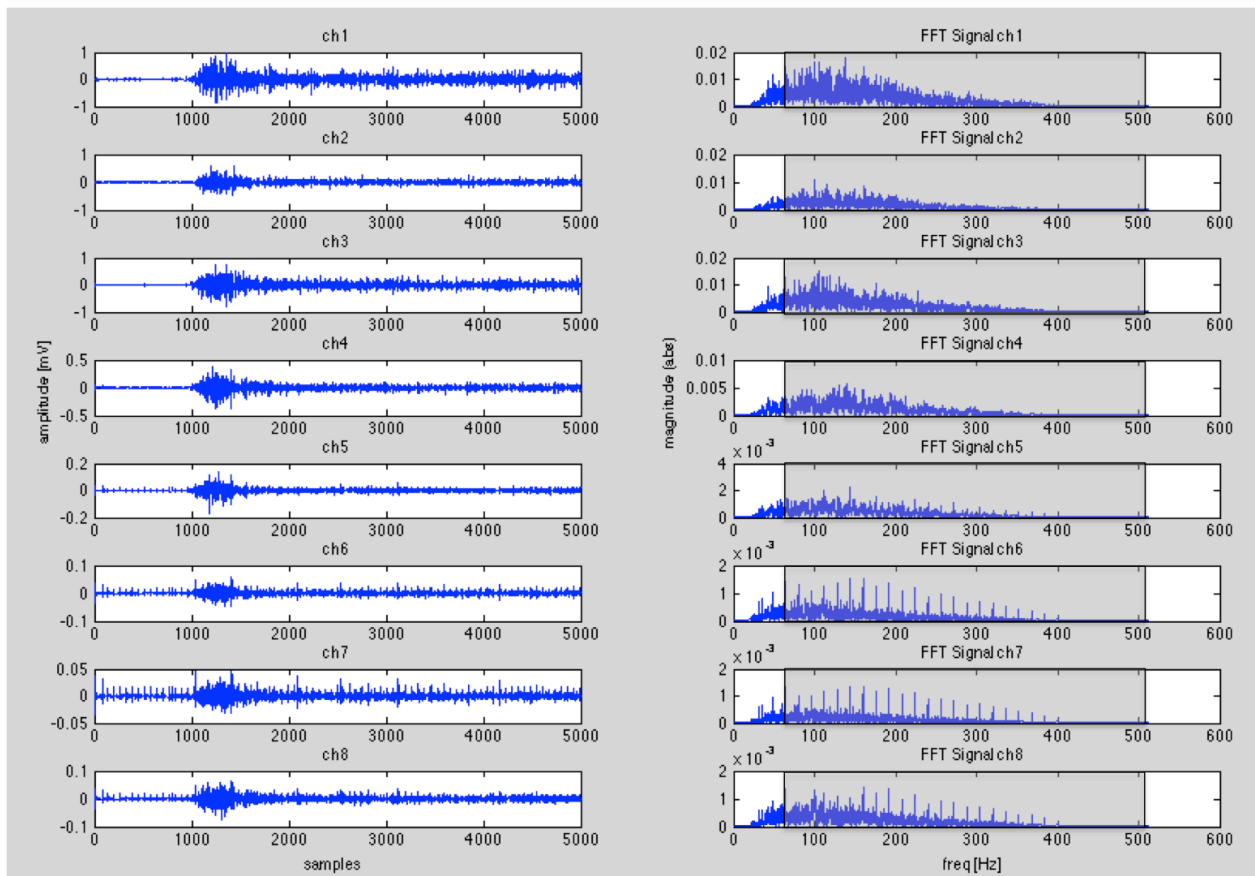


Fig. 4.2. Raw multichannel EMG signal of wrist extension and its FFT. The shadowed portion of the FFT for each channel represents the frequency band comprised within the first three levels of wavelet decomposition of the signal.

Moreover, the information contained in the frequency components for every level of wavelet decomposition can be obtained by calculating the corresponding FFT. Fig. 4.3 shows an example for channel 4 of the extension movement. The first column contains the transient segment and the coefficients of the first three levels of decomposition; the third column has the equivalent information for the steady state. The second and fourth columns present the FFTs of the original signals and of each of the wavelet decomposition levels. This allows corroborating their corresponding frequency band.

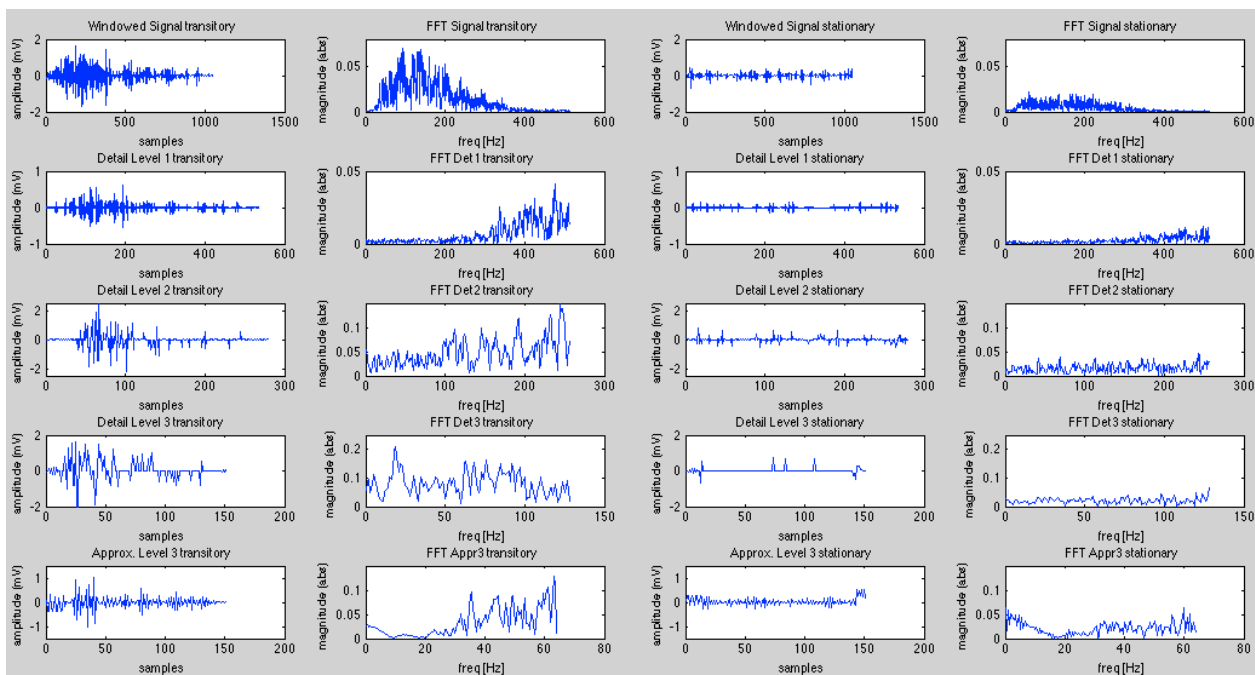


Fig. 4.3. De-noised EMG segment and corresponding frequency components. A DWT at third level of decomposition using a ‘coif4’ mother wavelet was applied to each segment of the signal. The first column shows, in the first row, the de-noised transient segment of the extension movement for channel 4. The second, third, and fourth rows contain the detail coefficients of the first three levels of decomposition. The fifth row corresponds to the approximation coefficients of the third level. The second column illustrates the corresponding frequency components obtained from the FFT. Columns three and four are the equivalent for the steady segment of the signal.

4.2 Hjorth's Parameters

In order to start using Hjorth's parameters as possible means to analyze and classify EMG signals, the window type and length for signal analysis was determined. These results are presented below.

4.2.1 Selection of Window Parameters

In order to analyze the data, it was essential to define an appropriate window for feature extraction. Both window type and length were chosen according to the following results.

4.2.1.1 Window Type

Four window types, previously mentioned in TABLE 3.3, were tested. The results are presented in Fig. 4.4 and Fig. 4.5. The first one contains the mean classification percentage of the 21 test subjects for each of the movements, while the second one shows the mean error percentage considering the six movements.

The test to select the most appropriate window type for this application was performed using the data from the transient EMG state and a window length of 128 ms. Hjorth's parameters were the features extracted from each window.

Finally, TABLE 4.1 gathers the information of the mean classification percentage and SD according to the window type for each of the movements. Based on the obtained results, the Hamming window was selected as the one yielding the best classification performance and the lowest SD for the whole sample. It was used in all the latter tests.

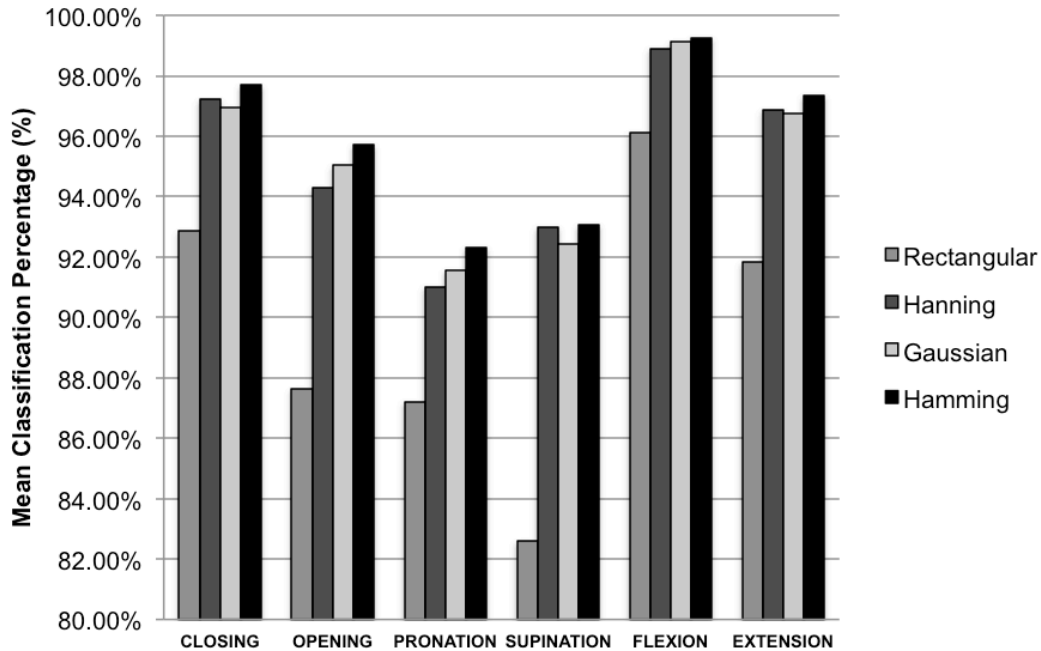


Fig. 4.4. Mean classification percentage depending on window type. This figure shows the mean classification percentage for the 21 subjects that participated in the study according to the selected window type. The test was done over the transient EMG segment using Hjorth's parameters and a window length of 128 ms.

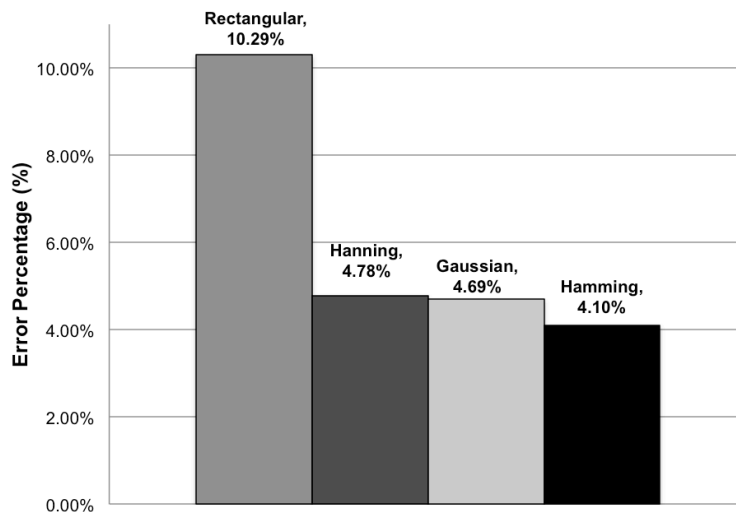


Fig. 4.5. Mean error percentage for window type selection. The error percentage is calculated from the mean classification of the six movements for the whole sample of 21 subjects. Hjorth's parameters and a window length of 128 ms were used over the transient EMG segment.

TABLE 4.1
MEAN CLASSIFICATION PERCENTAGE AND SD ACCORDING TO WINDOW TYPE

WINDOW TYPE	MOVEMENT						
	Closing	Opening	Pronation	Supination	Flexion	Extension	Mean
Rectangular	92.86±5.31%	87.62±9.14%	87.21±7.86%	82.59±8.14%	96.12±2.75%	91.84±4.70%	89.71±4.01%
Hanning	97.21±2.32%	94.29±4.72%	91.02±6.73%	92.99±6.92%	98.91±1.68%	96.87±3.15%	95.22±3.09%
Gaussian	96.94±2.13%	95.03±4.88%	91.56±5.77%	92.45±6.73%	99.12±1.24%	96.73±3.04%	95.31±3.04%
Hamming	97.69±2.14%	95.71±4.02%	92.31±5.41%	93.06±6.46%	99.25±1.16%	97.35±3.01%	95.90±2.56%

4.2.1.2 Window Length

Classification performance was tested using different window lengths. An overlap of 50% of the samples was maintained for every case. Shorter window lengths are desirable in order to obtain faster responses from the devices; however, it is harder to extract significant information from them. Without considering the processing time of the system, windows of less than 300 ms are suitable for real-time applications [6,9,10]. Fig. 4.6 and TABLE 4.2 show classification percentage for the transient EMG state depending on window length. Fig. 4.7 and TABLE 4.3 are the equivalent for the steady state. The comparison between the influence of window length in classification percentage for each of the EMG states is shown in Fig. 4.8 and TABLE 4.4.

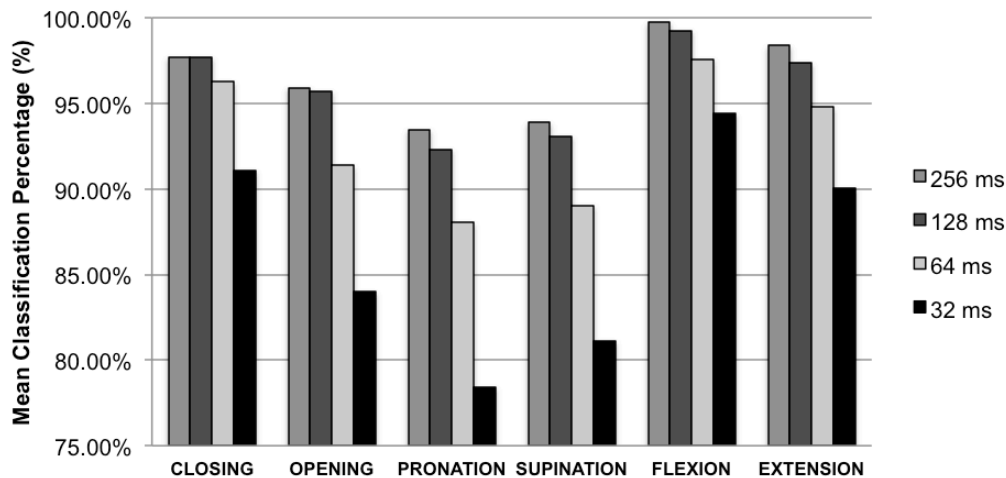


Fig. 4.6. Mean classification percentage of the transient EMG state depending on window length. This was tested using a Hamming window with an overlap of 50% of the samples.

TABLE 4.2
MEAN CLASSIFICATION PERCENTAGE AND SD FOR TRANSIENT EMG ACCORDING TO WINDOW LENGTH

WINDOW LENGTH [ms]	MOVEMENT						
	Closing	Opening	Pronation	Supination	Flexion	Extension	Mean
256	97.69±2.65%	95.92±4.20%	93.47±5.80%	93.88±5.59%	99.73±0.86%	98.37±1.93%	96.51±2.24%
128	97.69±2.14%	95.71±4.02%	92.31±5.41%	93.06±6.46%	99.25±1.16%	97.35±3.01%	95.90±2.56%
64	96.25±3.35%	91.37±6.42%	88.03±6.15%	89.05±7.70%	97.59±2.53%	94.79±4.30%	92.85±4.00%
32	91.07±2.91%	83.99±5.89%	78.42±8.03%	81.10±6.13%	94.39±2.79%	90.04±3.99%	86.50±3.44%

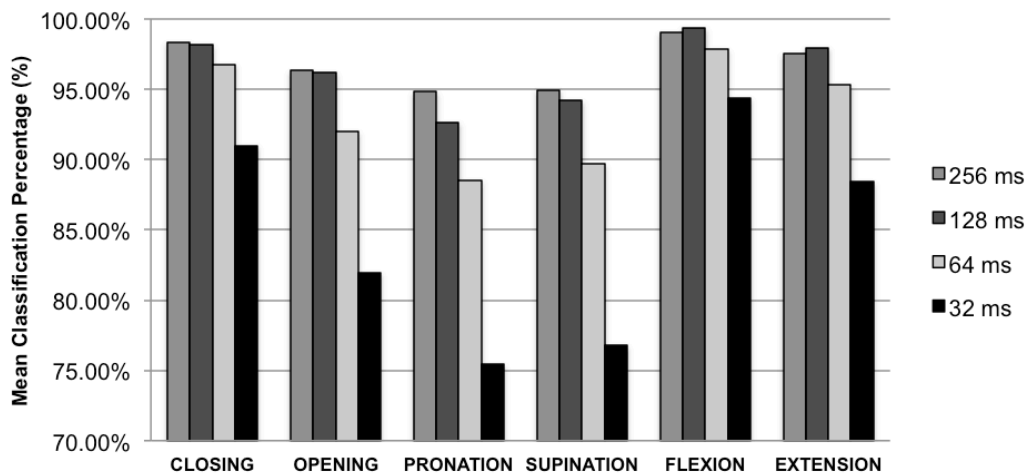


Fig. 4.7. Mean classification percentage of the steady EMG state depending on window length. This was tested using a Hamming window with an overlap of 50% of the samples.

TABLE 4.3
MEAN CLASSIFICATION PERCENTAGE AND SD FOR STEADY EMG ACCORDING TO WINDOW LENGTH

WINDOW LENGTH [ms]	MOVEMENT						
	Closing	Opening	Pronation	Supination	Flexion	Extension	Mean
256	98.37±2.80%	96.33±4.96%	94.83±5.90%	94.97±4.94%	99.05±1.65%	97.55±4.45%	96.85±2.29%
128	98.16±2.56%	96.19±3.24%	92.65±6.00%	94.22±5.37%	99.39±1.24%	97.96±1.78%	96.43±2.21%
64	96.79±2.77%	92.00±6.73%	88.54±6.65%	89.71±6.32%	97.84±1.76%	95.30±3.86%	93.37±3.66%
32	91.01±5.26%	81.93±5.92%	75.43±7.44%	76.77±7.34%	94.40±3.26%	88.42±4.95%	84.66±3.44%

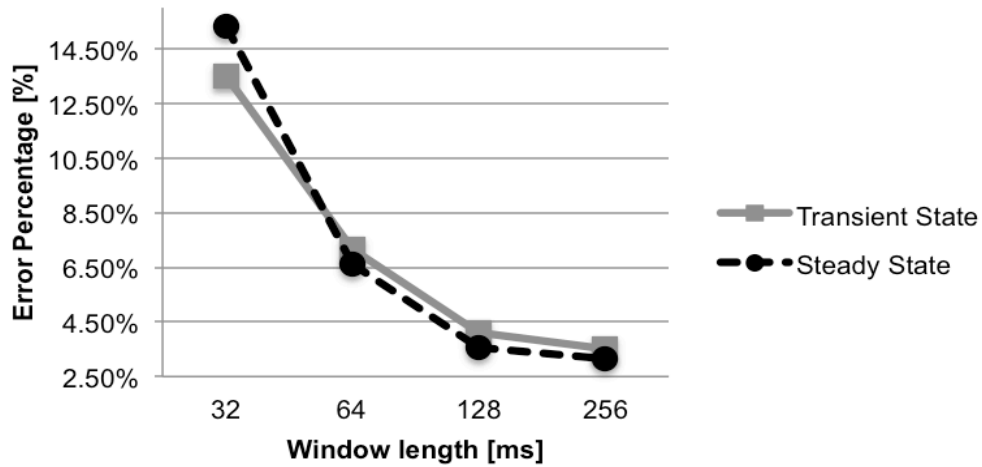


Fig. 4.8. Mean error percentage in classification performance depending on window length for transient and steady EMG states. The error is calculated from the mean classification percentage of the six movements for the 21 test subjects.

TABLE 4.4
COMPARISON OF MEAN ERROR PERCENTAGE AND SD FOR TRANSIENT AND STEADY EMG STATES ACCORDING TO WINDOW LENGTH

WINDOW LENGTH [ms]	EMG STATE	
	Transient	Steady
256	3.49±2.24%	3.15±2.29%
128	4.10±2.56%	3.57±2.21%
64	7.15±4.00%	6.63±3.66%
32	13.50±3.44%	15.34±3.44%

4.2.2 Neuron Number Selection

Both 256 ms and 128 ms Hamming window lengths yielded good classification performance; therefore, the number of neurons in the hidden layer of the model was defined by comparing classification performance of transient EMG segment using a 256 ms Hamming window with 50% sample overlap and extracting Hjorth's parameters as features for classification. The results obtained are shown in Fig. 4.9 and TABLE 4.5.

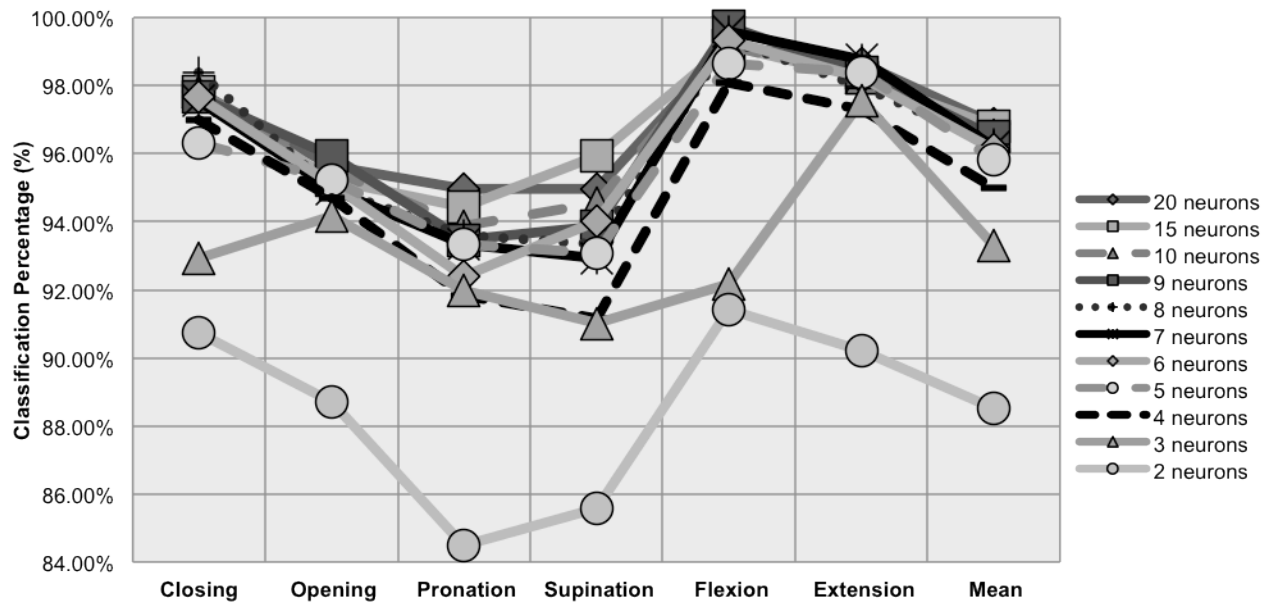


Fig. 4.9. Classification performance according to the number of neurons in the hidden layer of the ANN.

TABLE 4.5
CLASSIFICATION PERFORMANCE RELATED TO THE NUMBER OF NEURONS IN THE HIDDEN LAYER OF THE ANN

Number of Neurons	Closing	Opening	Pronation	Supination	Flexion	Extension	Mean	SD
20	97.82%	95.65%	94.97%	94.97%	99.18%	98.64%	96.87%	2.00%
15	97.82%	95.24%	94.42%	95.92%	99.18%	98.23%	96.80%	2.34%
10	97.82%	95.51%	93.88%	94.56%	99.18%	98.23%	96.53%	2.19%
9	97.69%	95.92%	93.47%	93.88%	99.73%	98.37%	96.51%	2.24%
8	98.37%	94.97%	93.61%	93.33%	99.32%	97.96%	96.26%	2.42%
7	97.55%	94.97%	93.33%	92.93%	99.59%	98.78%	96.19%	2.99%
6	97.69%	95.10%	92.38%	94.01%	99.32%	98.23%	96.12%	2.17%
5	96.33%	95.24%	93.33%	93.06%	98.64%	98.37%	95.83%	2.41%
4	97.01%	94.69%	91.83%	91.16%	98.10%	97.28%	95.01%	3.11%
3	92.93%	94.15%	91.97%	91.02%	92.18%	97.55%	93.30%	4.59%
2	90.75%	88.71%	84.49%	85.58%	91.43%	90.20%	88.53%	5.75%

The selected number of neurons for the hidden layer of the ANNs was adjusted for each of the methods. Nine, ten, and fifteen neurons were selected respectively for Hjorth's parameters, DWT's variance, and DWT using PCA methods, as the ones that allowed a

good balance between the model's complexity, the training time, and the classification performance (see TABLE 3.4).

4.2.3 Hjorth's Parameters Selection

Finally, the last parameter to define was the number of Hjorth's descriptors to be included in the feature matrix. Every possible combination between Hjorth's parameters was tested in order to find the one that performed the best. Previous studies [33,36,38,41], related to EEG signal analysis, have already reported to use just two of Hjorth's parameters or to find significant changes in just two of them, mainly Mobility and Complexity. The classification performance obtained from the different combinations of Hjorth's parameters used to build the feature matrix is shown in Fig. 4.10, and Fig. 4.11 illustrates the mean error for each method. The test was made over the transient EMG data using a 128 ms Hamming window with 50% overlap.

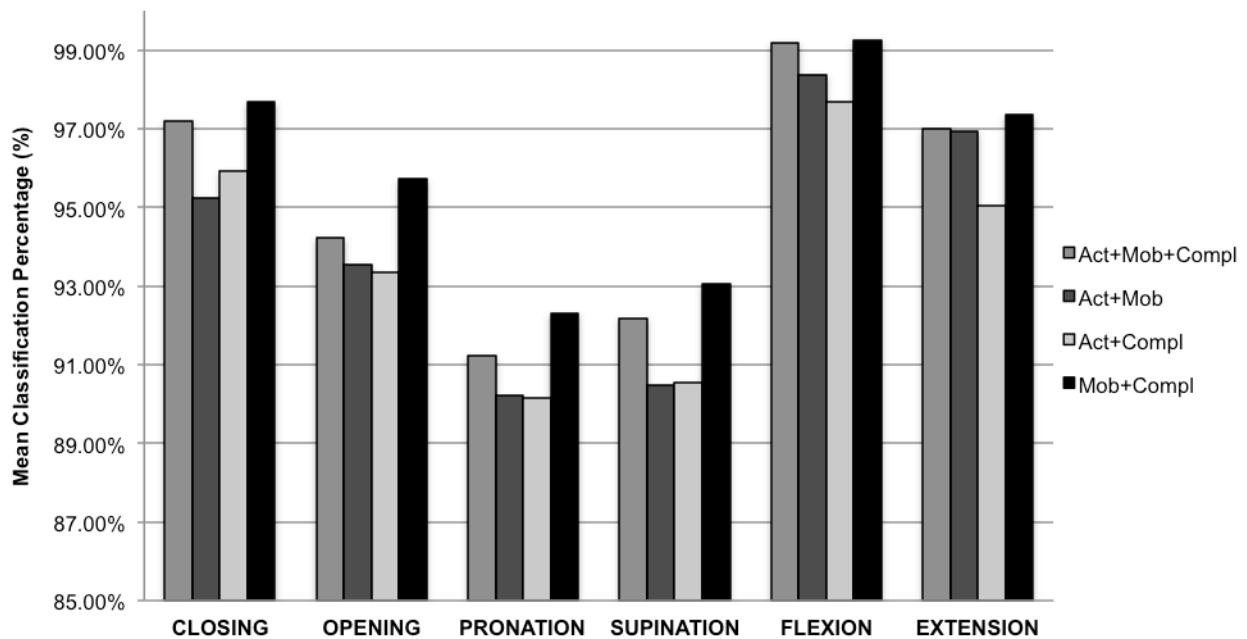


Fig. 4.10. Mean classification percentage according to the combination of Hjorth's parameters used to build the feature matrix. The test was conducted on the transient EMG state using a 128 ms Hamming window with 50% sample overlap.

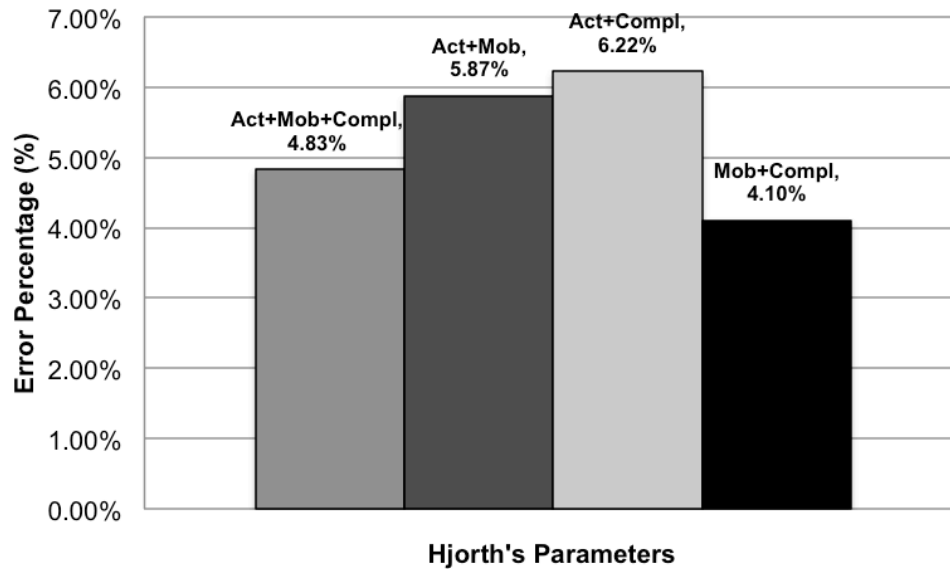


Fig. 4.11. Mean error percentage according to the combination of Hjorth's parameters used to build the feature matrix. The error is calculated from the mean classification percentage of the six movements for the 21 test subjects. The test was conducted on the transient EMG state using a 128 ms Hamming window with 50% sample overlap.

TABLE 4.6
MEAN CLASSIFICATION PERCENTAGE USING HJORTH'S PARAMETERS ARRANGED IN DIFFERENT FEATURE MATRIX SCHEMES

Hjorth's Parameters	MOVEMENT						Mean
	Closing	Opening	Pronation	Supination	Flexion	Extension	
Act+Mob+Compl	97.21±2.61%	94.22±5.85%	91.22±5.43%	92.18±6.85%	99.18±1.24%	97.01±2.71%	95.17±2.68%
Act+Mob	95.24±3.76%	93.54±4.60%	90.20±6.50%	90.48±7.09%	98.37±2.03%	96.94±3.36%	94.13±3.47%
Act+Compl	95.92±3.30%	93.33±5.81%	90.14±6.39%	90.54±6.59%	97.69±2.00%	95.03±4.11%	93.78±3.22%
Mob+Compl	97.69±2.14%	95.71±4.02%	92.31±5.41%	93.06±6.46%	99.25±1.16%	97.35±3.01%	95.90±2.56%

*Act = Activity, Mob = Mobility, Compl = Complexity

Based on the previous results, the feature matrix for this method was built using only Mobility and Complexity parameters, which performed the best as it can be appreciated in the last row of TABLE 4.6.

4.2.4 Transient Vs. Steady State Analysis

Englehart *et al.* [9] reported that steady state analysis considerably outperformed transient state analysis for EMG classification and suggested to discard its use in myoelectric controlled applications. As this is an important implication regarding the objective of the present study, the analysis was performed on both EMG states in order to corroborate this on the available data.

As both 128 and 256 ms window lengths were suitable for this method and can be applied in real-time applications, the test was repeated for each window length.

The classification performance of the transient and steady EMG states was computed and a comparison between them was made. Fig. 4.12 and TABLE 4.7 show the mean classification percentage for each of the subjects when using a 256 ms Hamming window with 50% overlap. The average classification percentages for each of the movements considering the whole test population, as well as the total mean, are shown in Fig. 4.13.

The same comparison procedure between the transient and state state using Hjorth's parameters was repeated with the 128 ms Hamming window with 50% overlap. The results are arranged in the same way that those for the 256 ms Hamming window, and can be found respectively in Fig. 4.14, TABLE 4.8, and Fig. 4.14.

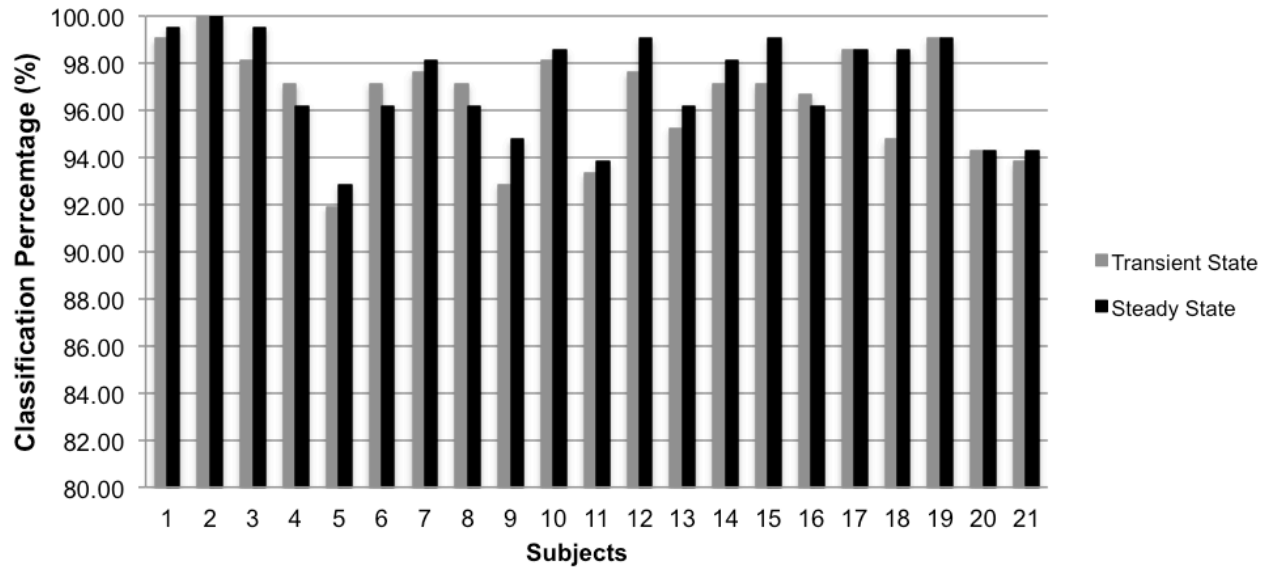


Fig. 4.12. Classification performance by subject for the transient and steady states using Hjorth's parameters and a window length of 256 ms.

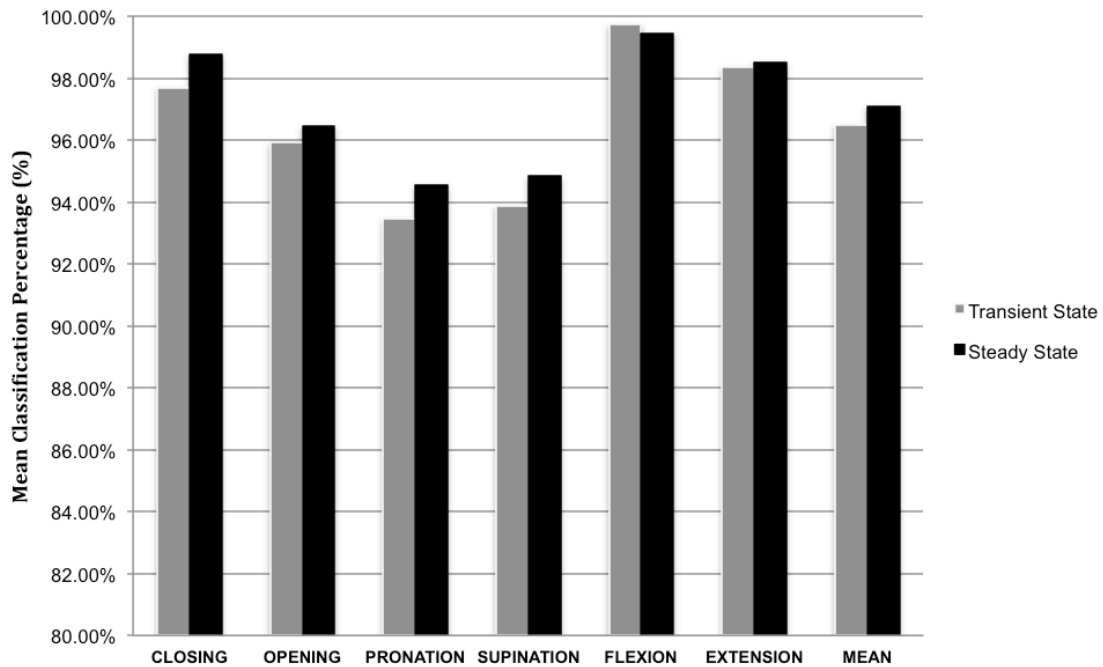


Fig. 4.13. Mean classification performance by movement for the transient and steady states using Hjorth's parameters and a window length of 256 ms.

TABLE 4.7
TRANSIENT VS. STEADY EMG CLASSIFICATION PERCENTAGE USING HJORTH'S PARAMETERS EXTRACTION FROM
A 256 MS HAMMING WINDOW

Subject	Closing		Opening		Pronation		Supination		Flexion		Extension	
	Trans.*	Steady	Trans.	Steady	Trans.	Steady	Trans.	Steady	Trans.	Steady	Trans.	Steady
1	100.00	100.00	100.00	100.00	97.14	97.14	97.14	100.00	100.00	100.00	100.00	100.00
2	100.00	100.00	100.00	100.00	100.00	100.00	100.00	100.00	100.00	100.00	100.00	100.00
3	97.14	100.00	97.14	97.14	97.14	100.00	97.14	100.00	100.00	100.00	100.00	100.00
4	97.14	97.14	97.14	97.14	100.00	97.14	88.57	88.57	100.00	100.00	100.00	97.14
5	97.14	100.00	82.86	82.86	91.43	88.57	82.86	88.57	100.00	100.00	97.14	97.14
6	94.29	100.00	100.00	94.29	97.14	91.43	91.43	91.43	100.00	100.00	100.00	100.00
7	100.00	100.00	97.14	97.14	100.00	94.29	91.43	100.00	100.00	100.00	97.14	97.14
8	100.00	100.00	100.00	94.29	88.57	91.43	97.14	91.43	100.00	100.00	97.14	100.00
9	97.14	97.14	97.14	97.14	80.00	85.71	88.57	94.29	97.14	100.00	97.14	94.29
10	100.00	100.00	97.14	97.14	94.29	97.14	97.14	97.14	100.00	100.00	100.00	100.00
11	97.14	91.43	94.29	97.14	82.86	80.00	88.57	94.29	100.00	100.00	97.14	100.00
12	97.14	100.00	94.29	100.00	97.14	94.29	100.00	100.00	100.00	100.00	97.14	100.00
13	100.00	100.00	94.29	97.14	91.43	91.43	85.71	94.29	100.00	94.29	100.00	100.00
14	91.43	97.14	94.29	94.29	97.14	97.14	100.00	100.00	100.00	100.00	100.00	100.00
15	97.14	100.00	97.14	97.14	91.43	97.14	100.00	100.00	100.00	100.00	97.14	100.00
16	97.14	97.14	100.00	100.00	94.29	94.29	94.29	91.43	100.00	100.00	94.29	94.29
17	97.14	100.00	97.14	94.29	97.14	100.00	100.00	97.14	100.00	100.00	100.00	100.00
18	100.00	100.00	97.14	100.00	82.86	100.00	91.43	97.14	97.14	97.14	100.00	97.14
19	100.00	100.00	97.14	100.00	97.14	100.00	100.00	94.29	100.00	100.00	100.00	100.00
20	100.00	100.00	88.57	94.29	94.29	94.29	85.71	80.00	100.00	97.14	97.14	100.00
21	91.43	94.29	91.43	94.29	91.43	94.29	94.29	91.43	100.00	100.00	94.29	91.43
MEAN	97.69	98.78	95.92	96.46	93.47	94.56	93.88	94.83	99.73	99.46	98.37	98.50
SD	2.65	2.32	4.20	3.82	5.80	5.18	5.59	5.24	0.86	1.46	1.93	2.49

* Trans. refers to the transient EMG state

** Every value in the table is expressed as a percentage (%)

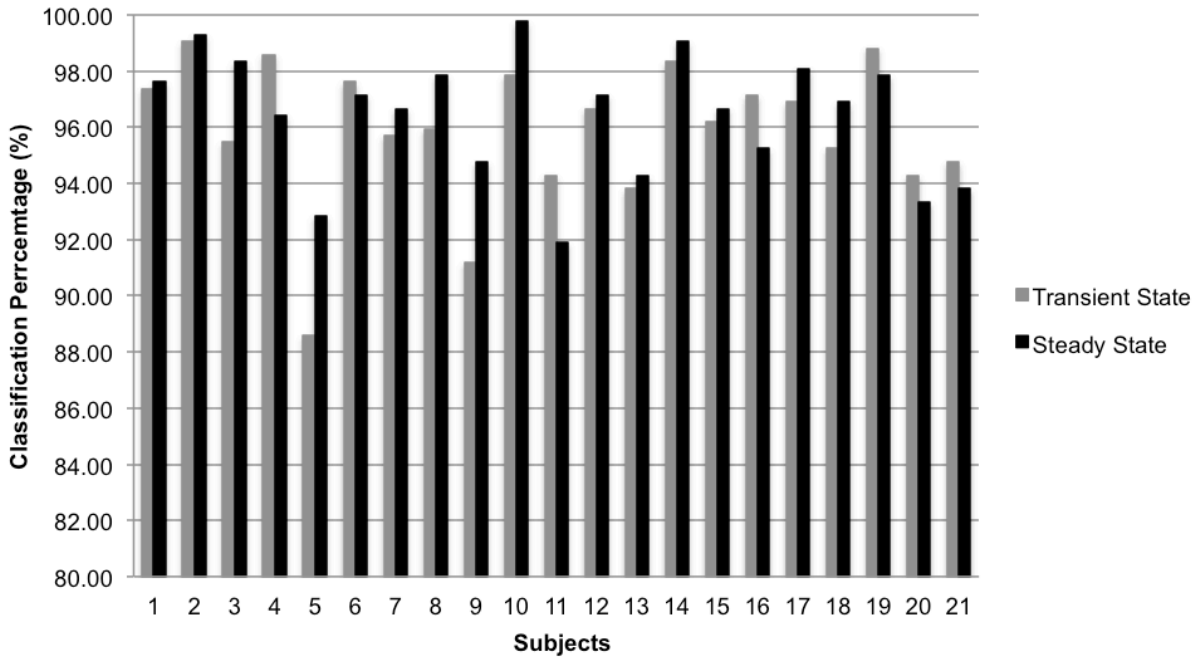


Fig. 4.14. Classification performance by subject for the transient and steady states using Hjorth's parameters and a window length of 128 ms.

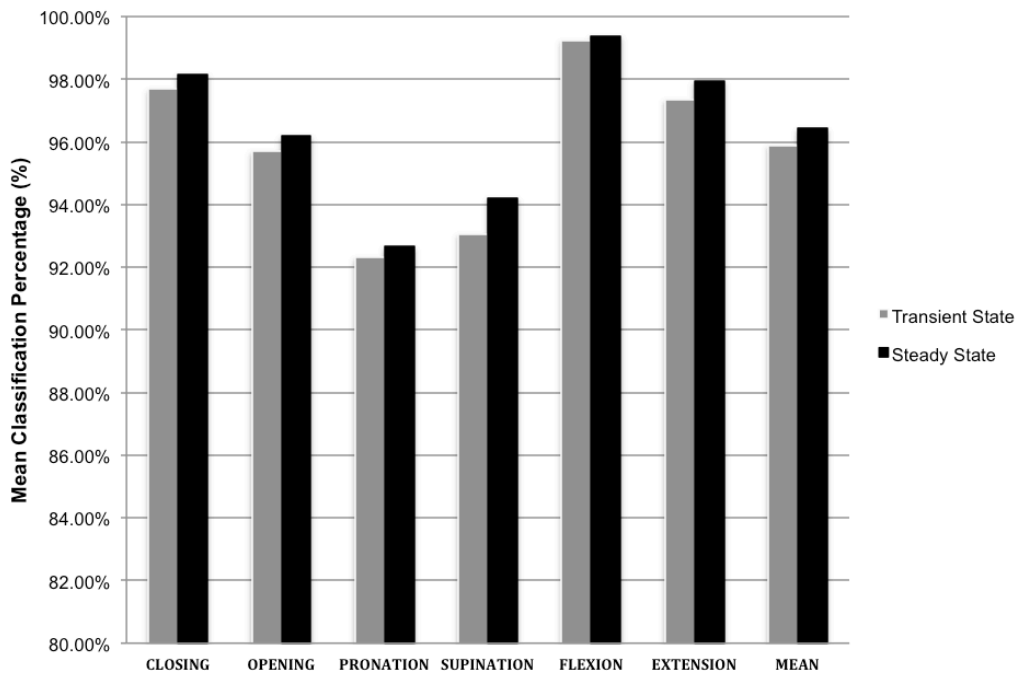


Fig. 4.15. Mean classification performance by movement for the transient and steady states using Hjorth's parameters and a window length of 128 ms.

TABLE 4.8
TRANSIENT VS. STEADY EMG CLASSIFICATION PERCENTAGE USING HJORTH'S PARAMETERS EXTRACTION FROM
A 128 MS HAMMING WINDOW

Subject	Closing		Opening		Pronation		Supination		Flexion		Extension	
	Trans.*	Steady	Trans.	Steady	Trans.	Steady	Trans.	Steady	Trans.	Steady	Trans.	Steady
1	98.57	100.00	97.14	94.29	95.71	94.29	94.29	97.14	100.00	100.00	98.57	100.00
2	100.00	100.00	98.57	100.00	97.14	98.57	100.00	98.57	100.00	100.00	98.57	98.57
3	97.14	100.00	94.29	95.71	92.86	95.71	94.29	100.00	95.71	100.00	98.57	98.57
4	98.57	98.57	100.00	97.14	100.00	95.71	95.71	90.00	100.00	100.00	97.14	97.14
5	100.00	97.14	84.29	91.43	90.00	85.71	71.43	85.71	98.57	100.00	87.14	97.14
6	98.57	98.57	95.71	94.29	94.29	97.14	97.14	97.14	100.00	97.14	100.00	98.57
7	98.57	97.14	94.29	98.57	94.29	92.86	94.29	94.29	98.57	100.00	94.29	97.14
8	98.57	100.00	97.14	100.00	85.71	90.00	97.14	97.14	100.00	100.00	97.14	100.00
9	91.43	98.57	92.86	94.29	82.86	88.57	85.71	94.29	98.57	100.00	95.71	92.86
10	98.57	100.00	97.14	98.57	92.86	100.00	100.00	100.00	100.00	100.00	98.57	100.00
11	97.14	88.57	98.57	95.71	81.43	81.43	88.57	87.14	100.00	98.57	100.00	100.00
12	95.71	100.00	95.71	98.57	92.86	90.00	97.14	97.14	100.00	100.00	98.57	97.14
13	95.71	98.57	91.43	94.29	87.14	85.71	90.00	87.14	98.57	100.00	100.00	100.00
14	98.57	100.00	97.14	97.14	98.57	100.00	95.71	100.00	100.00	100.00	100.00	97.14
15	98.57	97.14	95.71	100.00	88.57	90.00	97.14	97.14	98.57	100.00	98.57	95.71
16	97.14	98.57	98.57	95.71	97.14	81.43	97.14	100.00	100.00	98.57	92.86	97.14
17	100.00	98.57	98.57	100.00	95.71	97.14	90.00	97.14	100.00	100.00	97.14	95.71
18	95.71	100.00	100.00	97.14	85.71	98.57	92.86	90.00	97.14	97.14	100.00	98.57
19	100.00	97.14	98.57	97.14	98.57	100.00	98.57	94.29	100.00	100.00	97.14	98.57
20	98.57	97.14	87.14	87.14	97.14	95.71	87.14	81.43	98.57	100.00	97.14	98.57
21	94.29	95.71	97.14	92.86	90.00	87.14	90.00	92.86	100.00	95.71	97.14	98.57
MEAN	97.69	98.16	95.71	96.19	92.31	92.65	93.06	94.22	99.25	99.39	97.35	97.96
SD	2.14	2.56	4.02	3.24	5.41	6.00	6.46	5.37	1.16	1.24	3.01	1.78

* Trans. refers to the transient EMG state

** Every value in the table is expressed as a percentage (%)

The mean classification performance and SD for each of the subjects along the transient and steady EMG states for both windows sizes is condensed in TABLE 4.9.

TABLE 4.9
MEAN CLASSIFICATION AND SD PERCENTAGE PER SUBJECT FOR TRANSIENT AND STEADY EMG STATES USING
HJORTH'S PARAMETERS

Subject	Transient EMG State 256 ms	Steady EMG State 256 ms	Transient EMG State 128 ms	Steady EMG State 128 ms
	Mean±SD	Mean±SD	Mean±SD	Mean±SD
1	99.05±1.48%	99.52±1.17%	97.38±2.10%	97.62±2.81%
2	100.00±0.00%	100.00±0.00%	99.05±1.17%	99.29±0.78%
3	98.10±1.48%	99.52±1.17%	95.48±2.10%	98.33±2.10%
4	97.14±4.43%	96.19±3.90%	98.57±1.81%	96.43±3.47%
5	91.90±7.54%	92.86±7.17%	88.57±10.46%	92.86±6.19%
6	97.14±3.61%	96.19±4.30%	97.62±2.33%	97.14±1.56%
7	97.62±3.34%	98.10±2.33%	95.71±2.21%	96.67±2.66%
8	97.14±4.43%	96.19±4.30%	95.95±5.14%	97.86±4.02%
9	92.86±7.17%	94.76±4.92%	91.19±5.95%	94.76±4.11%
10	98.10±2.33%	98.57±1.56%	97.86±2.67%	99.76±0.58%
11	93.33±6.43%	93.81±7.54%	94.29±7.61%	91.90±7.32%
12	97.62±2.15%	99.05±2.33%	96.67±2.50%	97.14±3.73%
13	95.24±5.90%	96.19±3.46%	93.81±5.08%	94.29±6.45%
14	97.14±3.61%	98.10±2.33%	98.33±1.67%	99.05±1.48%
15	97.14±3.13%	99.05±1.48%	96.19±3.90%	96.67±3.69%
16	96.67±2.81%	96.19±3.46%	97.14±2.39%	95.24±6.92%
17	98.57±1.56%	98.57±2.39%	96.90±3.77%	98.10±1.73%
18	94.76±6.62%	98.57±1.56%	95.24±5.40%	96.90±3.55%
19	99.05±1.48%	99.05±2.33%	98.81±1.08%	97.86±2.17%
20	94.29±5.99%	94.29±7.45%	94.29±5.57%	93.33±7.38%
21	93.81±3.34%	94.29±3.13%	94.76±4.11%	93.81±3.90%
Mean±SD	96.51±2.24%	97.10±2.17%	95.90±2.56%	96.43±2.21%

The results from the classification performance on the transient and steady states using both 256 ms and 128 ms Hamming windows with 50% sample overlap are summarized, for each movement type, in Fig. 4.16 and in TABLE 4.10.

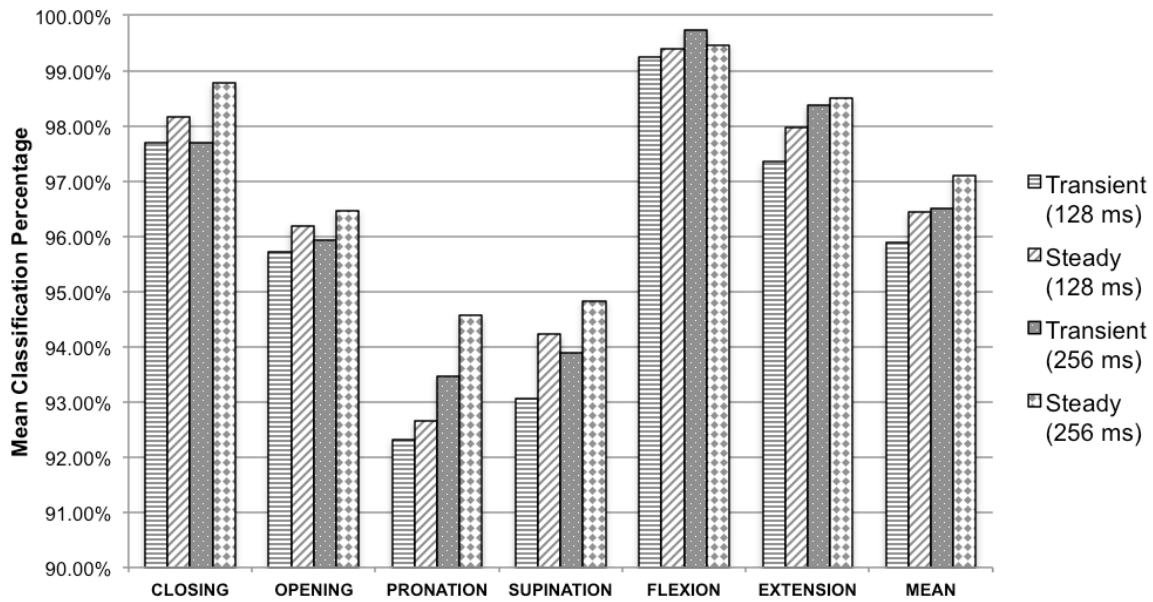


Fig. 4.16. Summary of transient and steady EMG states classification using window lengths of both 256 ms and 128 ms.

TABLE 4.10
SUMMARIZED RESULTS FROM TRANSIENT VS. STEADY STATE CLASSIFICATION USING HJORTH'S PARAMETERS

EMG State	Window Length [ms]	MOVEMENT							
		Closing	Opening	Pronation	Supination	Flexion	Extension	MEAN	
Transient	256	MEAN	97.69%	95.92%	93.47%	93.88%	99.73%	98.37%	96.51%
		SD	2.65%	4.20%	5.80%	5.59%	0.86%	1.93%	2.24%
Steady		MEAN	98.78%	96.46%	94.56%	94.83%	99.46%	98.50%	97.10%
		SD	2.32%	3.82%	5.18%	5.24%	1.46%	2.49%	2.17%
Transient	128	MEAN	97.69%	95.71%	92.31%	93.06%	99.25%	97.35%	95.90%
		SD	2.14%	4.02%	5.41%	6.46%	1.16%	3.01%	2.56%
Steady		MEAN	98.16%	96.19%	92.65%	94.22%	99.39%	97.96%	96.43%
		SD	2.56%	3.24%	6.00%	5.37%	1.24%	1.78%	2.21%

4.3 DWT's Variance

The reported results for this method were obtained using a 256 ms Hamming window with an overlap of 50% of the samples. The method was tested as well with a smaller window length (128 ms), but classification decreased approximately 1% over the whole data for the transient state and 3% for the steady state. Moreover, the SD between subjects increased almost 1%; therefore variability in the algorithm's performance between subjects was higher when decreasing the window length. These results are not reported because classification was considered to be too low for some individual movements as to be used in a control algorithm.

The ANN model for this method was trained using 10 neurons in the hidden layer. This number was defined experimentally and was tried to be kept as similar as possible to the previous method in order to maintain similar conditions. The variance was calculated from the detail coefficients of the second and third levels of decomposition as previously explained in section 3.3.2.2. A fourth order Coiflet mother wavelet was used.

4.3.1 Transient Vs. Steady State Analysis

The comparison in classification performance for both the transient and steady EMG states was tested. The results for each of the subjects are presented in Fig. 4.17, in TABLE 4.11, and in TABLE 4.12. Additionally, Fig. 4.18 and TABLE 4.13 condense the mean classification for each of the movements in both EMG states.

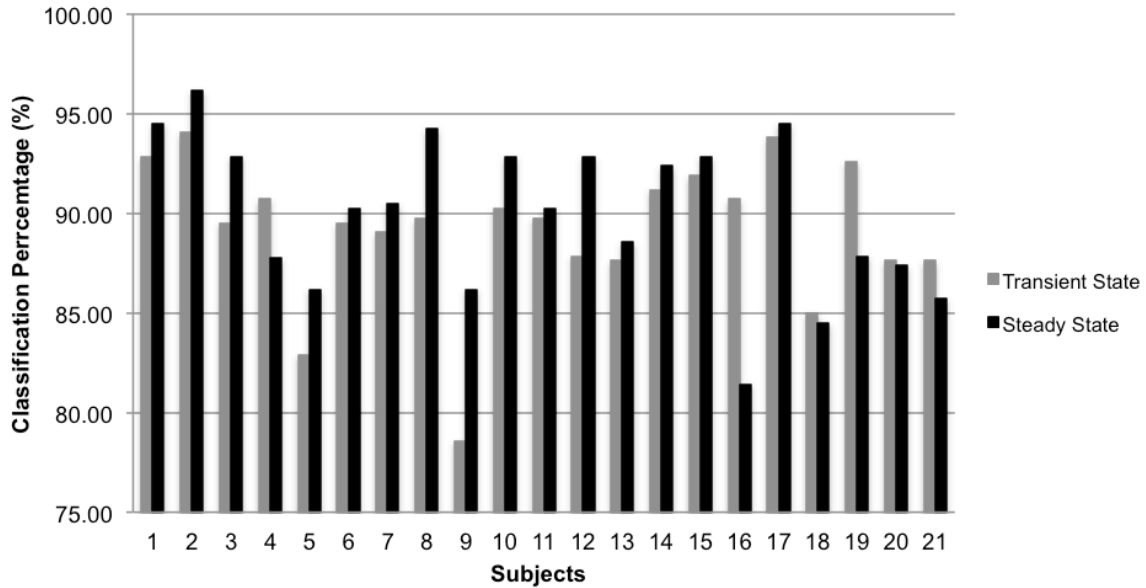


Fig. 4.17. Classification performance for the transient and steady states using the DWT's variance. The variance was calculated from the wavelet coefficients extracted using a 'coif4' mother wavelet and a window length of 256 ms with 50% overlap.

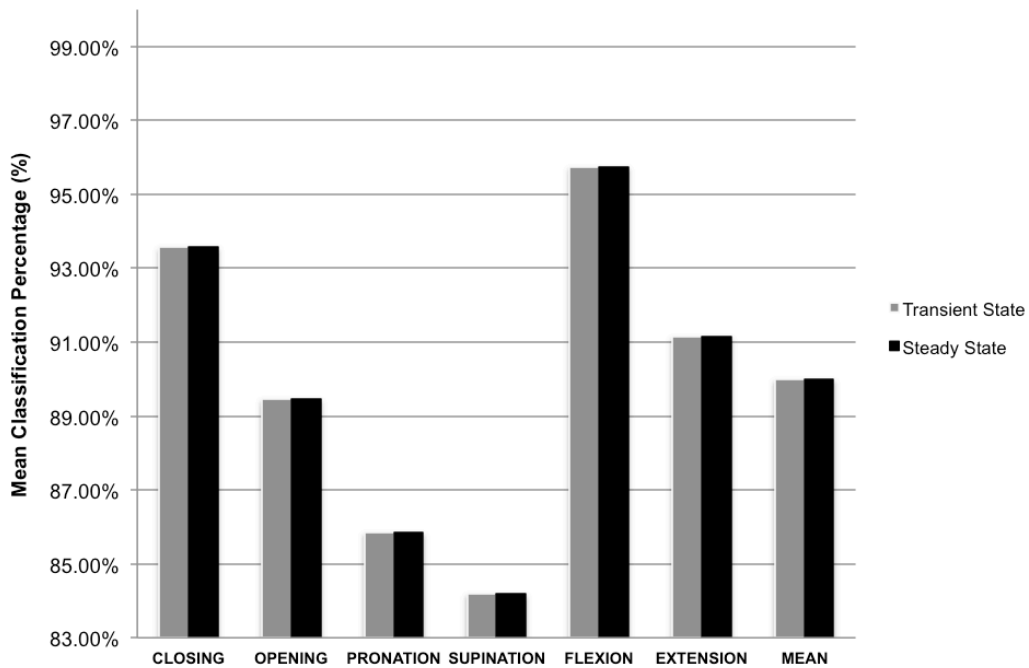


Fig. 4.18. Mean classification performance by movement for the transient and steady states using the DWT's variance method. A 256 ms Hamming window with 50% overlap was used.

TABLE 4.11
TRANSIENT VS. STEADY EMG CLASSIFICATION PERCENTAGE USING DWT'S VARIANCE EXTRACTION FROM A
256 MS HAMMING WINDOW

Subject	Closing		Opening		Pronation		Supination		Flexion		Extension	
	Trans.*	Steady	Trans.	Steady	Trans.	Steady	Trans.	Steady	Trans.	Steady	Trans.	Steady
1	91.43	97.14	92.86	94.29	87.14	91.43	92.86	94.29	100.00	97.14	92.86	92.86
2	100.00	98.57	95.71	98.57	90.00	94.29	91.43	87.14	95.71	98.57	91.43	100.00
3	88.57	95.71	84.29	84.29	92.86	92.86	82.86	92.86	98.57	100.00	90.00	91.43
4	92.86	94.29	95.71	92.14	95.71	87.14	82.86	76.43	97.14	95.71	80.00	80.71
5	91.43	94.29	72.86	78.57	85.71	84.29	62.86	71.43	91.43	95.71	92.86	92.86
6	97.14	100.00	84.29	87.14	87.14	85.71	81.43	78.57	95.71	92.86	91.43	97.14
7	94.29	87.14	90.00	90.00	84.29	87.14	80.00	91.43	92.86	91.43	92.86	95.71
8	94.29	100.00	92.86	97.14	75.71	84.29	82.86	92.86	100.00	94.29	92.86	97.14
9	72.86	94.29	82.86	84.29	70.00	81.43	71.43	81.43	88.57	88.57	85.71	87.14
10	90.00	95.00	91.43	89.29	84.29	96.43	85.71	84.29	98.57	96.43	91.43	95.71
11	94.29	88.57	90.00	98.57	71.43	75.71	90.00	84.29	97.14	100.00	95.71	94.29
12	92.86	92.86	87.14	94.29	77.14	84.29	82.86	90.00	91.43	100.00	95.71	95.71
13	91.43	91.43	85.71	90.00	80.00	78.57	77.14	80.00	97.14	97.14	94.29	94.29
14	87.14	96.43	88.57	83.57	92.86	95.71	90.00	88.57	97.14	98.57	91.43	91.43
15	91.43	90.00	94.29	97.14	88.57	91.43	94.29	95.71	94.29	97.14	88.57	85.71
16	95.71	85.71	91.43	82.86	91.43	75.71	81.43	74.29	94.29	97.14	90.00	72.86
17	97.14	100.00	94.29	98.57	92.86	91.43	85.71	87.14	100.00	100.00	92.86	90.00
18	92.86	97.14	85.71	85.71	68.57	75.71	81.43	77.14	88.57	84.29	92.86	87.14
19	98.57	87.86	90.00	86.43	92.86	83.57	82.86	82.86	100.00	97.14	91.43	89.29
20	88.57	90.00	85.71	85.71	84.29	87.14	72.86	77.14	97.14	94.29	97.14	90.00
21	85.71	88.57	91.43	80.00	84.29	78.57	78.57	80.00	95.71	94.29	90.00	92.86
MEAN	91.84	93.57	88.91	89.46	84.63	85.85	82.45	84.18	95.78	95.75	91.50	91.16
SD	5.70	4.51	5.36	6.34	8.07	6.61	7.47	7.09	3.54	3.97	3.66	6.13

* Trans. refers to the transient EMG state

** Every value in the table is expressed as a percentage (%)

TABLE 4.12
MEAN CLASSIFICATION AND SD PERCENTAGE PER SUBJECT FOR TRANSIENT AND STEADY EMG STATES USING
DWT'S VARIANCE

Subject	Transient EMG State	Steady EMG State
	256 ms	256 ms
	Mean±SD	Mean±SD
1	92.86±4.14%	94.52±2.29%
2	94.05±3.77%	96.19±4.84%
3	89.52±5.76%	92.86±5.19%
4	90.71±7.38%	87.74±7.79%
5	82.86±12.29%	86.19±9.80%
6	89.52±6.30%	90.24±7.95%
7	89.05±5.69%	90.48±3.22%
8	89.76±8.83%	94.29±5.50%
9	78.57±8.08%	86.19±4.92%
10	90.24±5.06%	92.86±4.99%
11	89.76±9.45%	90.24±9.28%
12	87.86±6.93%	92.86±5.35%
13	87.62±8.01%	88.57±7.61%
14	91.19±3.55%	92.38±5.64%
15	91.90±2.81%	92.86±4.61%
16	90.71±5.01%	81.43±9.21%
17	93.81±4.84%	94.52±5.67%
18	85.00±9.16%	84.52±7.74%
19	92.62±6.22%	87.86±5.17%
20	87.62±9.11%	87.38±5.81%
21	87.62±6.04%	85.71±7.06%
Mean±SD	89.18±3.66%	89.99±3.91%

TABLE 4.13
SUMMARIZED RESULTS FROM TRANSIENT VS. STEADY STATE CLASSIFICATION USING DWT'S VARIANCE

EMG State	Window Length [ms]	MOVEMENT							
		Closing	Opening	Pronation	Supination	Flexion	Extension	MEAN	
Transient	256	MEAN	91.84%	88.91%	84.63%	82.45%	95.78%	91.50%	89.18%
		SD	5.70%	5.36%	8.07%	7.47%	3.54%	3.66%	3.66%
Steady		MEAN	93.57%	89.46%	85.85%	84.18%	95.75%	91.16%	89.99%
		SD	4.51%	6.34%	6.61%	7.09%	3.97%	6.13%	3.91%

4.4 Models' Tolerance to Additive White Gaussian Noise

Previous to noise contamination, and regarding that not a great amount of data was available for each of the subjects, a new recording was created by averaging the transient segments of the 5 available recordings for each type of movement. Fig. 4.19 shows an example of one EMG channel from one of the subjects during wrist extension. The first five signals correspond to the EMG recordings that were taken, and the sixth one is a signal generated by averaging the previous recordings.

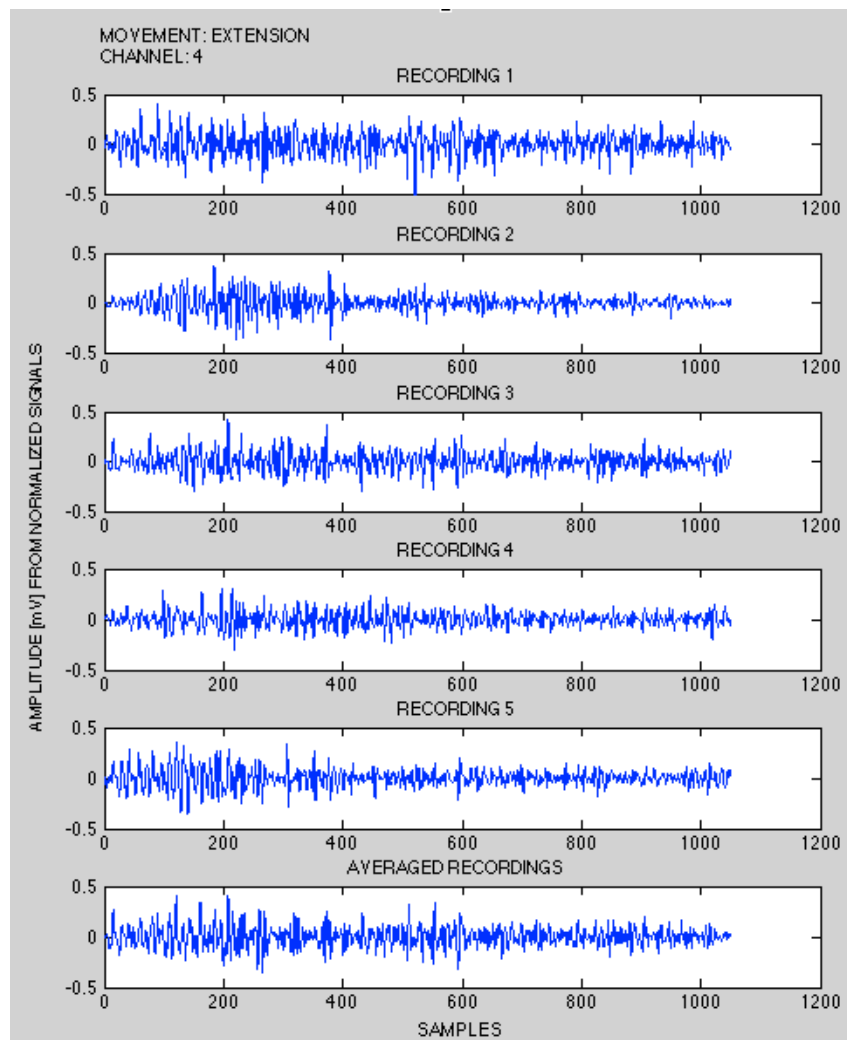


Fig. 4.19. New signal generated by averaging previous recorded EMG signals. This particular one shows channel 4 during a wrist extension.

In order to test the model's tolerance to AWGN, original recordings and the new generated ones were used. After applying the sliding window to the signal, each windowed segment was contaminated as previously explained in Chapter III, taking into consideration that in an on-line application, each recorded segment of the signal at a certain instant of time can be affected by noise. Fig. 4.20 shows an example of a windowed segment of one EMG channel with different levels of noise. The contaminated signal is shown in white behind the original one (black). In the right, the FFTs of the original (black) and contaminated (white) signals are shown in order to see how the frequency spectrum was affected by noise. It is important not to forget that white Gaussian noise has uniform power across the frequency band.

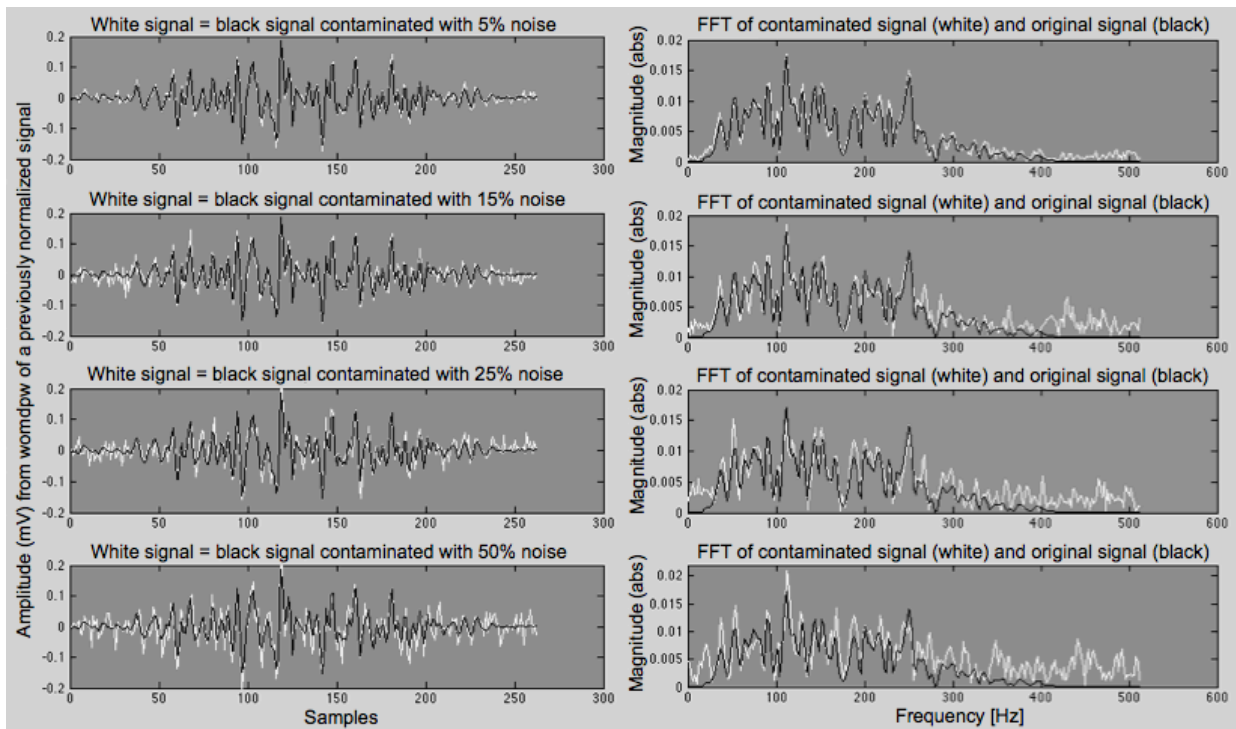


Fig. 4.20. EMG segment contaminated with different levels of additive white Gaussian noise. In the left side, the original windowed segment from one EMG channel (black) is contaminated with AWGN at 5% (first row), 15% (second row), 25% (third row), and 50% (fourth row) with respect to the signal's power. The contaminated signals are shown in white behind the original ones. The right side of the image shows the FFT for both the original and contaminated signals.

The trained ANN models for each subject, using both the Hjorth's parameters and the DWT's variance methods, were tested with the contaminated averaged transient state recordings. Different levels of white noise were added to the new recordings – namely, 5%, 10%, 15%, 20%, 25%, 30%, and 50%. The obtained results are presented in Fig. 4.21 and in TABLE 4.14.

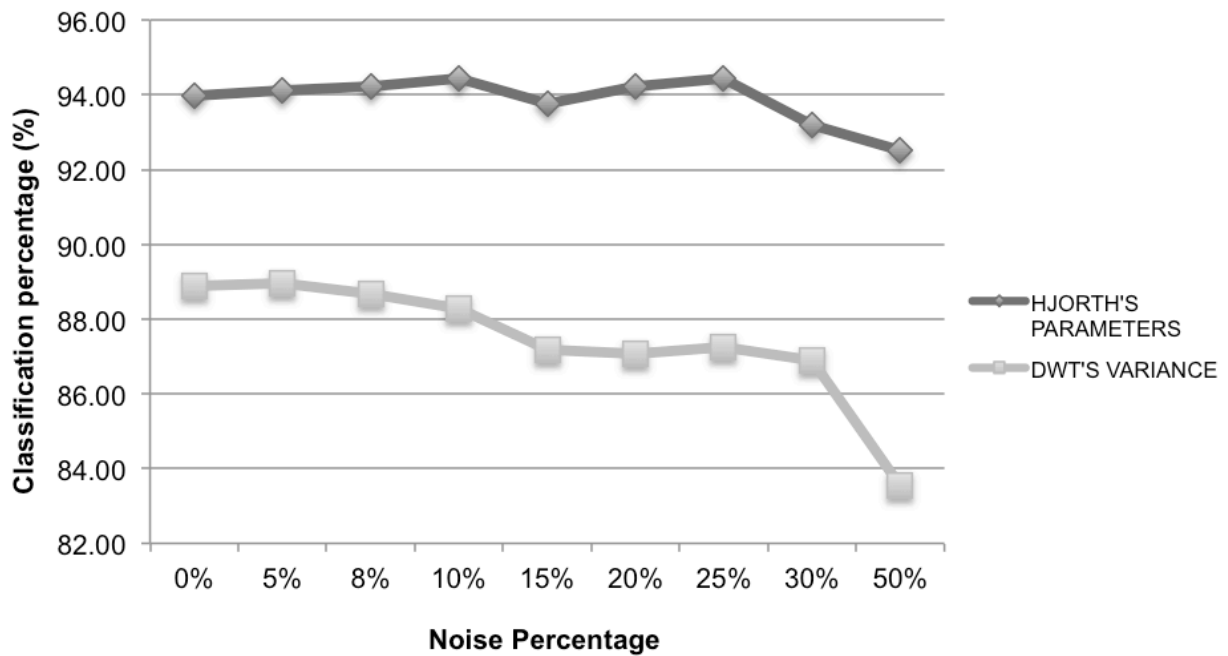


Fig. 4.21. Models' responses to AWGN.

TABLE 4.14
MEAN CLASSIFICATION ACCURACY OF THE TRAINED MODELS WHEN TESTING WITH AVERAGED TRANSIENT STATE RECORDINGS CONTAMINATED WITH DIFFERENT NOISE LEVELS

MODEL	NOISE PERCENTAGE								
	0%	5%	8%	10%	15%	20%	25%	30%	50%
Hjorth's Parameters	93.99%	94.10%	94.22%	94.44%	93.76%	94.22%	94.44%	93.20%	92.52%
DWT's Variance	88.89%	88.95%	88.66%	88.27%	87.19%	87.07%	87.24%	86.90%	83.56%

4.5 DWT Using PCA

This method was tested using a 256 ms Hamming window with a 50% overlap in order to compare the results with the two previous ones under similar conditions.

Wavelet decomposition was applied until the third level. A fourth order Coiflet mother wavelet was used. The resulting feature matrix was of greater dimensions than those of the two previous methods and it was more difficult for the ANN model to reach convergence during the training state. The number of neurons in the hidden layer of the ANN model was adjusted experimentally to 15 neurons.

As this method is similar to previously reported ones [9,27,69,70] and was intended only for comparison purposes, it was only tested over the transient EMG state. The obtained results will be subsequently presented.

4.4.1 Transient State Analysis

As previously explained in Chapter III, PCA was applied for dimensionality reduction of the matrix containing the detail coefficients of the first three decomposition levels and the approximation coefficients of the third level. The feature matrix was built using eight principal components for each movement type.

The classification percentages per subject are presented in Fig. 4.22 and in TABLE 4.15; additionally, Fig. 4.23 shows the mean classification per movement type achieved by this method over the whole test population.

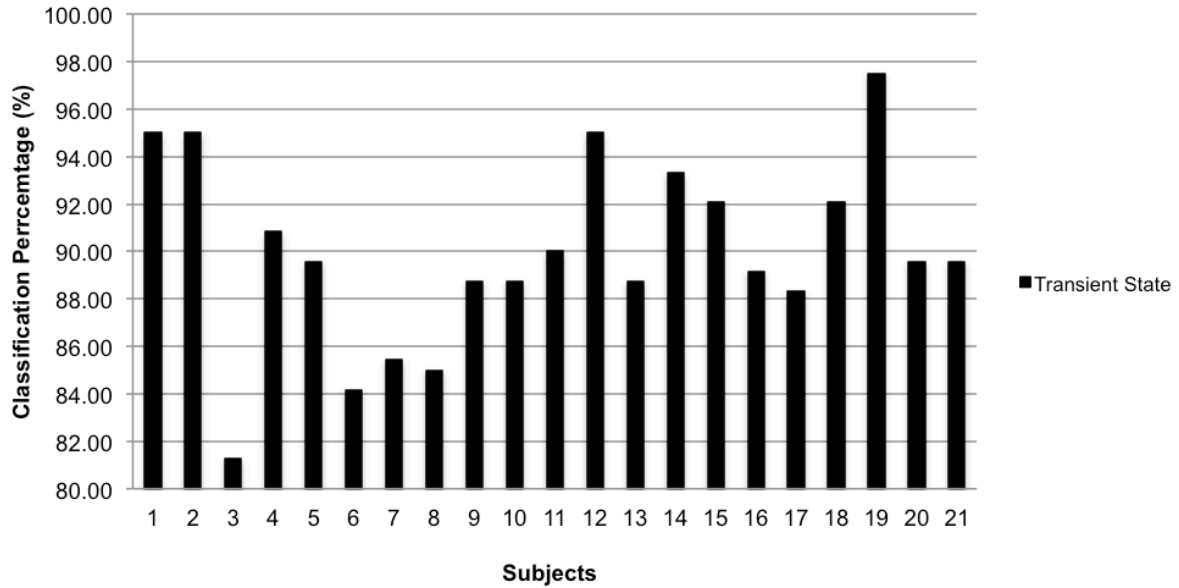


Fig. 4.22. Classification performance for the transient EMG state using DWT reduced by PCA. The feature matrix was built with the principal components extracted from the first three detail levels and the third approximation level using a 'coif4' mother wavelet and a window length of 256 ms with 50% overlap.

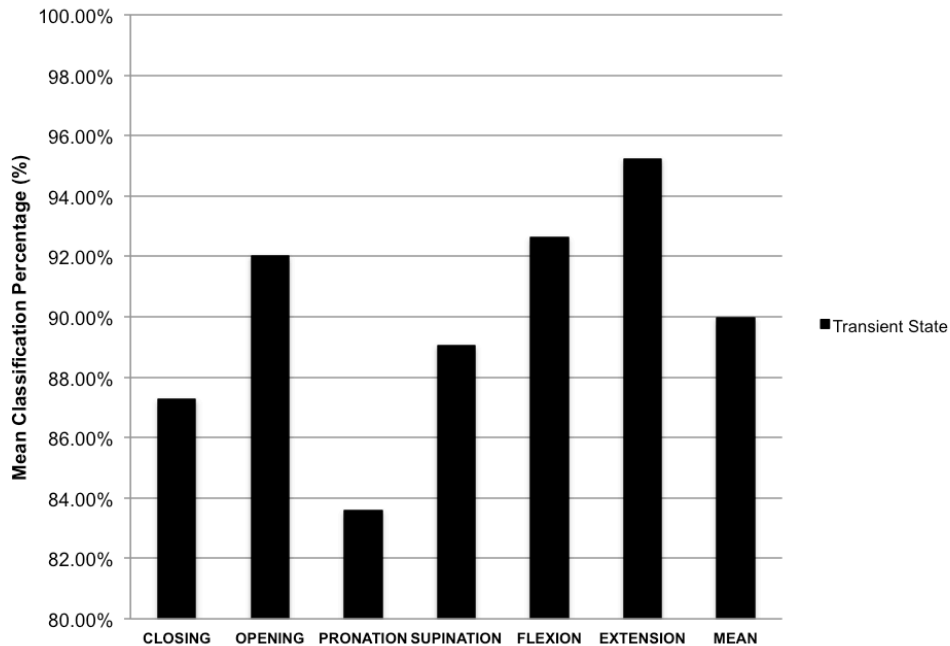


Fig. 4.23. Mean classification performance by movement for the transient EMG state using DWT reduced by PCA. A 256 ms Hamming window with 50% overlap was used.

TABLE 4.15
TRANSIENT EMG CLASSIFICATION PERCENTAGE USING DWT REDUCED BY PCA

Subject	MOVEMENT						MEAN±SD
	Closing	Opening	Pronation	Supination	Flexion	Extension	
1	92.50	100.00	92.50	97.50	95.00	92.50	95.00±3.16
2	100.00	95.00	85.00	95.00	100.00	95.00	95.00±5.48
3	67.50	87.50	75.00	80.00	82.50	95.00	81.25±9.59
4	92.50	85.00	95.00	87.50	87.50	97.50	90.83±4.92
5	80.00	97.50	82.50	92.50	85.00	100.00	89.58±8.28
6	72.50	85.00	72.50	90.00	85.00	100.00	84.17±10.57
7	77.50	92.50	75.00	87.50	82.50	97.50	85.42±8.72
8	97.50	77.50	70.00	77.50	95.00	92.50	85.00±11.40
9	90.00	95.00	80.00	87.50	90.00	90.00	88.75±4.94
10	85.00	95.00	87.50	80.00	92.50	92.50	88.75±5.65
11	80.00	95.00	77.50	87.50	100.00	100.00	90.00±9.87
12	92.50	100.00	82.50	100.00	97.50	97.50	95.00±6.71
13	72.50	82.50	87.50	95.00	100.00	95.00	88.75±10.09
14	90.00	100.00	87.50	82.50	100.00	100.00	93.33±7.69
15	92.50	97.50	90.00	82.50	90.00	100.00	92.08±6.21
16	90.00	95.00	82.50	77.50	92.50	97.50	89.17±7.69
17	72.50	92.50	85.00	85.00	100.00	95.00	88.33±9.70
18	90.00	90.00	85.00	100.00	90.00	97.50	92.08±5.57
19	97.50	100.00	95.00	100.00	92.50	100.00	97.50±3.16
20	100.00	97.50	87.50	87.50	87.50	77.50	89.58±8.13
21	100.00	72.50	80.00	97.50	100.00	87.50	89.58±11.56
Mean±SD	87.26±10.21	92.02±7.73	83.57±6.96	89.05±7.52	92.62±6.15	95.24±5.41	89.96±3.98

* Trans. refers to the transient EMG state

** Every value in the table is expressed as a percentage (%)

4.6 Transient State Analysis: Comparison in Performance Between Methods

As the interest EMG segment for this study is the transient state, a comparison between classification performances of the three methods was made. The obtained results for mean classification percentage of each of the movements are displayed below in Fig. 4.24. A comparison between the standard deviation among subjects for each movement type according to the applied method was also made. The intention was to appreciate how much performance varies from one subject to another. The results are shown in Fig. 4.25. General results from the three methods are also presented in TABLE 4.16.

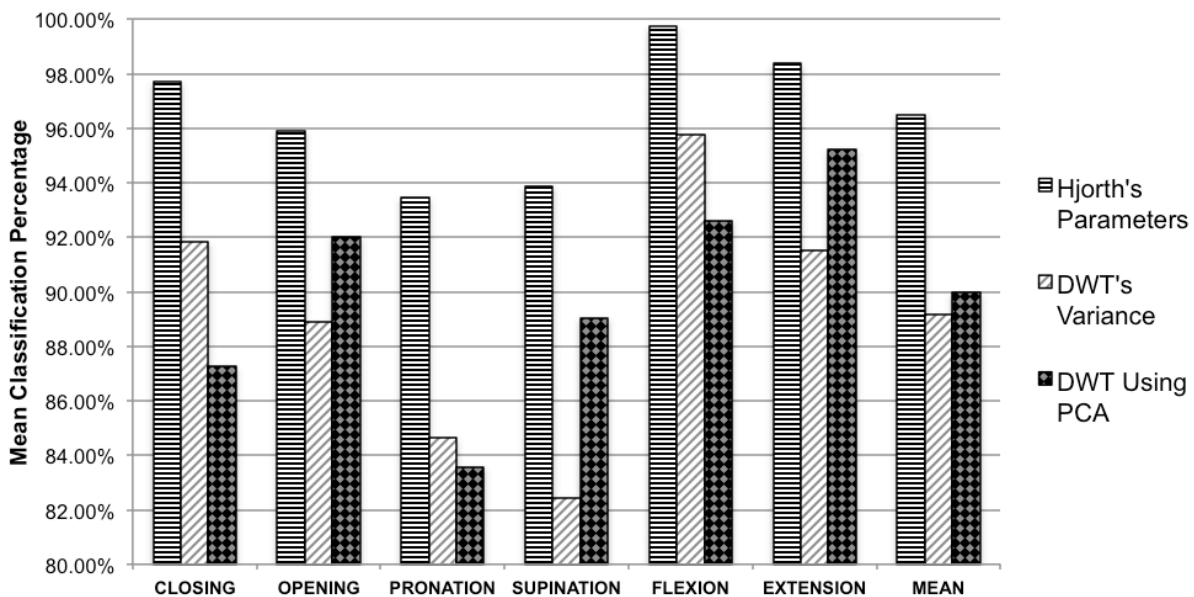


Fig. 4.24. Comparison in the mean classification percentage of the transient EMG state for each movement type using the three methods. A window length of 256 ms with 50% overlap was used for feature extraction.

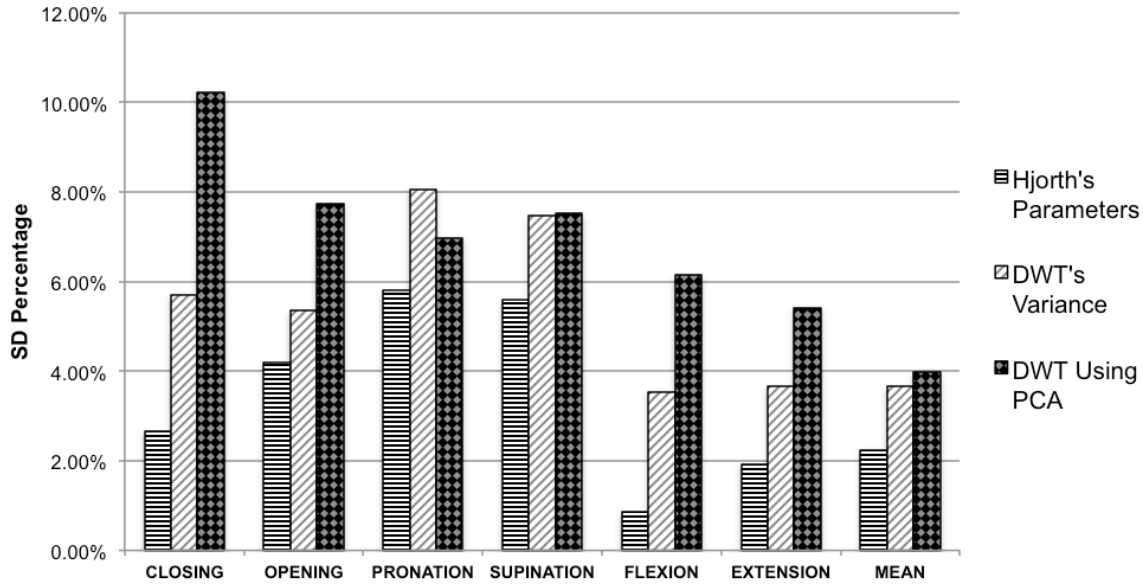


Fig. 4.25. Comparison in the standard deviation of the whole test population for each movement type using the three methods. A window length of 256 ms with 50% overlap was used for feature extraction.

TABLE 4.16
SUMMARIZED RESULTS OF THE COMPARISON OF THE MEAN CLASSIFICATION AND SD PERCENTAGES FOR EACH MOVEMENT TYPE USING THE THREE METHODS

EMG State	Window Length [ms]	MOVEMENT							
		Closing	Opening	Pronation	Supination	Flexion	Extension	MEAN	
Hjorth's Parameters	256	MEAN	97.69%	95.92%	93.47%	93.88%	99.73%	98.37%	96.51%
		SD	2.65%	4.20%	5.80%	5.59%	0.86%	1.93%	2.24%
DWT's Variance		MEAN	91.84%	88.91%	84.63%	82.45%	95.78%	91.50%	89.18%
		SD	5.70%	5.36%	8.07%	7.47%	3.54%	3.66%	3.66%
DWT Using PCA		MEAN	87.26%	92.02%	83.57%	89.05%	92.62%	95.24%	89.96%
		SD	10.21%	7.73%	6.96%	7.52%	6.15%	5.41%	3.98%

4.7 Proposed Control Algorithm

Fig. 4.26 illustrates the proposed control algorithm. Even while the ANN model was capable of identifying the movement since the first 128 ms of the transient state, this scheme suggests analyzing the features extracted from the first 3 windows with 50% overlap that will represent a total delay of 256 ms, but that will allow having more

information for movement identification. This diagram also suggests the implementation of an automatic detection algorithm for the transient state of the EMG signal that can be done as future work.

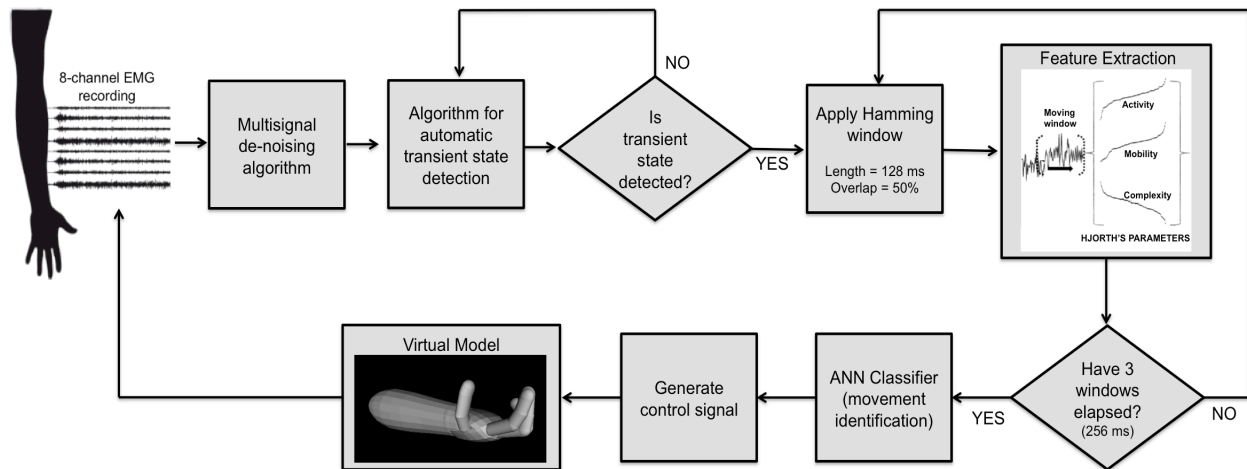


Fig. 4.26. Flow diagram of the proposed control algorithm.

Discussion

The first challenge in EMG transient state analysis for on-line control of a myoelectric device is the proper identification of the onset of the movement. In order to ensure a good performance of the system, it should be reliable enough when identifying the beginning of the muscle contraction as to trigger feature extraction. If the onset of the movement is incorrectly designated earlier than it actually occurs, noise and low-level EMG signals from the subject's rest position will be included and translated inaccurately in low force levels. In the contrary, if a late identification of the onset is made, the initial MUAPs will be excluded from the analysis and essential information to the classifier will be lost. The database used for this study was not made considering the analysis of the transient state; hence, it does not take much care of the quality of the signal before the sustained contraction. Furthermore, several signals appeared truncated in the beginning of the onset of the contraction. This together made automatic transient state detection really challenging and the decision to identify the onset of the contraction by supervision was taken. The shadowed regions in Fig. 4.1 give an example of how the signals were segmented in transient and steady states for feature extraction.

In order to decide on appropriate signal processing techniques, it is necessary to study the frequency and time domain properties of the signals of interest. Using multichannel EMG signals allows recording information from several muscle sites. The amplitude for each of the EMG channels allows seeing the participation of corresponding muscles on a certain movement. The first column in Fig. 4.2 gives an example of the raw multichannel EMG from a wrist extension movement. The first four channels that correspond to extensor muscles as named in TABLE 3.2 have higher amplitude values than the last four. In the same way, the FFT that appears in the second column shows

magnitudes in the order of 10^{-3} for these last channels. The shadowed region allows seeing the frequency band that was considered for feature extraction. In order to assure analysis over this band, the wavelet shrinkage algorithm was applied. This has also the advantage of being a good noise cancelling technique that filters according to an adaptive threshold calculated relative to the amount of noise in each level of the wavelet decomposition. The selected frequency band for analysis is located within the first three levels of decomposition. As shown in Fig. 4.3, when obtaining the FFT from the coefficients at each level, it is possible to corroborate the frequency band they correspond to. The frequency spectrum of the steady segment is flatter than that of the transient one, which suggests that a constant firing rate has been reached.

Window functions were applied for signal segmentation in order to build up the patterns used to feed the classifier model. However, when choosing the window, the question of which type yields a better performance for data segmentation is hard to answer. Hence, a test was applied. The objective of using windows on signal processing is to be able to smoothly truncate a segment of the signal in order to extract features from it and analyze it modifying the signal as least as possible. The simplest type of window is the rectangular one; however, it truncates data abruptly, which causes high sidelobe behavior and is not recommended for the application. Other types of window have been more suitable for EMG analysis. Fig. 4.4 and TABLE 4.1 present the classification percentage when using each window type. As it can be appreciated in Fig. 4.5, the greatest error is obtained with the rectangular window. Even if the Hamming window performed the best, the Gaussian and Hanning windows had similar performances and their use could also be considered.

Applying window functions allows defining which time interval is used in the computation; and therefore, the extracted features represent the data from that time interval. Extrapolating these features to other times has no meaning; however, when window overlapping is used, contiguous windows share similar characteristics.

Stationarity can be assumed when a finite block of data is taken to be representative and therefore, analysis can be made within the window [102]. As for window length selection, the main limitation in the system is the real-time constrain. As mentioned before, the maximum accepted delay for myoelectric controlled devices is 300 ms [6,9,10]. Fig. 4.6 and Fig. 4.7 demonstrate that among the tested window lengths, wider windows (256 ms) yield better classification accuracy for both the transient and steady EMG states (see specific data in TABLE 4.2 and TABLE 4.3). This occurs because features extracted from a larger segment of the signal tend to be more representative. However, it is important to find a good balance between the system's response time and its accuracy, which is why a 128 ms window length is proposed as more adequate for the Hjorth's parameters method. The classification percentage obtained by applying 256 and 128 ms window lengths was similar. The 256 ms window outperformed the 128 ms one by just 0.61% for the mean classification using the transient state and 0.42% for the steady state. Fig. 4.8 and TABLE 4.4 show the mean error percentage while applying different window lengths for feature extraction in both the transient and steady states. These results were not consistent for the other discussed methods (DWT's variance and DWT using PCA) where a 256 ms window length was kept.

The ANN was a good approach for building the model. ANNs are suitable for difficult signal processing problems because they are capable to generalize, and they possess the ability to learn from experience without requiring an a priori mathematical model of the underlying signal characteristics. However, difficulties exist when only a limited numbers of examples are available for the training process [1]. It would be important to have more information from each subject; however, in order to counteract the limited amount of available data, k-fold cross-validation was carried out. Moreover, Bayesian regulation backpropagation was used as the training algorithm, which is recommended when there is not much information available. The number of neurons in the hidden layer of the ANN model was determined experimentally. The classification performance regarding different neuron numbers can be seen in Fig. 4.9 and more precisely in

TABLE 4.5. When using Hjorth's parameters calculated over the transient EMG state, the error did not change much between using 9 and 20 neurons as shown in TABLE 4.5. Nine neurons were chosen for the hidden layer of the ANN model because they yielded a good balance between classification performance and model's complexity. Convergence was harder to achieve for the other two models due to more complicated feature sets. Therefore, 10 neurons were determined for the DWT's variance model and 15 neurons for the DWT model using PCA. TABLE 3.4 summarizes the final ANNs' architectures.

Hjorth's descriptors have been used successfully in EEG analysis and sleep stage scoring as previously described in section 2.3.4.1. As it is known, the EEG signal is formed by the superposition of characteristic responses. In the same way, the EMG signal is a superposition of MUAPs, which seems to make Hjorth's parameters suitable for EMG analysis due to the nature of myoelectric sources. As supported by clinical results previously described in chapter II, these descriptors convey information concerning physiological states.

The auto-correlation function applies particularly well to physical situations because the constants that define a physical system and its characteristic response also determine the auto-correlation function of the response. A basic way of expressing the characteristics of a time series in statistical terms is to refer to its auto-correlation function, which defines statistically the interdependence between any two values in the series as a function of their difference in time. Applying Hjorth's parameters for time domain analysis is in fact a means to derive the auto-correlation function of the curve in terms of polynomial coefficients [30].

Most generally applied techniques for EMG analysis are based on feature extraction in both the time and frequency domains; however, Hjorth's parameters serve as a bridge

between a physical time domain interpretation and the conventional frequency domain description [30-33]. The auto-correlation function conveys all the information that can be obtained from power spectral analysis or from conventional frequency analysis [30]. In fact, a high correlation has been found between the NSD 'Mobility' and the FFT [34], which has also been used for EMG analysis. Nonetheless, the methods for frequency domain analysis imply a transformation that is usually more time-consuming and requires more complex processing. Although Hjorth's parameters are based on spectral moments, they are also calculated by time variances (time domain analysis) that can be performed continuously during on-line recording, making the computational cost more affordable than for other methods and hence making it more suitable for real-time applications.

The question of which combination of parameters was more representative for EMG signal analysis was formulated since the beginning. For non-periodic phenomena with a limited complexity, as it is the case of the EMG signal, the basic information is essentially contained in the first few polynomial coefficients; therefore, the number of required (non-redundant) descriptors correspond to the complexity of the system under observation [30]. Binnie *et al.* [101] showed that two descriptors give sufficient information to replace frequency analysis in monitoring the state of patients suffering minimal hepatic encephalopathy. Other studies have reported to find significant changes using just two of Hjorth's parameters to interpret EEG signals [33,36,38,41]; furthermore, the last three have reported to find them in Mobility and Complexity, as it was the case in the present study. The highest classification performance was achieved using the last two Hjorth's descriptors as shown in Fig. 4.10 and Fig. 4.11. (To find the exact numerical data refer also to TABLE 4.6).

In general terms, the system response of a first order system is an exponentially decaying impulse that can be mathematically expressed as $e^{-\alpha t}$, where α is the inverse time constant of the system. When computing Hjorth's descriptors for this response,

Mobility turns to be identical to α and hence describes the system. For a second order system, the response is modeled as a decaying sinusoid with the mathematical expression $e^{-\alpha t} \cdot \sin(\beta \cdot t)$. In this case, when computing the parameters, the relationship between them and the constants of the system shown in (5.1) are obtained [30].

$$\begin{cases} M (\text{mobility}) = (\alpha^2 + \beta^2)^{\frac{1}{2}} \\ C (\text{complexity}) = 2 \alpha \end{cases} \quad (5.1)$$

As defined in [30], making some algebraic manipulations, the constants can be expressed as a function of Hjorth's parameters as shown in (5.2).

$$\begin{cases} \alpha = C/2 \\ \beta = M \cdot (1 - C^2/4M^2)^{\frac{1}{2}} \end{cases} \quad (5.2)$$

Based on the previous assumptions, the system is fully determined by Mobility and first order Complexity. The number of required descriptors to convey the basic information of the system corresponds to the system's order. The muscle contraction can be modeled as a second order system, which would justify the performance achieved by using these two parameters. Moreover, the descriptor values, except for Activity, referring to a single response are valid also for a superposition of responses since the ratios are not affected by the addition of further responses of arbitrary phase and amplitude [30]. The MES is, however, a summation of MUAPs that do not have the same characteristics among them. Motor units fire asynchronously with different rates and with certain amplitude that depends on the force of the contraction; therefore, the parameter Activity seems to be less suitable to describe it. In an experiment made by [30], in which Mobility and Complexity parameters were computed from a computer-implemented superposition of 10,000 responses of a system and converted mathematically to system constants, they turned to be identical with the constants of the system from which the superimposed

responses were originally derived. In sEMG, the electrode in the skin captures the random nature of the joint activity of the motor units. Taking into consideration Hjorth's experiment, applying the descriptors to these superimposed responses should convey relevant information to describe the myoelectric system.

Previously reported studies [9,69,70] comparing transient and steady EMG states have found that steady state analysis significantly outperforms transient state analysis. In [70], the feature set that yielded the best results for a six-class problem was built using WPT. However, an approximate 2% mean error was found for the steady state, while the mean error for transient state analysis was 5%. As it can be appreciated in Fig. 4.12 and TABLE 4.7 for the 256 ms window and in Fig. 4.14 and TABLE 4.8 for the 128 ms window, the steady state tends to have a higher mean classification than the transient state. TABLE 4.9 and TABLE 4.10 allow comparing mean classification performances between the transient and steady states obtained using Hjorth's parameters. The mean classification percentage for the steady state in a six-class problem using the 256 ms window was just 0.59% higher than the transient state and 0.53% higher in the 128 ms window case. When analyzing classification percentages for each movement type (Fig. 4.13 using the 256 ms window and Fig. 4.15 using the 128 ms window), the highest difference between both states was of just 1.16% for supination movement, which is lower than that reported in [70]. Fig. 4.16 summarizes the results from all the aforementioned cases. As it can be seen, the lowest classification performances were found for pronation and supination. This suggests that the muscles recorded by the EMG channels had less participation in these two movement types. When referring to TABLE 3.2 and Fig. 3.3, it is possible to see that almost every recorded muscle have flexion and extension purposes. This explains as well why flexion, extension, opening, and closing were so accurately classified. When observing an example in the confusion matrices obtained from both the training and testing stages of the ANN of a random subject (Fig. 5.1), it is possible to appreciate by the change of color that confusion occurred in the pronation/supination class. It often happened that misclassification corresponded to confusion between these two movements suggesting that the recorded

muscles have similar performance in both pronation and supination and that more specialized muscles should be considered in order to achieve higher classification accuracy.

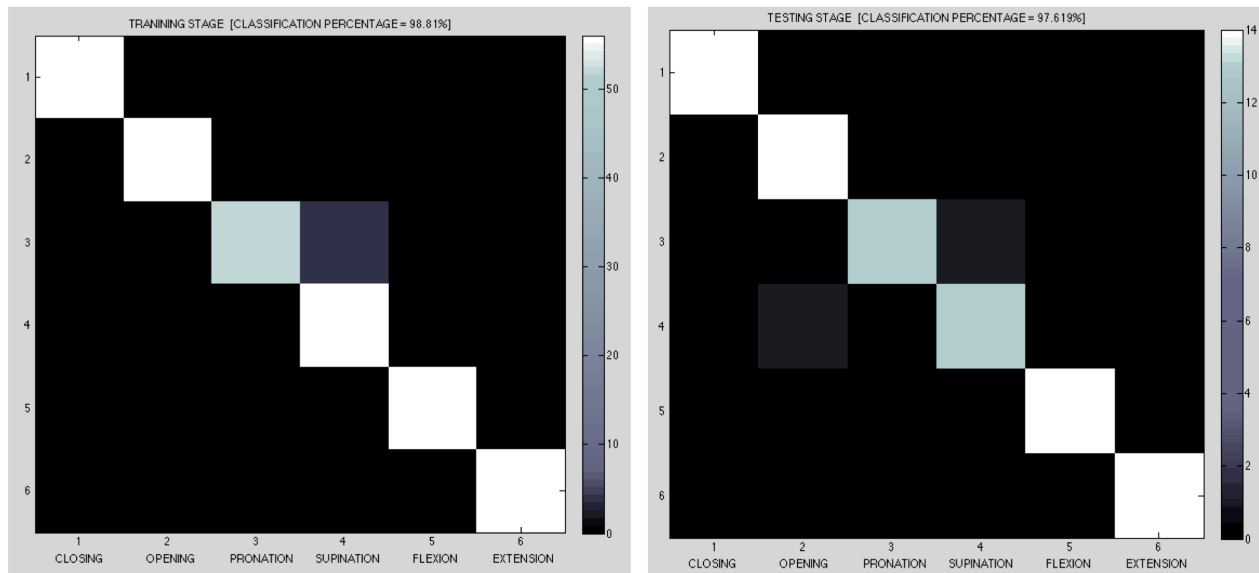


Fig. 5.1. Confusion matrix of the training and testing stages of the ANN from one of the subjects using Hjorth's parameters and a window length of 128 ms. The left side of the image shows the confusion matrix for the training stage. From a total of 56 windows used for the training, four windows corresponding to wrist pronation were misclassified as wrist supination. The training percentage was 98.81%. The right side of the image shows the confusion matrix for the testing stage. From a total of 14 windows used for the testing stage, one window corresponding to wrist pronation was misclassified as wrist supination, and one window corresponding to wrist supination was misclassified as hand opening. The test percentage was 97.619%. This corresponds to the first of five foldings used for k-fold cross-validation.

Both methods applying DWT depart from the use of representative wavelet coefficients from each of the EMG signals as the main tool for feature extraction. The method that used the variance of the wavelet coefficients from the second and third levels of decomposition to build the feature matrix had a worse performance than the method using Hjorth's parameters. Moreover, the values of SDs are significantly higher between subjects as it can be seen in TABLE 4.11 and in Fig. 4.17, where for some subjects the differences between mean classification of the transient and steady states are

considerably more noticeable than for the previous method; however, the mean classification performance for the whole test population did not change much between EMG states as appreciated in Fig. 4.18, TABLE 4.12, and TABLE 4.13. Pronation and supination continued to be the worst classified movement types from the set.

The tolerance to AWGN was tested for the transient EMG state on the two previously explained models. In order to test the performance with information that did not participate in the training state, a new recording was created by averaging the available ones. An example of this is shown in Fig. 4.19. These new recordings were contaminated using different noise levels calculated relative to the signal's power. The result of contamination for different noise percentages in both the time and frequency domains appears in Fig. 4.20.

The model using Hjorth's parameters showed a greater tolerance to white noise (see Fig. 4.21). Mean classification performance decreased approximately 1.5% when 50% noise was added relative to the signal's power. In the case of the model using DWT's variance, classification performance decreased a bit more abruptly (approximately 4.5% as it can be inferred from TABLE 4.14); however, it still showed a good tolerance. This could be associated to the performance of the de-noising algorithm that was applied for pre-processing. In the case of Hjorth's parameters, the fact that they are calculated as ratios of time variances could also suggest that they help in noise cancelling. More tests should be made on this matter in order to solidly conclude on the reaction that this parameters have with respect to noise.

Finally, a third method was tested for transient state analysis. It consisted in using PCA to reduce wavelet coefficients extracted from the first three levels of decomposition as previously explained in Chapter III. This method is similar to that reported in [9,27,70]. Fig. 4.22 shows the mean classification performance per subject and Fig. 4.23 the mean

classification for each movement type. The obtained performance using this method was lower than previously reported ones. As shown in TABLE 4.15 and later in Fig. 4.25, this method had the highest standard deviation between subjects for almost every movement type.

The method using Hjorth's parameters clearly outperformed the other two as presented in Fig. 4.24 and TABLE 4.16. It presented the highest classification percentages for every movement type and the lowest standard deviations between subjects. This suggests it is worthy to continue studying the performance that Hjorth's parameters have in EMG analysis.

Finally, a flow diagram of a proposed control algorithm is presented in Fig. 4.26. As initially mentioned in the discussion, in order to make on-line analysis, a reliable method for detection of the onset of the muscle contraction should be implemented. The aforementioned analysis has proven that the first 128 ms of the transient EMG state contain relevant information as to be able to classify different movement types; however, it was also seen that wider sections provide more representative information from the signal. The algorithm suggests using 3 windows of 128 ms with 50% overlap for feature extraction (using Hjorth's parameters) before feeding the classifier. This would represent an overall delay of 256 ms that is still fitted within the real-time constrain and would ensure a better accuracy in the classifier's decision. The future objective would be to extrapolate the control signal used for the virtual model to control a myoelectric prosthetic device and moreover, be able to extrapolate the whole system to be controlled by an amputee user.

Conclusions and Future Work

It has been widely discussed whether or not the transient state of the muscle contraction contains enough relevant information as to accurately discriminate between different types of motions. Most myoelectric controlled devices have been based on the assumption that there is no information in the instantaneous value of the MES; therefore, it is necessary to wait until a sustained stable contraction is reached in order to generate the control signal and start actuating the device, which is not desirable in a clinical application. The present study reaffirms the existence of deterministic components within the onset part of the muscle contraction as initially proposed by Hudgins *et al.* [6], and the fact that the information is relevant enough as to discriminate between the proposed movements.

Hjorth's parameters seem to adapt well enough to the nature of myoelectric signals as to extract highly representative information from them; moreover, the classification performance obtained from the transient and steady EMG states does not differ much between them as it has been previously reported using other methods.

The fact that Hjorth's parameters are a time domain analysis technique implies simpler processing and makes it more suitable for continuous on-line calculations as compared to frequency domain methods that normally require complex transformations. Furthermore, the analyzed data proved to contain significant information as to be able to classify the movements within the first 128 ms of the onset of the contraction. Movement classification was more accurate when using 256 ms windows for feature extraction; however, this value gets really close to the clinically recognized maximum delay for real-

time applications (200 to 300 ms), and the total system's delay has yet to be considered. Therefore, a 128 ms window, which yielded an average classification percentage higher than 95%, seems to provide a good compromise between system's accuracy and response time.

Even if classification is slightly higher when using the steady state of the EMG signal, including transient MES information can lead to more robust usability and performance. If the system is capable of identifying the transient EMG state, the subject is simply prompted to perform a contraction in a natural manner instead of needing long training periods to learn how to make sustained stable contractions to control the device. Moreover, changing from one position to another should be possible without going to an intermediate inactive position. If transitions are included in the training data, the need to constrain the subject to be in a steady state position prior to data collection could be eliminated. As proposed by [80], the classification error should not be the sole measure to evaluate a system's usability and performance.

Design of clinical devices cannot be focused only on using the highest technology, but it should be intimately related to the patient's needs and demands. It is necessary to communicate with the patient during the whole developing process in order to come up with solutions that will adapt as closely as possible to the patient's needs. The acceptance of a myoelectric controlled system by the user depends on a number of factors including client motivation, control complexity, and system reliability [64]. Therefore, to develop a useful device that has a successful acceptance by the user, none of these criteria should be left aside.

It is true that recording multichannel EMG signals requires a higher computational cost; however, it provides localized information at several muscle sites, and it has the advantage that the positions of the electrodes become less critical. If there is noise

affecting one of the channels, or one of the electrodes moves slightly, the system still relies in the information from the rest of the channels; whereas for a single-channel system, all the information would be lost.

The use of Hjorth's parameters for EMG analysis seems a promising alternative for movement classification using both the steady and transient EMG states. Being able to identify which is the desired movement from the beginning of the contraction is in fact a predictive technique that has the potential of reducing significantly the delay when actuating a myoelectric controlled device. In a future, this could result on a more natural control capable of identifying in real-time the user's movement intention.

5.1 Future Work

Even if this work represents an advance in EMG signal processing, there is still a lot to be done. As future work, it would be important to consider the following aspects:

- Use a greater number of subjects to test the algorithm's performance.
- Test the virtual model control during on-line analysis while the subject has the electrodes on instead of using the signals in the database.
- Develop a reliable method to automatically identify the onset of the contraction regardless of the noise affecting the system. This will allow the system to identify when the contraction is being generated and hence to automatically initiate feature extraction in order to generate the control signal.
- Increase the number of movements to identify, and test the system's performance using combined movements.

- Define the tolerance in electrode displacement with respect to each muscle in order to continue obtaining acceptable results.
- Test reducing the number of channels, and determine which is the best as to accurately classify the movements of interest.
- Test tolerance to noise on the on-line analysis application.
- Make EMG recordings including changes from one movement to another without passing through an inactive state. This will allow testing the model's robustness. It could also be helpful to train the ANN model using data from both the transient and steady states in order to evaluate if classification accuracy increases and if it is easier to identify the transitions between movements.
- In the present database, the movement speed was not considered during data recording; therefore, it was assumed to be more or less constant throughout the whole database. It would be important to evaluate the model's performance when the movements are executed at various speeds. For this matter, inclusion of accelerometers in the arm's joints for speed monitoring while making data collection is proposed.
- Evaluate the system's performance in data recorded from amputee subjects.
- Extrapolate the system to amputees considering how to position the electrodes in the stump, and evaluate whether it is feasible to keep the same number of EMG channels.
- Implement the control algorithm in a myoelectric controlled prosthesis, and test it during on-line analysis for both normally limbed subjects and amputees.

It is important to continue research on the field to eventually be able to develop a reliable, on-line myoelectric controlled system that will allow amputees replacing the lost functions as most naturally as possible and will help them improve their quality of life.

References

- [1] M. Zecca, S. Micera, M. C. Carrozza, and P. Dario, "Control of multifunctional prosthetic hands by processing the electromyographic Signal," *Critical Reviews in Biomedical Engineering*, vol. 30, no. 4-6, pp. 459-485, 2002.
- [2] H. A. Romo, J. C. Realpe, and P. E. Jojoa, "Surface EMG signals analysis and its applications in hand prosthesis control," *Revista Avances en Sistemas e Informática*, vol. 4, no. 1, pp. 127-136, Jun. 2007.
- [3] D. Staudenmann, I. Kingma, D. F. Stegeman, and J. H. van Dieën, "Towards optimal multi-channel EMG electrode configurations in muscle force estimation: a high density EMG study," *Journal of Electromyography and Kinesiology*, vol. 15, pp. 1-11, 2005.
- [4] D. Desmond and M. MacLachlan, "Psychological issues in prosthetic and orthotic practice: a 25 year review of psychology in Prosthetics and Orthotics International," *Prosthetics and Orthotics International*, vol. 26, no. 3, pp. 182-188, 2002.
- [5] P. Chrapka, "EMG controlled hand prosthesis: EMG classification system," Bachelor of Engineering dissertation, Electrical and Biomed. Eng. Program, McMaster University, Hamilton, Ontario, Canada, 2010.
- [6] B. Hudgins, P. Parker, and R. N. Scott, "A new strategy for multifunction myoelectric control," *IEEE Trans. Biomed. Eng.*, vol. 40, no. 1, pp. 82-94, Jan. 1993.

- [7] M. F. Lucas, A. Gaufriau, S. Pascual, C. Doncarli, and D. Farina, "Multi-channel surface EMG classification using support vector machines and signal-based wavelet optimization," *Biomedical Signal Processing and Control*, vol. 3, no. 2, pp. 169-174, Apr. 2008.
- [8] R. Merletti, "Surface electromyography. Half a century of research," presented at the conference Outils et méthodes en traitement des signaux électromyographiques, Paris, 2013.
- [9] K. Englehart, B. Hudgins, and P. A. Parker, "A wavelet based continuous classification scheme for multifunction myoelectric control," *IEEE Trans. Biomed. Eng.*, vol. 48, pp. 302-311, 2001.
- [10] F. H. Y. Chan, Y. Yang, F. K. Lam, Y. Zhang, and P. A. Parker, "Fuzzy EMG classification for prosthesis control," *IEEE Transactions on Rehabilitation Engineering*, vol. 8, no. 3, pp. 305-311, Sept. 2000.
- [11] K. Englehart and B. Hudgins, "A robust, real-time control scheme for multifunction myoelectric control," *IEEE Trans. Biomed. Eng.*, vol. 50, no. 7, pp. 848-854, July 2003.
- [12] B. Karlik, M. O. Tokhi, and M. Alci, "A novel technique for classification of myoelectric signals for prosthesis," in *CD-ROM Proc. of the 15th Triennial World Congress of the International Federation of Automatic Control (IFAC)*, Barcelona, Spain, vol. 2, 2002.
- [13] U. Kuruganti, B. Hudgins, and R. N. Scott, "Two-channel enhancement of a multifunction control system," *IEEE Trans. Biomed. Eng.*, vol. 42, no. 1, pp. 109-111, Jan. 1995.

- [14] M. García, “Valoración de la electromiografía de superficie multicanal para el análisis de la mialgia de esfuerzo en músculos del antebrazo,” proyecto de fin de carrera. Escuela Técnica Superior de Ingeniería de Telecomunicaciones de Barcelona, Universidad Politécnica de Catalunya. Barcelona, 2010.
- [15] R. C. Miralles, M. Granados y X. Balcells, “Mano,” en *Biomecánica Clínica del Aparato Locomotor*, R. C. Miralles Marrero y M. Puig Cunillera, Ed. Masson, 1998, ch. 10, pp. 147-169.
- [16] C. L. Taylor and R. J. Schwarz, “The Anatomy and Mechanics of the Human Hand,” *Artificial Limbs*, vol. 2, no. 2, The Orthotics and Prosthetics Virtual Library Project, 1955, pp. 22-35.
- [17] N. Palastanga, D. Field y R. Siames, *Anatomía y Movimiento Humano. Estructura y Funcionamiento*. Barcelona, España, Ed. Paidotribo, 2000, pp. 161-172.
- [18] M. B. I. Raez, M. S. Hussain, and F. Mohd-Yasin, “Techniques of EMG signal analysis: detection, processing, classification and applications,” *Biol. Proced. Online*, vol. 8, no. 1, pp. 11-35, March 2006.
- [19] J. Rafiee, M. A. Rafiee, F. Yavari, and M. P. Schoen, “Feature extraction of forearm EMG signals for prosthetics,” *Expert Systems with Applications*, vol. 38, pp. 4058-4067, 2011.
- [20] M. Khezri and M. Jahed, “Real-time intelligent pattern recognition algorithm for surface EMG signals,” *Biomed. Eng. Online*, vol. 6, no. 45, Dec. 2007.
- [21] R. André Mezzarane, L. Abdala Elias, F. Henrique Magalhães, V. Martins Chaud, and A. Fabio Kohn, “Experimental and simulated EMG responses in the study of the human spinal cord,” in *Electrodiagnosis in New Frontiers of Clinical Research*, InTech, 2013, ch. 4, pp. 57-87.

- [22] C. J. De Luca, *Surface Electromyography: Detection and Recording*. Boston, DelSys Incorporated, 2002, pp. 1-10.
- [23] A. Merlo, D. Farina, and R. Merletti, "A fast and reliable technique for muscle activity detection from surface EMG signals," *IEEE Transactions on Biomedical Engineering*, vol. 50, no. 3, pp. 316-323, March 2003.
- [24] L. Chun-Lin, (2010, Feb. 23). *A Tutorial of the Wavelet Transform*. [Online]. Available: <http://disp.ee.ntu.edu.tw/tutorial/WaveletTutorial.pdf>
- [25] M. Flanders, "Choosing a wavelet for single-trial EMG," *Journal of Neuroscience Methods*, vol. 116, pp. 165-177, February 2002.
- [26] J. Altmann, (1996). *Surfing the Wavelets. Wavelets Basics*, École Polytechnique Fédérale de Laussane. [Online]. Available: <http://www.wavelet.org/tutorial/wbasic.htm>
- [27] J. Camacho Navarro, F. León-Vargas, and J. Barrero Pérez. "EMG-Based system for basic hand movement recognition," *Dyna*, vol. 79, no. 171, pp. 41-49, February 2012.
- [28] J. Shlens, (2009, April 22). *A Tutorial on Principal Component Analysis*. Version 3.01. [Online]. Available: <http://www.sn1.salk.edu/~shlens/pca.pdf>
- [29] L. I. Smith, (2002, Feb. 26). *A tutorial on Principal Component Analysis*. [Online]. Available: http://www.cs.otago.ac.nz/cosc453/student_tutorials/principal_components.pdf

- [30] B. Hjorth, "Technical contribution. The physical significance of time domain descriptors in EEG analysis," *Electroencephalography and Clinical Neurophysiology*, vol. 34, pp. 321-325, 1973.
- [31] P. P. Balestrassi, A. P. Paiva, A. C. Zambroni de Souza, J. B. Turrioni, and E. Popova, "A multivariate descriptor method for change-point detection in nonlinear time series," *Journal of Applied Statistics*, vol. 38, no. 2, pp. 327-342, February 2011.
- [32] B. Hjorth, "EEG analysis based on time domain properties," *Electroencephalography and Clinical Neurophysiology*, vol. 29, no. 3, pp. 306-310, September 1970.
- [33] T. Cecchin, R. Ranta, L. Koessler, O. Caspary, H. Vespignani, and L. Maillard, "Seizure lateralization in scalp EEG using Hjorth parameters," *Clinical Neurophysiology*, vol. 121, pp. 290-300, 2010.
- [34] M. Mouzé-Amady and F. Horwat, "Evaluation of Hjorth parameters in forearm surface EMG analysis during an occupational repetitive task," *Electroencephalography and Clinical Neurophysiology*, vol. 101, pp. 181-183, 1996.
- [35] F. Aparisi and C. L. Haro, "Hotelling's T^2 control chart with variable sampling intervals," *International Journal of Production Research*, vol. 39, no. 14, pp. 3127-3140, 2001.
- [36] W. Spehr, H. Sartorius, K. Berglund, B. Hjorth, C. Kablitz, U. Plog, P. G. Wiedermann, K. Zapf, "EEG and haemodialysis. A structural survey of EEG spectral analysis, Hjorth's EEG descriptors, blood variables and psychological data," *Electroencephalography and Clinical Neurophysiology*, vol. 43, no. 6, pp. 787-797, December 1977.

- [37] A. Persson and B. Hjorth, "EEG topogram – an aid in describing EEG to the clinician," *Neurophysiology*, vol. 56, no. 5, pp. 399-405, November 1983.
- [38] O. Kanno and P. Clarenbach, "Effect of clonidine and yohimbine on sleep in man: Polygraphic study and EEG analysis by normalized slope descriptors," *Electroencephalography and Clinical Neurophysiology*, vol. 60, no. 6, pp. 478-484, June 1985.
- [39] W. Spehr, G. Stemmler, "Postalcoholic diseases: Diagnostic relevance of computerized EEG," *Electroencephalography and Clinical Neurophysiology*, vol. 60, no. 2, pp. 106-114, February 1985.
- [40] H. Depoortere, D. Francon, P. Granger, M. G. Terzano, "Evaluation of the stability and quality of sleep using Hjorth's descriptors," *Physiology & Behavior*, vol. 54, no. 4, pp. 785-793, October 1993.
- [41] M. Ziller, K. Frick, W. M. Herrmann, S. Kubicki, I. Spieweg, and G. Winterer, "Bivariate global frequency analysis versus chaos theory," *Neuropsychobiology*, vol. 32, no. 1, pp. 45-51, 1995.
- [42] K. Ansari-Asl, G. Chanel, and T. Pun, "A channel selection method for EEG classification in emotion assessment based on synchronization likelihood," in *Proc. 15th European Signal Processing Conference (EUSIPCO 2007)*, EURASIP, Poznan, Poland, pp. 1241-1245, Sept. 2007.
- [43] S. Pourzare, O. Aydemir, and T. Kayikcioglu, "Classification of various facial movement artifacts in EEG signals," in *Proc. of the 35th International Conference on Telecommunications and Signal Processing (TSP)*, Prague, pp. 529-533, July 2012.

- [44] W. Szelenberger, J. Wackermann, M. Skalski, S. Niemcewicz, and J. Drojewski, "Analysis of complexity of EEG during sleep," *Acta Neurobiol. Exp.*, vol. 56, pp. 165-169, 1996.
- [45] C. Fyfe, "Artificial neural networks," in *Do Smart Adaptive Systems Exist?*, Springer Berlin - Heidelberg, 2005, ch. 4, pp. 57-79.
- [46] I. A. Basheer and M. Hajmeer, "Artificial neural networks: fundamentals, computing, design, and application," *Journal of Microbiological Methods*, vol. 43, pp. 3-31, 2000.
- [47] A. K. Jain, J. Mao, and K. M. Mohiuddin, "Artificial neural networks: A tutorial," *IEEE Computer*, vol. 29, no. 3, pp.31-44, Mar. 1996.
- [48] J. Dalton and A. Deshmane, "Artificial neural networks," *Potentials, IEEE*, vol. 10, no. 2, pp. 33-36, April 1991.
- [49] T. P. Vogl, J. K. Mangis, A. K. Rigler, W. T. Zink, and D. L. Alkon, "Accelerating the convergence of the back-propagation method," *Biol. Cybern.*, vol. 59, pp. 257-263, 1988.
- [50] N. Friedman, M. Linial, I. Nachman, and D. Pe'er, "Using bayesian networks to analyze expression data," *Journal of Computational Biology*, vol. 7, no. 3,4, pp. 601-620, 2000.
- [51] K. Englehart, B. Hudgins, M. Stevenson, and P. A. Parker, "Classification of myoelectric signal burst patterns using a dynamic neural network," in *Proc. of the 21st IEEE Annual Northeast Bioengineering Conference (NEBC)*, Bar Harbor, ME, pp. 63-64, May 1995.

- [52] K. Englehart, B. Hudgins, M. Stevenson, and P. A. Parker, "A dynamic feedforward neural network for subset classification of myoelectric signal patterns," in *Proc. of the 17th IEEE Annual Conference, Engineering in Medicine and Biology Society (IEMBS)*, Montreal, Que., vol. 1, pp. 819-820, Sept. 1995.
- [53] H. Liu, X. Chen, and Y. Chen, "Wavelet transform and real-time learning method for myoelectric signal in motion discrimination," in *Proc. of the 7th International Symposium on Measurement Technology and Intelligent Instruments*, Journal of Physics: Conference Series 13, pp. 250-253, 2005.
- [54] M. Gazzoni, D. Farina, and R. Merletti, "A new method for the extraction and classification of single motor unit action potentials from surface EMG signals," *Journal of Neuroscience Methods*, vol. 136, pp. 165-177, 2004.
- [55] S. Arlot and A. Celisse, "A survey of cross-validation procedures for model selection," *Statistics Surveys*, vol. 4, pp. 40-79, 2010.
- [56] R. Gutiérrez-Osuna, "Lecture 13: Cross-Validation", Introduction to Pattern Analysis, Texas A&M University, pp. 1-15, [Online].
Available: http://www.cs.tau.ac.il/~nin/Courses/NC05/pr_113.pdf
- [57] J. Kodovský, "Ensemble classification in steganalysis – Cross-validation and AdaBoost," *Technical report*, pp. 1-8, August 2011.
- [58] U. M. Braga-Neto and E. R. Dougherty, "Is cross-validation valid for small-sample microarray classification?," *Bioinformatics*, vol. 20, no. 3, pp. 374-380, 2004.
- [59] R. Kohavi, "A study of cross-validation and bootstrap for accuracy estimation and model selection," in *Proc. of the International Joint Conference on Artificial Intelligence (IJCAI)*, vol. 14, no. 2, pp. 1137-1145, August 1995.

- [60] N. A. Diamantidis, D. Karlis, and E. A. Giakoumakis, "Unsupervised stratification of cross-validation for accuracy estimation," *Artificial Intelligence*, vol. 116, pp. 1-16, 2000.
- [61] J. D. Rodríguez, A. Pérez, and J. A. Lozano, "Sensitivity analysis of k-fold cross validation in prediction error estimation," *IEEE Transactions on Pattern Analysis and Machine Intelligence*, vol. 32, no. 3, pp. 569-575.
- [62] R. Reiter, "A new electronic hand (Eine Neue ElektroKunsthand)," *Grenzgebiete der Medizin*, vol. 1, no. 4, pp. 133-135, 1948.
- [63] A. Attenberger and K. Buchenrieder, "Modeling and visualization of classification-based control schemes for upper limb prostheses," in *Proc. of the 19th IEEE International Conference and Workshops on Engineering of Computer-Based Systems (ECBS)*, IEEE Computer Society, Novi Sad, Serbia, pp.188-194, Apr. 2012.
- [64] P. Parker, K. Englehart, and B. Hudgins, "Myoelectric signal processing for control of powered limb prostheses," *Journal of Electromyography and Kinesiology*, vol. 16, pp. 541-548, 2006.
- [65] D. Graupe and W. Cline, "Functional separation of EMG signal via ARMA identification methods for prosthetic control purposes," *IEEE Trans. on Systems, Man and Cybernetics*, vol. SMC-5, no. 2, pp. 252-259, March 1975.
- [66] T. Basha, R. N. Scott, P. A. Parker, and B. S. Hudgins, "Deterministic components in the myoelectric signal," *Tech. Note, Med. & Biol. Eng. & Comput.*, vol. 32, pp. 233-235, 1994.

- [67] Y. Yamazaki, M. Suzuki, and T. Mano, "An electromyographic volley at the initiation of rapid isometric contractions of the elbow," *Brain Res. Bullet.*, vol. 30, pp. 181-187, 1993.
- [68] C. M. Light, P. H. Chappell, B. Hudgins, and K. Englehart, "Intelligent multifunction myoelectric control of hand prostheses," *Journal of Medical Engineering and Technology*, vol. 26, no. 4, pp. 139-146, 2002.
- [69] K. Englehart, B. Hudgins, P. A. Parker, and M. Stevenson, "Time-frequency representation for classification of the transient myoelectric signal," in *Proc. of the 20th Annual International Conference of the IEEE Engineering in Medicine and Biology Society (EMBS)*, Hong Kong, IEEE Press, vol. 20, no. 5, pp. 2627-2630, 1998.
- [70] K. Englehart, B. Hudgins, and P. A. Parker, "Time-frequency based classification of the myoelectric signal: static vs. dynamic contractions," in *Proc. of the 22nd Annual International Conference of the IEEE Engineering in Medicine and Biology Society (EMBS)*, Chicago, IL, IEEE Press, vol. 1, pp. 317-320, July 2000.
- [71] B. Hudgins, K. Englehart, P. A. Parker, and R. N. Scott, "A microprocessor-based multifunction myoelectric control system," in *Proc. of the 23rd Canadian Medical and Biological Engineering Society Conference*, Toronto, pp. 138-139, 1997.
- [72] F. H. Y. Chan, Y. Yang, F. K. Lam, Y. Zhang, and P. A. Parker, "Fuzzy EMG classification for prosthesis control," *IEEE Trans. Rehab. Eng.*, vol. 8, no. 3, pp. 305-311, Sept. 2000.
- [73] A. B. Ajiboye and R. F. Weir, "A heuristic fuzzy logic approach to EMG pattern recognition for multifunctional prosthesis control," *IEEE Trans. on Neural Systems and Rehabilitation Engineering*, vol. 13, no. 3, pp. 280-291, Sept. 2005.

- [74] S. Karlsson, J. Yu, and M. Akay, "Time-frequency analysis of myoelectric signals during dynamic contractions: a comparative study," *IEEE Trans. Biomed. Eng.*, vol. 47, no. 2, pp. 228-238, Feb. 2000.
- [75] D. Nishiwaka, W. Yu, H. Yokoi, and Y. Kakazu, "EMG prosthetic hand controller using real-time learning method," in *Proc. of the 1999 IEEE International Conference on Systems, Man, and Cybernetics (SMC '99)*, Tokyo, IEEE Press, vol. 1, pp. 153-158, Oct. 1999.
- [76] D. Nishiwaka, W. Yu, H. Yokoi, and Y. Kakazu, "EMG prosthetic hand controller discriminating ten motions using real-time learning method," in *Proc. of the 1999 IEEE/RSJ International Conference on Intelligent Robots and Systems (IROS '99)*, Kyongju, IEEE Press, vol. 3, pp. 1592-1597, Oct. 1999.
- [77] D. Nishiwaka, W. Yu, H. Yokoi, and Y. Kakazu, "On-line learning method for EMG prosthetic hand control," *Electron. Comm. Jpn.*, part 3, vol. 84, no. 10, pp. 35-46, 2001.
- [78] J. Chu, I. Moon, Y. Lee, S. Kim, and M. Mun, "A supervised feature-projection-based real-time EMG pattern recognition for multifunction myoelectric hand control," *IEEE/ASME Trans. on Mechatronics*, vol. 12, no. 3, pp. 282-290, June 2007.
- [79] Y. Huang, K. B. Englehart, B. Hudgins, and A. D. C. Chan, "A Gaussian mixture model based classification scheme for myoelectric control of powered upper limb prostheses," *IEEE Trans. Biomed. Eng.*, vol. 52, no. 11, pp. 1801-1811, Nov. 2005.
- [80] L. Hangrove, Y. Losier, B. Lock, K. Englehart, and B. Hudgins, "A real-time pattern recognition based myoelectric control usability study implemented in a virtual environment," in *Proc. of the 29th Annual International Conference of the*

IEEE Engineering in Medicine and Biology Society (EMBS 2007), Lyon, France, IEEE Press, pp. 4842-4845, Aug. 2007.

- [81] L. Hangrove, K. Englehart, and B. Hudgins, "A comparison of surface and intramuscular myoelectric signal classification," *IEEE Trans. Biomed. Eng.*, vol. 54, no. 5, pp. 847-853, May 2007.
- [82] K. Davidge, "Multifunction myoelectric control using a linear electrode array," M.Sc. dissertation, Electronics and Electrical Engineering, University of New Brunswick, Canada, 2005.
- [83] M. León Ponce, "Desarrollo de un sistema para la identificación de 7 movimientos de la mano basado en la señal mioeléctrica del antebrazo," tesis de M. en C., Sección de Bioelectrónica, Departamento de Ingeniería Eléctrica, Centro de Investigación y de Estudios Avanzados del Instituto Politécnico Nacional (CINVESTAV), México, D.F., 2003.
- [84] J. A. Barraza Madrigal, "Desarrollo de una prótesis virtual para extremidad superior con amputación por arriba de la articulación del codo," tesis de M. en C., Sección de Bioelectrónica, Departamento de Ingeniería Eléctrica, Centro de Investigación y de Estudios Avanzados del Instituto Politécnico Nacional (CINVESTAV), México, D.F., 2010.
- [85] A. D. Moreno Pérez, "Desarrollo de control para una prótesis de brazo con cuatro grados de libertad activos y actuadores paralelos," tesis de M. en C., Sección de Bioelectrónica, Departamento de Ingeniería Eléctrica, Centro de Investigación y de Estudios Avanzados del Instituto Politécnico Nacional (CINVESTAV), México, D.F., 2010.
- [86] A. P. Márquez Lázaro, "Estrategia para la descomposición de señales mioeléctricas basadas en las técnicas de transformada wavelet y vector soporte,"

tesis de M. en C., Sección de Bioelectrónica, Departamento de Ingeniería Eléctrica, Centro de Investigación y de Estudios Avanzados del Instituto Politécnico Nacional (CINVESTAV), México, D.F., 2011.

- [87] A. Ramírez García, "Implementación funcional de una prótesis para un amputado por encima del codo," tesis de Dr. en C., Sección de Bioelectrónica, Departamento de Ingeniería Eléctrica, Centro de Investigación y de Estudios Avanzados del Instituto Politécnico Nacional (CINVESTAV), México, D.F., 2011.
- [88] A. Ramírez-García, L. Leija, and R. Muñoz, "Active upper limb prosthesis based on natural movement trajectories," in *Prosthetics and Orthotics International*, vol. 34, no. 1, pp. 58-72, 2010.
- [89] D. A. Meléndrez Armada, "Sistema electrónico para el desarrollo, evaluación e implementación de algoritmos de control para una prótesis de cuatro grados de libertad," tesis de M. en C., Sección de Bioelectrónica, Departamento de Ingeniería Eléctrica, Centro de Investigación y de Estudios Avanzados del Instituto Politécnico Nacional (CINVESTAV), México, D.F., 2012.
- [90] M. León Ponce, "Clasificación de patrones mioeléctricos para la operación de un dispositivo antropomórfico," tesis de Dr. en C., Sección de Bioelectrónica, Departamento de Ingeniería Eléctrica, Centro de Investigación y de Estudios Avanzados del Instituto Politécnico Nacional (CINVESTAV), México, D.F., 2012.
- [91] M. León, J. M. Gutiérrez, L. Leija, R. Muñoz, J. M. de la Cruz, and M. Santos, "Multiclass motion identification using myoelectric signals and support vector machines," in *Proc. of the 2011 Third World Congress on Nature and Biologically Inspired Computing (NaBIC)*, Salamanca, pp. 189-194, Oct. 2011.
- [92] C. M. Stein, "Estimation of the mean of a multivariate normal distribution," *The Annals of Statistics*, vol. 9, no. 6, pp. 1135-1151, 1981.

- [93] D. L. Donoho, "De-noising by soft-thresholding," *IEEE Transactions on Information Theory*, vol. 41, no. 3, pp. 613-627, May 1995.
- [94] D. L. Donoho and I. M. Johnstone, "Ideal spatial adaptation by wavelet shrinkage," *Biometrika Trust*, vol. 81, no. 3, pp. 425-455, Aug. 1994.
- [95] X. Zhang and M. D. Desai, "Adaptive denoising based on SURE risk," *IEEE Signal Processing Letters*, vol. 5, no. 10, pp. 265-267, Oct. 1998.
- [96] S. Wang, X. Liu, J. Yianni, T. Z. Aziz, J. F. Stein, "Extracting burst and tonic components from surface electromyograms in dystonia using adaptive wavelet shrinkage," *Journal of Neuroscience Methods*, vol. 139, pp. 177-184, 2004.
- [97] I. M. Johnstone and B. M. Silverman, "Wavelet threshold estimators for data with correlated noise," *J. R. Statist. Soc. B*, vol. 59, no. 2, pp. 319-351, 1997.
- [98] D. L. Donoho and I. M. Johnstone, "Adapting to unknown smoothness via wavelet shrinkage," *J. Amer. Stat. Assoc.*, vol. 90, pp. 1200-1224, 1995.
- [99] J. A. Barraza-Madriral, A. Ramírez-García, R. Muñoz-Guerrero, "A virtual upper limb prosthesis as a training system," in *Proc. Of the 2010 7th International Conference on Electrical, Computing Science and Automatic Control (CCE 2010)*, Tuxtla Gutierrez, Mexico, pp. 210-215, Sept. 2010.
- [100] J. A. Barraza-Madriral and R. Muñoz-Guerrero, "Virtual system for training and evaluation of candidates to use a myoelectric prosthesis," in *Proc. of the 2011 Pan American Health Care Exchanges (PAHCE)*, Rio de Janeiro, Brasil, pp. 225-230, March 2011.

- [101] C. D. Binnie, R. Brown, D. S. L. Lloyd, and M. Smith, "Some electroencephalographic and psychological findings in minimal hepatic encephalopathy," *Electroenceph. Clin. Neurophysiol.*, vol. 34, 108 p., 1973.
- [102] B. Hannaford and S. Lehman, "Short Time Fourier Analysis of the Electromyogram: Fast Movements and Constant Contraction," *IEEE Trans. Biomed. Eng.*, vol. BME-33, no. 12, pp. 1173-1181, Dec. 1986.

Submitted Papers

Papers submitted in international conferences.

First Paper (Accepted)

M. Pla Mobarak, R. Muñoz Guerrero, J. M. Gutiérrez Salgado, and V. Louis Dorr, “Hand movement classification using transient state analysis of surface multichannel EMG signal,” in *2014 Pan American Health Care Exchanges (PAHCE)*, Brasilia, Brazil, April 2014.

Second Paper (Submitted – Waiting for reply)

M. Pla Mobarak, J. M. Gutiérrez Salgado, R. Muñoz Guerrero, and V. Louis Dorr, “Transient state analysis of the multichannel EMG signal using Hjorth’s parameters for identification of hand movements,” in *Ninth International Multi-Conference on Computing and Global Information Technology (ICCGI 2014)*, Seville, Spain, June 2014.

Hand movement classification using transient state analysis of surface multichannel EMG signal

M. Pla Mobarak¹, R. Muñoz Guerrero¹, J. M. Gutiérrez Salgado¹, V. Louis Dorr²

¹Department of Electrical Engineering, Bioelectronics Section, CINVESTAV-IPN, Mexico D.F., Mexico

²Centre de Recherche en Automatique de Nancy (CRAN), CNRS : UMR7039 - University of Lorraine, Nancy, France

Email: ¹{mpla, rmunoz, mgutierrez}@cinvestav.mx, ²valerie.louis@univ-lorraine.fr

Abstract — This paper presents two methods for the classification of six different hand motions based on the analysis of the transient state of surface multichannel electromyographic signals recorded from 10 normally limbed subjects. The signals were classified using the coefficients extracted from a discrete wavelet transform analysis. While the first method uses a feature vector based on the variance of the wavelet coefficients, the second analysis considers a PCA treatment focused on dimensionality reduction. These vectors were used to feed an artificial neural network. The first method was applied for both the transient and steady states obtaining an average classification accuracy of 89.43% (SD 2.05%) and 91.86% (SD 3.17%) respectively. The second method gave a classification accuracy of 92.58% (SD 3.07%) for the transient state. This proves the existence of deterministic information within the transient state of the EMG signal and the possibility to classify different movements since the beginning of the muscle contraction.

Keywords — Discrete Wavelet Transform, EMG steady state, EMG transient state, principal component analysis, surface multichannel EMG

I. INTRODUCTION

Surface electromyography (sEMG) is widely used in different areas of the biomedical field such as rehabilitation, clinical diagnosis of neuromuscular disorders, prosthesis control, among many others. Its popularity has increased due to the relative simplicity of signal acquisition and its possibility to be non-invasive.

One of the main challenges when using myoelectric control is subject dependency. This occurs because the myoelectric signal (MES) is based on the anatomical and physiological properties of muscles, which vary between subjects [1,2]. Moreover, when extrapolating the system to high-level amputees, several electrode sites are hard or even not possible to locate [3].

Since the 1940's [4,5], research on the use of sEMG for upper limb prosthesis control has been conducted. However, most prosthetic devices have been designed using a limited number of channels, which can only control a reduced number of degrees of freedom (DoFs). This has motivated the research on multichannel systems.

Although multichannel signal processing requires a greater use of computational resources, it provides a better representation of the real muscle activity in the collected signal, reducing EMG variability and improving its quality [6].

The sEMG signal is stochastic due to the random summation of motor unit action potential (MUAP) trains within the capturing region of the electrodes; however, two main states can be well distinguished during a muscle contraction as shown in Fig. 1. The transient state is described as the bursts of myoelectric activity that accompany sudden muscular effort, while the steady state consists of a constant firing rate and corresponds to the muscular effort during a sustained contraction when the movement's final position is reached and the muscle length is no longer modified [7].

Myoelectric controlled systems are usually based on the premise that there is no information in the instantaneous value of the MES due to its stochastic nature. However, the steady state contains very little temporal structure of the active modification of recruitment and firing patterns involved in the contraction, which can be found within the transient state [3,5]. This suggests that the EMG transient state analysis could provide with useful information for classification while the muscle contraction is being generated, and constitutes the main motivation for this study. Basha *et al.* [8] and Yamazaki *et al.* [9] found further evidence of deterministic components in the transient state of the MES.

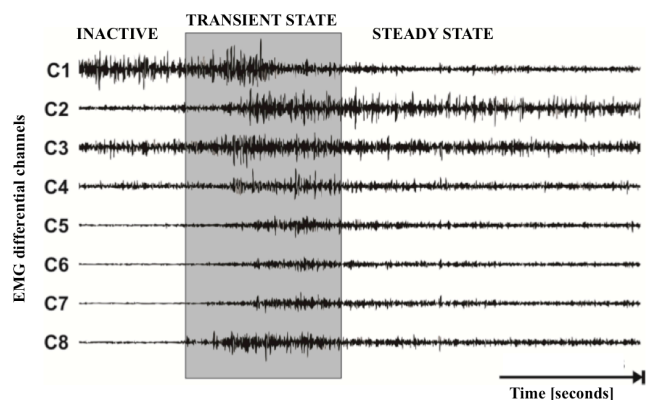


Fig. 1. Two main states found in EMG signals. They appear identified in an 8-channel EMG record of hand closure [10].

In 1993, Hudgins *et al.* [3] proposed a new control strategy for artificial devices introducing the analysis of the transient state of the EMG signal. This work was based on the observation that there is considerable structure in the MES during the onset of a contraction, which changes between different limb movements. They were able to discriminate between four movements (elbow flexion/extension and medial/lateral humeral rotation) using just one bipolar electrode. They obtained roughly 90% accuracy. A few years later, Englehart *et al.* [11-13] introduced the use of wavelet transform (WT) and wavelet packet transform (WPT) for classification of EMG signals. They compared these methods to the short-time Fourier transform (STFT) and the time domain feature set (TD) obtaining the best performance from WT and WPT. They applied principal component analysis (PCA) for data dimensionality reduction. Their results showed a significant improvement in classification using four channels as compared to two. They also classified more accurately the steady state data than the transient data. Nonetheless, there are still unanswered questions about the information contained within the onset part of the muscle contraction that continue to motivate future research.

This paper will provide a detailed description of the methods that were followed to analyze the EMG signals collected from 10 subjects in order to identify six different hand motions. The results from each of the participants will be presented and subsequently discussed in relation to previous works. Finally, we will comment on some ideas about the future work that can be done.

II. METHODOLOGY

A. Data Acquisition Protocol

The EMG data for this study was obtained from the database used in [10]. The signals were collected using 8 differential channels placed on the dominant forearm of 10 normally limbed subjects, aged between 23 and 50, and with no register of neuromuscular disorders. Each subject was asked to repeat five times six different hand motions, namely hand opening/closing, wrist pronation/supination, and wrist flexion/extension. A one-minute rest was given after concluding each set of six movements in order to avoid muscle fatigue.

Each recording is 20 seconds in length. It starts with the subject's forearm in an inactive position followed by the dynamic part of the contraction, and finished by sustaining the movement in the final position until the end of the recording. In order to standardize electrode positioning, each subject was asked to repeatedly close and open the hand until the desired muscles, which are mentioned in table I, were localized. The skin was carefully cleaned, and eight

pairs of Ag-AgCl surface electrodes (model VERMED NeuroPlus A10043) with an inter-electrode distance of 1.5 cm were located in the designated areas. The reference electrode was subsequently placed on the elbow. The electrode disposition that was used can be seen in Fig. 2.

TABLE I
FOREARM MUSCLES RECORDED BY EACH EMG DIFFERENTIAL CHANNEL

EMG Channel	Forearm Muscle
1	Extensor digitorum communis
2	Extensor carpi ulnaris
3	Differential measure between extensor digitorum communis and extensor carpi ulnaris
4	Extensor carpi radialis longus
5	Brachioradial
6	Flexor carpi radialis
7	Palmaris longus
8	Flexor carpi ulnaris

Written consent was obtained from every subject before starting the study. A test session, consisting of explaining the protocol to the participants and making amplification gain calibration of the eight differential EMG channels, was made previous to the actual recording of the signals. Each participant was asked to perform the study in a standing position with the dominant arm extended to the front and the hand relaxed in order to reduce variability.

The acquisition system consisted of 8 differential channels with adjustable amplification gain and a first order analog band-pass filter with a low cut-off frequency of 20 Hz and a high cut-off frequency of 400 Hz. Each analog output was connected to a National Instruments acquisition card (model DAQ-Card 6024E) for 12-bit A/D conversion. The sampling rate was 1024 Hz.

B. Data Processing

The EMG data was processed and analyzed using MATLAB® (version R2012b). Each recording was divided by supervision in transient and steady states as shown in Fig.1. A hamming window of 256 ms with 50% overlapping was applied in order to define each segment for feature extraction. A multisignal denoising algorithm using the principle of Stein's unbiased risk was applied to each segment, and rescaling was made using a noise level dependent estimation.

Since the information channel of the sEMG signal goes from 20-500 Hz, but the main concentration of energy is located within the frequency band of 50-150 Hz [1,7], the signal was decomposed until the third level. For a sEMG signal sampled at 1024 Hz, the components of interest are mainly located within the second and third levels of decomposition as shown in table II.

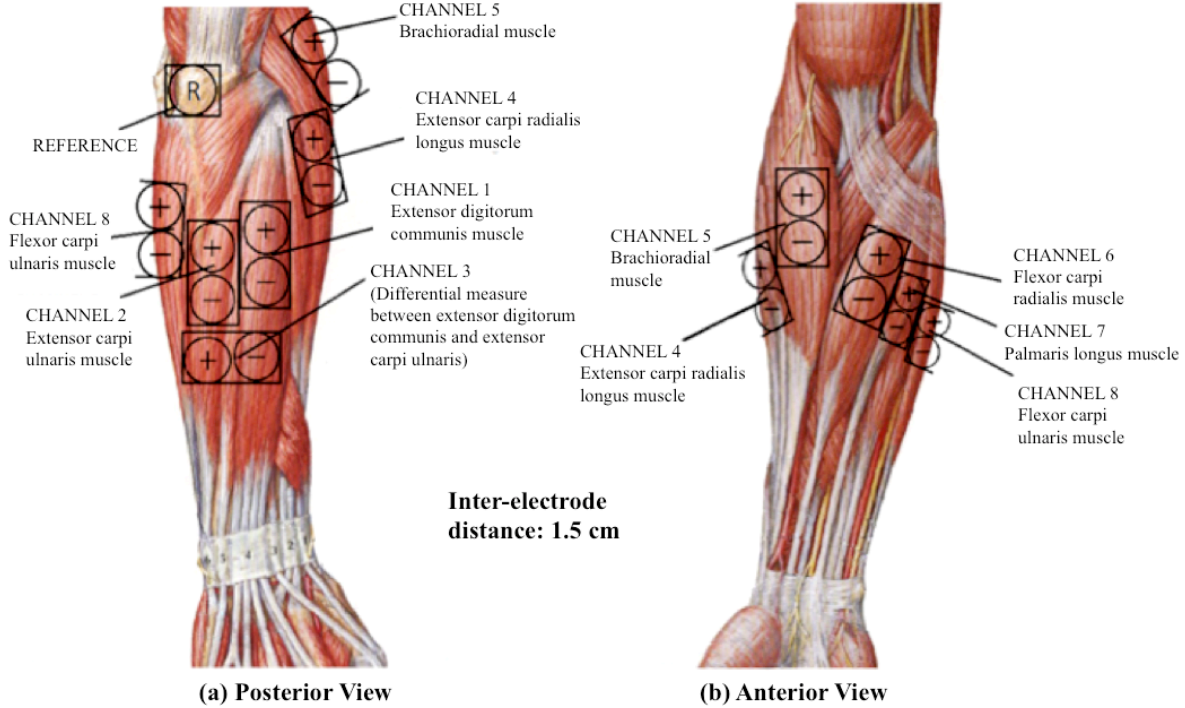


Fig. 2. Posterior (a) and anterior (b) views of electrode placement for EMG signal recording.

The discrete wavelet transform (DWT) analysis was applied using a fourth order Coiflet mother wavelet that has been proven to yield better accuracy for EMG analysis [13]; this was also tested experimentally.

TABLE II
DECOMPOSITION LEVEL AND CORRESPONDING FREQUENCY RANGE OF SEMG SAMPLED AT 1024 Hz

DECOMPOSITION LEVEL	FREQUENCY RANGE [Hz]
1 st Level	256 to 512
2 nd Level	128 to 256
3 rd Level	64 to 128
4 th Level	32 to 64
5 th Level	16 to 32

The two methods followed for discriminating between six different hand movements are described below.

C. First Method

The feature vector for this method was created extracting the variance from the detail coefficients obtained from the second and third levels of decomposition after the discrete wavelet analysis was applied. The variance was extracted as an approach to preserve the tendency of the coefficients but reducing the size of the feature vector.

This method was a both applied to the transient and steady states of each EMG recording. The feature vector was normalized for each of the extracted characteristics.

D. Second Method

This method was only applied to the transient state of the EMG signals. The procedure that was followed is similar as the one described in [12]; however, the procedure for the first method is a novel proposal. In this case, the feature vector was created using the detail coefficients of the first three levels of decomposition, and the approximation coefficients of the third level. Principal component analysis (PCA) was applied in order to reduce dimensionality of the data.

E. Artificial Neural Network's Parameters

To build the classifier models, different artificial neural networks were trained using a Bayesian regulation back-propagation algorithm. Final architecture depends of the available feature vector. In this way, the hidden layer consisted of 10 neurons for the first method and 15 neurons for the second one. In both cases, the network output was binary codified. The number of neurons established for both models was determined based on experimental testing.

In order to evaluate the network's performance, K-fold cross-validation (k = 5) process was carried out.

III. RESULTS

The results of each of the aforementioned methods are presented in this section. The different movements that were considered for the study are illustrated in Fig. 3. There are six different movements condensed in three classes, each of them consisting of an agonist and an antagonist movement labeled as stated in table III.

TABLE III
MOVEMENTS USED FOR CLASSIFICATION

Class	Movement 1 (Agonist)	Movement 2 (Antagonist)
I	Hand Closing (C)	Hand Opening (O)
II	Wrist Pronation (P)	Wrist Supination (S)
III	Wrist Flexion (F)	Wrist Extension (E)

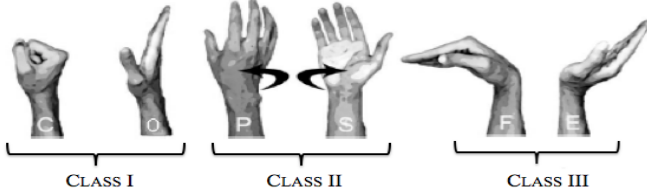


Fig. 3. Three classes of antagonist movements analyzed in this study. The first class includes hand closing/opening, the second one wrist pronation/supination, and the third one consists of wrist flexion/extension [10].

The following tables contain the classification percentages obtained for each of the methods that were applied. These percentages were calculated by quantifying the number of windows of 256 ms in length that were correctly identified by the classifier for each of the corresponding movements.

Tables IV and V respectively present the results obtained from the first method applied to the transient and the steady states of the EMG signal. Both tables condense the mean classification results for each type of movement within a population of 10 subjects and the standard deviation (SD) found between them. The last column contains the total mean classification per subject.

Table VI shows a comparison between the mean classification obtained from the 10 subjects when using the transient state (first column) and the steady state (second column). Each row stands for each of the movements that were classified. The last two rows contain the mean and standard deviation. This information is graphically represented in Fig. 4.

A. First Method – Transient State

TABLE IV
PERCENTAGE CLASSIFICATION ACCURACY USING THE FIRST METHOD APPLIED TO THE TRANSIENT STATE OF THE EMG SIGNAL

Subj.	C	O	P	S	F	E	Mean
1	88.57	91.43	81.43	81.43	97.14	90.00	88.33
2	97.14	92.86	95.71	90.00	92.86	90.00	93.10
3	92.86	95.71	95.71	82.86	97.14	80.00	90.71
4	90.00	92.86	88.57	80.00	97.14	88.57	89.52
5	85.71	90.00	75.71	90.00	98.57	95.71	89.29
6	82.86	91.43	75.71	70.00	95.71	94.29	85.00
7	95.71	87.14	77.14	77.14	100.00	95.71	88.81
8	91.43	94.29	82.86	91.43	95.71	88.57	90.71
9	91.43	92.86	85.71	84.29	95.71	87.14	89.52
10	91.43	90.00	94.29	78.57	95.71	85.71	89.29
Mean	90.71	91.86	85.29	82.57	96.57	89.57	89.43
SD	4.27	2.43	8.03	6.69	1.93	4.86	2.05

B. First Method – Steady State

TABLE V
PERCENTAGE CLASSIFICATION ACCURACY USING THE FIRST METHOD APPLIED TO THE STEADY STATE OF THE EMG SIGNAL

Subj.	C	O	P	S	F	E	Mean
1	97.14	94.29	91.43	94.29	97.14	92.86	94.52
2	98.57	98.57	94.29	87.14	98.57	100.00	96.19
3	95.71	91.43	90.00	64.29	100.00	74.29	85.95
4	92.86	88.57	91.43	84.29	98.57	95.71	91.90
5	88.57	98.57	75.71	84.29	100.00	94.29	90.24
6	92.86	94.29	84.29	90.00	100.00	95.71	92.86
7	94.29	82.86	92.86	97.14	94.29	90.00	91.90
8	90.00	97.14	91.43	95.71	97.14	85.71	92.86
9	100.00	98.57	91.43	87.14	100.00	90.00	94.52
10	92.86	85.71	81.43	82.86	95.71	87.14	87.62
Mean	94.29	93.00	88.43	86.71	98.14	90.57	91.86
SD	3.63	5.69	5.96	9.36	2.03	7.17	3.17

TABLE VI
COMPARISON BETWEEN CLASSIFICATION APPLYING THE FIRST METHOD TO TRANSIENT AND STEADY STATES OF THE EMG DATA

Movement	Transient State	Steady State
Hand Closing	90.71%	94.29%
Hand Opening	91.86%	93.00%
Wrist Pronation	85.29%	88.43%
Wrist Supination	82.57%	86.71%
Wrist Flexion	96.57%	98.14%
Wrist Extension	89.57%	90.57%
Mean	89.43%	91.86%
SD	2.05%	3.17%

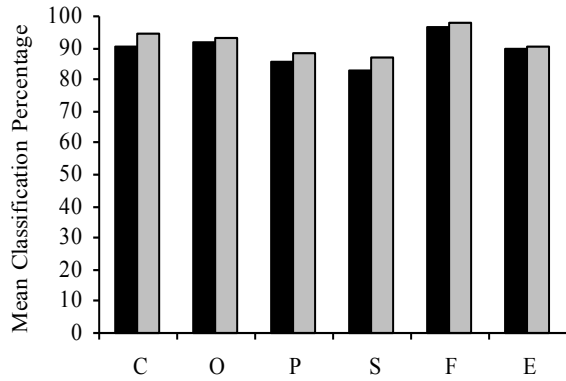


Fig. 4. Comparison between classification accuracy for the first method using EMG transient state (black) and EMG steady state (gray).

The mean classification results obtained by applying the second method to the transient state of the EMG signal are presented in table VII. A further comparison between the classification accuracy of both methods is shown in table VIII, where each column contains the results from the first and second methods respectively.

C. Second Method – Transient State

TABLE VII
PERCENTAGE CLASSIFICATION ACCURACY USING THE SECOND METHOD APPLIED TO THE TRANSIENT STATE OF THE EMG SIGNAL

Subj.	C	O	P	S	F	E	Mean
1	92.50	100.00	92.50	97.50	95.00	92.50	95.00
2	100.00	95.00	85.00	95.00	100.00	95.00	95.00
3	92.50	85.00	95.00	87.50	87.50	97.50	90.83
4	85.00	95.00	87.50	80.00	92.50	92.50	88.75
5	80.00	95.00	77.50	87.50	100.00	100.00	90.00
6	92.50	100.00	82.50	100.00	97.50	97.50	95.00
7	90.00	100.00	87.50	82.50	100.00	100.00	93.33
8	92.50	97.50	90.00	82.50	90.00	100.00	92.08
9	72.50	92.50	85.00	85.00	100.00	95.00	88.33
10	97.50	100.00	95.00	100.00	92.50	100.00	97.50
Mean	89.50	96.00	87.75	89.75	95.50	97.00	92.58
SD	8.23	4.74	5.58	7.68	4.68	3.07	3.07

TABLE VIII
COMPARISON BETWEEN CLASSIFICATION OF THE EMG TRANSIENT STATE USING THE FIRST AND SECOND METHODS

Movement	First Method	Second Method
Hand Closing	90.71%	89.50%
Hand Opening	91.86%	96.00%
Wrist Pronation	85.29%	87.75%
Wrist Supination	82.57%	89.75%
Wrist Flexion	96.57%	95.50%
Wrist Extension	89.57%	97.00%
Mean	89.43%	92.58%
SD	2.05%	3.07%

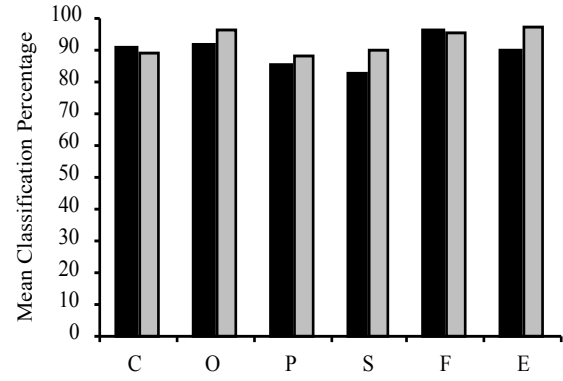


Fig. 5. Comparison between classification accuracy of the EMG transient state for the first method (black) and the second method (gray).

Fig. 5 shows graphically the classification performance obtained from methods 1 and 2 while using the transient state of the signals. The black bars represent the mean classification rate for each of the movements when applying the first method, while the gray bars are the equivalent for the second method.

IV. DISCUSSION

All the proposed methods depart from the use of representative wavelet coefficients from each of the EMG signals as the main tool for feature extraction. The WT analysis was both tested using a fourth order Daubechies mother wavelet and a fourth order Coiflet mother wavelet. Classification performance was better when the Coiflet wavelet was applied; Englehart, et al. [13] also report that a fourth order Coiflet mother wavelet yielded better accuracy than a host of other wavelet families of varying order.

The classification was made based on the features extracted for each 256 ms window. Thus, classification percentage is based on the windows that were properly identified by the classifier.

Classification accuracy using the steady state segment of the EMG signal (table V) outperformed the percentages obtained when using the transient state (table IV). The comparison between mean classification performance for steady and transient states of each of the movements appears in table VI and Fig. 4. These results are consistent with those obtained by Englehart, et al. in [12,13], where they report that the steady state data was classified more accurately than the transient data.

Almost for every method that was tested, the lowest classification rates were those of pronation and supination. This could be related to the electrode placement chosen for this study that might not be significant enough as to

accurately discriminate between these two types of movements.

In general, the second method had a better performance for classification of the transient EMG state. The results obtained for each of the movements are shown in table VII. Both table VIII and Fig. 5 make evident the general performance improvement when using the second method that includes all the coefficients obtained from the wavelet decomposition. This could suggest that even if the main concentration of energy is located within the frequency band of 50-150 Hz, there are frequency components outside this band that contribute to classification of the transient EMG segment.

V. CONCLUSION

The present study allowed obtaining appropriate classification percentages for identification of six different hand movements by processing the transient state of the multichannel sEMG signals recorded from 10 subjects.

These results reaffirm the existence of deterministic components within the onset part of the muscle contraction as initially proposed by Hudgins *et al.* in [3], and the fact that the information is relevant enough to discriminate between movements. However, the use of the steady state of the EMG signal still has a better classification performance, which could be associated to a greater amount of significant information present on this part of the contraction as concluded by Englehart *et al.* [12], or to the fact that a more appropriate processing tool has yet not been applied.

Some future work that can be done in order to improve this study is to implement a tool for automatic detection of the transient state of multichannel EMG considering that channels are activated according to the recorded muscle's participation in the movement. Other processing tools could be explored as well for further analysis of the transient EMG state and attempting to optimize classification accuracy.

ACKNOWLEDGMENT

The authors would like to acknowledge the master scholarship granted to Michele Pla by CONACYT.

REFERENCES

- [1] M. B. I. Reaz, M. S. Hussain, and F. Mohd-Yasin, "Techniques of EMG signal analysis: detection, processing, classification and applications," *Biol. Proced. Online*, vol. 8, no. 1, pp. 11-35, March 2006.
- [2] J. Rafiee, M. A. Rafiee, F. Yavari, and M. P. Schoen, "Feature extraction of forearm EMG signals for prosthetics," *Expert Systems with Applications*, vol. 38, pp. 4058-4067, 2011.

- [3] B. Hudgins, P. Parker, and R. N. Scott, "A new strategy for multifunction myoelectric control," *IEEE Trans. Biomed. Eng.*, vol. 40, no. 1, pp. 82-94, Jan. 1993.
- [4] R. Reiter, "A new electronic hand (Eine Neue Elektrokunsthand)," *Grenzgebiete der Medizin*, vol. 1, no. 4, pp. 133-135, 1948.
- [5] M. Zecca, S. Micera, M. C. Carrozza, and P. Dario, "Control of multifunctional prosthetic hands by processing the electromyographic signal," *Critical Reviews in Biomedical Engineering*, vol. 30, no. 4-6, pp. 459-485, 2002.
- [6] D. Staudenmann, I. Kingma, D. F. Stegeman, and J. H. van Dieën, "Towards optimal multi-channel EMG electrode configurations in muscle force estimation: a high density EMG study," *Journal of Electromyography and Kinesiology*, vol. 5, pp. 1-11, 2005.
- [7] H. A. Romo, J. C. Realpe, and P. E. Jojoa, "Surface EMG signal analysis and its applications in hand prosthesis control (Análisis de señales EMG superficiales y su aplicación en el control de prótesis de mano)," *Revista Avances en Sistemas e Informática*, vol. 4, no. 1, pp. 127-136, Jun. 2007.
- [8] T. Basha, R. N. Scott, P. A. Parker, and B. S. Hudgins, "Deterministic components in the myoelectric signal," *Tech. Note, Med. & Biol. Eng. & Comput.*, vol. 32, pp. 233-235, 1994.
- [9] Y. Yamazaki, M. Suzuki, and T. Mano, "An electromyographic volley at the initiation of rapid isometric contractions of the elbow," *Brain Res. Bullet.*, vol. 30, pp. 181-187, 1993.
- [10] M. León Ponce, "Classification of myoelectric patterns for the operation of an antropomorphic device (Clasificación de patrones mioeléctricos para la operación de un dispositivo antropomórfico)," Ph.D. dissertation, Bioelectronics Program, Electrical Engineering Department, CINVESTAV, Mexico City, Mexico, Dec. 2012.
- [11] K. Englehart, B. Hudgins, P. A. Parker, and M. Stevenson, "Time-frequency representation for classification of the transient myoelectric signal," in *Proc. of the 20th Annual International Conference of the IEEE Engineering in Medicine and Biology Society*, IEEE Press, vol. 20, no. 5, pp. 2627-2630, 1998.
- [12] K. Englehart, B. Hudgins, and P. A. Parker, "Time-frequency based classification of the myoelectric signal: static vs. dynamic contractions," in *Proc. of the 22nd Annual EBMS International Conference*, IEEE Press, pp. 317-320, July 2000.
- [13] K. Englehart, B. Hudgins, and P. A. Parker, "A wavelet based continuous classification scheme for multifunction myoelectric control," Department of Electrical and Computer Engineering and the Institute of Biomedical Engineering, University of New Brunswick, Canada, vol. 48, pp. 302-311, 2001.

Transient State Analysis of the Multichannel EMG Signal Using Hjorth's Parameters for Identification of Hand Movements

Michele Pla Mobarak, Juan Manuel Gutiérrez Salgado,
Roberto Muñoz Guerrero
Department of Electrical Engineering, Bioelectronics
CINVESTAV
Mexico City, Mexico
e-mail: {mpla, mgutierrez, rmunoz}@cinvestav.mx

Valérie Louis-Dorr
Centre de Recherche en Automatique de Nancy (CRAN)
CNRS : UMR7039 – University of Lorraine
Nancy, France
e-mail: valerie.louis@univ-lorraine.fr

Abstract—Most myoelectric controlled systems are based on the common assumption that there is no information in the instantaneous value of the myoelectric signal and therefore, analysis is made on the steady state of the muscle contraction. However, two main drawbacks of this control scheme are that the user needs to be trained in order to produce the sustained contractions, and that the control signal can only be generated when the steady state is reached. Using the transient state would allow classifying the movement during the dynamic part of the contraction decreasing the delay and allowing a more natural control. This paper proposes a novel method for transient EMG classification based on the use of Hjorth's parameters. Surface multichannel EMG signals were recorded from 10 normally limbed subjects for both the transient and steady EMG states. Six different hand motions were accurately classified using a window length of 128 ms and an artificial neural network model. An average classification accuracy of 97.45% (SD 1.10%) was obtained for the transient EMG state and of 97.93% (SD 1.11%) for the steady state, suggesting the existence of deterministic information in the transient state of the muscle contraction and the fact that Hjorth's parameters seem to adapt well enough to the nature of myoelectric signals as to extract highly representative information from them.

Keywords—EMG steady state; EMG transient state; Hjorth's parameters; multichannel EMG; normalized slope descriptors

I. INTRODUCTION

Research on the use of electromyography (EMG) for upper limb prostheses control has been conducted since the 1940's [1] and has had an outstanding improvement throughout the years; however, still numerous challenges remain in signal processing in order to achieve a more reliable and natural control. To be able to make the most out of the potential of technological innovations in prostheses, development on this area should be closely related to the understanding of the psychological complexities that the amputee faces [2]. The performance of a myoelectric control system is evaluated with regards to three important aspects of controllability [3]: the accuracy of movement selection, the intuitiveness of the actuating control, and the response time of the control system. A 200 to 300 ms interval is a clinically recognized maximum delay that users find acceptable before they get frustrated with the response time of the prosthesis [3-5]. Hence, the motivation to analyze the

transient state of the EMG signal arises in order to identify movements while the muscle contraction is being generated and not until it reaches a steady state.

The EMG signal is a non-stationary, non-linear, and stochastic process produced as a result of the summation of several motor unit action potential trains (MUAPTs) [1,6-8]. However, two main states can be recognized during the muscle contraction. The transient state is described as the bursts of myoelectric activity that accompany sudden muscular effort while executing the movement. The steady state will be considered as the muscular effort during a sustained contraction when the movement's final position is reached, and the muscle length is no longer modified; i.e., the myoelectric signal produced by a stable muscle contraction [9,10].

EMG classification has been most often based on the steady state analysis of the muscle contraction. This has greatly simplified commercial myoelectric controlled systems that usually rely on the premise of the accepted myoelectric signal generation models. However, the steady state contains a short temporal structure of the active modification of recruitment and firing patterns involved in the contraction and that can be found within the transient state [1,4,5,9]. In 1993, Hudgins *et al.* [4] were the first to consider the structure in the myoelectric signal (MES) during the onset of the contraction to develop a new control strategy based on the analysis of the transient EMG state. They were able to discriminate between four movements with roughly 90% accuracy. Only a few studies, such as [11-14], have reported the use of the transient state to classify EMG signals. Englehart *et al.* [5] introduced the use of wavelet transform (WT) and wavelet packet transform (WPT) for classification of transient EMG signals. They classified more accurately the steady state than the transient data. However, in 2007, Hangrove *et al.* [15] showed that including transient data along with steady state data for classifier training increases the classification error, but it also increases real-time performance and system usability, which should be considered when evaluating the system.

The use of multichannel EMG helps reducing unwanted variability and provides a better representation of the real muscle activity in the collected signal [16-18]. The increase in classification performance while increasing the number of channels was investigated in [19]. Moreover, with

multichannel EMG, the positions of the electrodes become less critical [20], making it a promising technique. However, when extrapolating the system to high-level amputees, an excessive number of electrode sites could be hard or even not possible to locate.

Interference and muscle crosstalk introduce non-linearity into the EMG signal. The combination of muscle tissue, adipose tissue, skin, and the skin-electrode interface behaves like a non-linear low pass filter that attenuates and distorts the surface EMG signal; nevertheless, methods for non-linear time series analysis have not been widely applied to EMG [6].

The aim of this work is to propose a novel method for transient state analysis of the multichannel EMG signal by using normalized slope descriptors as features for classification. This paper will provide a general overview on Hjorth's parameters and their use in biomedical applications. Subsequently, it will explain the method that was followed and the results obtained from the analysis of both the transient and steady EMG signals recorded from 10 normally limbed subjects in order to identify a set of hand and wrist movements. Results will be compared to previously reported methods.

II. HJORTH'S PARAMETERS

Hjorth introduced, in 1970, three parameters based on time domain properties [21-24]. They were intended as a clinically useful tool capable of describing quantitatively the graphical characteristics of an electroencephalography (EEG) trace in terms of amplitude, slope, and slope spread, so that they receive the name of normalized slope descriptors (NSDs). These parameters are named "activity", "mobility", and "complexity".

Activity measures the variance of the amplitude of the signal as shown in (1). In the frequency domain, it can be conceived as the surface of the power spectrum.

Mobility measures the ratio between the standard deviation of the slope and the standard deviation of the amplitude given per time unit; hence, it represents dominant frequency. This ratio depends on the curve shape in such a way that it measures the relative average slope. Its mathematical definition is presented in (2).

Complexity is a dimensionless parameter that quantifies any deviation from the sine shape as an increase from unit. It is calculated as shown in (3). It can be interpreted as a measure of the signal's bandwidth.

$$\text{Activity} = m_0 = \sigma_a^2, \quad (1)$$

$$\text{Mobility} = \sqrt{m_2/m_0} = \sigma_d/\sigma_a, \quad (2)$$

$$\text{Complexity} = \sqrt{(m_4/m_2) - (m_2/m_0)} = \frac{\sigma_{dd}/\sigma_d}{\sigma_d/\sigma_a}, \quad (3)$$

where m_n is the spectral moment at order n calculated using (4), σ_a^2 is the variance from the analyzed segment of the non-linear time series $f(t)$, and σ_d and σ_{dd} are the

standard deviations of the first and second derivatives of $f(t)$, respectively.

$$m_n = \int_{-\infty}^{+\infty} \omega^n \cdot S(\omega) d\omega \quad (4)$$

$S(\omega)$ corresponds to the power density spectrum. As the frequency description from the Fourier transform is always symmetrical with respect to zero frequency, in a statistical approach to the shape of the frequency distribution, all odd moments will become zero, and the information will be contained in the even moments.

Hjorth's parameters serve as a bridge between a physical time domain interpretation and the conventional frequency domain description [22]. The transformation between both domains is based on the energy equality within the actual epoch and can be calculated by the time-frequency relationship shown in (5)-(7).

$$m_0 = \int_{-\infty}^{+\infty} S(\omega) d\omega = \frac{1}{T} \int_{t-T}^t f^2(t) dt \quad (5)$$

$$m_2 = \int_{-\infty}^{+\infty} \omega^2 S(\omega) d\omega = \frac{1}{T} \int_{t-T}^t \left(\frac{df(t)}{dt} \right)^2 dt \quad (6)$$

$$m_4 = \int_{-\infty}^{+\infty} \omega^4 S(\omega) d\omega = \frac{1}{T} \int_{t-T}^t \left(\frac{d^2f(t)}{dt^2} \right)^2 dt \quad (7)$$

Hjorth's parameters were originally formulated for EEG analysis and description and have been widely used in sleep EEG processing for data reduction and discrimination of sleep stages [25-27]. Other studies related with EEG signal analysis have reported the use of Hjorth's descriptors for applications such as psychotropic drug research [25,26], assessment of postalcoholic diseases [28], temporal lobe seizures lateralization [24], classification of facial movement artifacts in the EEG signal [29], monitoring changes in EEG signals of patients with renal failure before and after hemodialysis [30], creating ink topographic displays for visual monitoring of changes in EEG signals [31], evaluation of performance in channel reduction for EEG classification in emotion assessment [32], among others. Mouz -Amady and Horwat (1996) [33] applied NSDs to EMG signals and concluded that they could be used to describe the spectral content of surface EMG during repetitive movements due to their results of high correlation coefficients (ranging from 0.81 to 0.93) between Hjorth's mobility and the FFT mean frequency. Hjorth's parameters have also been applied successfully in non-biomedical fields [21].

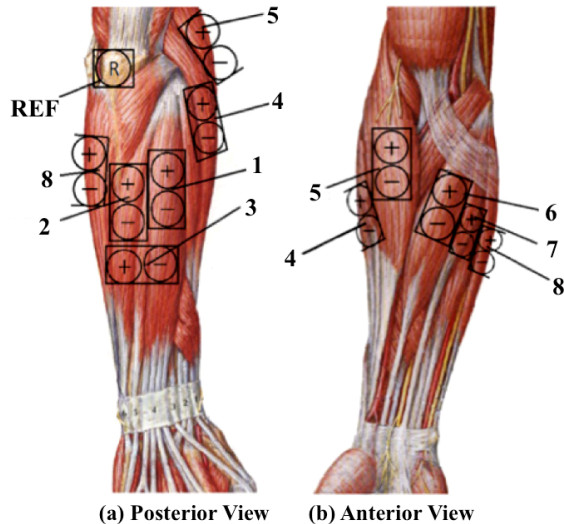


Figure 1. Posterior (a) and anterior (b) views of electrode placement for EMG signal recording. Corresponding muscles are identified in Table I.

III. METHOD

A. Data Acquisition Protocol

The surface EMG signals used for this study were those recorded in [34] using 8 differential channels (Ag-AgCl surface electrodes model VERMED NeuroPlus A10043 with an inter-electrode distance of 1.5 cm) placed on the dominant forearm of 10 normally limbed subjects, aged between 23 and 50, and with no register of neuromuscular disorders. The electrode disposition is shown in Fig. 1. To ensure the positioning of the electrodes over the muscles of interest, each participant was asked to repeatedly close and open the hand in order to identify the muscles mentioned in table I. The skin was carefully cleaned before electrode placement, and the reference electrode was located on the elbow.

Each subject was asked to execute six different hand motions, namely hand opening/closing, wrist pronation/supination, and wrist flexion/extension. The series of movements were repeated five times with a one-minute rest between them in order to avoid muscle fatigue. Each recording is 20 seconds in length. It starts with the forearm in an inactive position, followed by the dynamic part of the contraction, and finished by sustaining the contraction, once the final position is reached, until the end of the recording.

Written consent was obtained from every subject before starting the study. In a previous session, the protocol was explained to each of the participants and the amplification gain of the eight differential EMG channels was calibrated according to the amplitude of the contraction for each subject.

In order to reduce unwanted variability, every participant was asked to perform the study in a standing position with the dominant arm extended to the front and the hand relaxed.

The acquisition system consisted of 8 differential channels with adjustable amplification gain and a first order analog band-pass filter with a low cut-off frequency of 20 Hz

TABLE I. FOREARM MUSCLES RECORDED BY EACH EMG DIFFERENTIAL CHANNEL

EMG Channel	Forearm Muscle
1	Extensor digitorum communis
2	Extensor capri ulnaris
3	Differential measure between extensor digitorum communis and extensor carpi ulnaris
4	Extensor carpi radialis longus
5	Brachioradial
6	Flexor carpi radialis
7	Palmaris longus
8	Flexor carpi ulnaris

and a high cut-off frequency of 400 Hz. Each analog output was connected to a National Instruments acquisition card (model DAQ-Card 6024WE) for 12-bit A/D conversion. EMG signals were recorded with a sampling rate of 1024 Hz.

B. Data Processing

The multichannel EMG signals were processed and analyzed using MATLAB® (version R2012b). Each recording was divided in transient and steady states as illustrated in Fig. 2. A hamming window was applied to segment the signal for feature extraction. Classification performance was tested with two window lengths, 256 and 128 ms, both with 50% sample overlap.

A wavelet shrinkage method at third level of decomposition and based on Stein's unbiased risk estimate (SURE) was applied to each windowed segment for denoising purposes and to narrow the signal's frequency band. The decomposition level was chosen considering that the main concentration of energy in the surface EMG signal is located within the band of 50-150 Hz. The de-noised signals were rescaled using a noise level dependent estimation.

Once the window length was selected, Hjorth's parameters were calculated for each segment using (1)-(3). Different combinations of these parameters were arranged to build various feature matrices and evaluate which one yielded the best performance. The first matrix consisted of the three Hjorth's parameters, and the other three were formed from the possible combinations of two different parameters.

C. Artificial Neural Network's Parameters

For classification of the EMG signals, an artificial neural network (ANN) model was trained using the aforementioned feature matrices. A Bayesian regularization backpropagation algorithm was used to train the model.

The final ANN's architecture depended on the available feature matrix dimension; however, the model consisted of only one hidden layer with 9 neurons in it. This number of neurons was defined based on experimental testing. For classification purposes, the network output was binary codified.

In order to evaluate the network's performance, a k-fold cross-validation process ($k=5$) was carried out.

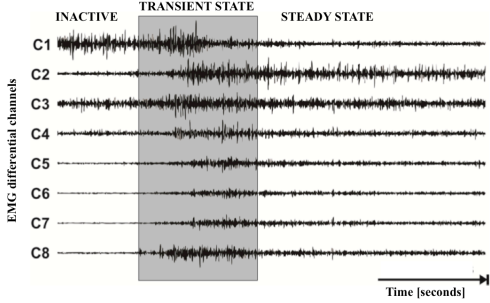


Figure 2. Division in transient and steady states of an eight multichannel EMG signal.

IV. RESULTS

A. Window Length Selection

Two hamming windows of different size were tested over the whole transient data set. The first one had a length of 256 ms and the second one of 128 ms. Both windows were applied with a 50% sample overlap. Table II and Fig. 3 show the classification percentage obtained for each window length.

TABLE II. MEAN CLASSIFICATION PERCENTAGE AND STANDARD DEVIATION ACCORDING TO WINDOW LENGTH

Movement Type	Window Length [ms]	
	256 ms	128 ms
<i>Closing</i>	97.71±2.95%	98.71±1.25%
<i>Opening</i>	97.43±2.11%	96.86±1.48%
<i>Pronation</i>	96.86±2.50%	94.86±3.03%
<i>Supination</i>	97.71±3.51%	96.43±3.03%
<i>Flexion</i>	100.00±0.00%	99.71±0.60%
<i>Extension</i>	99.14±1.38%	98.14±1.66%
<i>Mean</i>	98.14±0.99%	97.45±1.10%

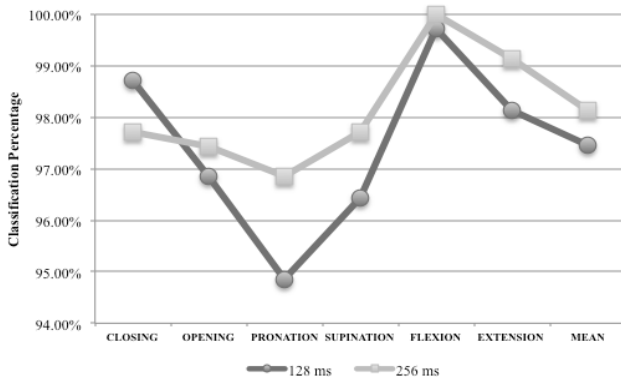


Figure 3. Comparison in classification percentage of the transient EMG state for each movement type using different window lengths.

B. Hjorth's Parameters Selection

Classification performance was evaluated with different combinations of Hjorth's parameters over the transient segment of the signals as it is shown in Table III. The column labeled 'A+M+C' contains the classification percentages obtained for each movement type using the three Hjorth's parameters. The following columns denote the classification percentages from combining two of the parameters.

The mean classification error percentage obtained from using each feature matrix was calculated and is presented in Fig. 4. These percentages include the mean classification for the whole test population including every movement type.

TABLE III. MEAN CLASSIFICATION PERCENTAGE ACCORDING TO THE COMBINATION OF HJORTH'S PARAMETERS USED IN THE FEATURE MATRIX

Movement Type	Hjorth's Parameters			
	A+M+C	A+M	A+C	M+C
<i>Closing</i>	98.14%	96.57%	97.14%	98.71%
<i>Opening</i>	96.86%	95.43%	96.14%	96.86%
<i>Pronation</i>	94.00%	94.43%	93.00%	94.86%
<i>Supination</i>	95.57%	94.29%	93.29%	96.43%
<i>Flexion</i>	99.86%	99.57%	97.87%	99.71%
<i>Extension</i>	97.86%	98.29%	96.71%	98.14%
<i>Mean</i>	97.05%	96.43%	95.69%	97.45%
<i>SD</i>	2.95%	3.57%	4.31%	2.55%

A stands for 'Activity', M for 'Mobility', and C for 'Complexity'

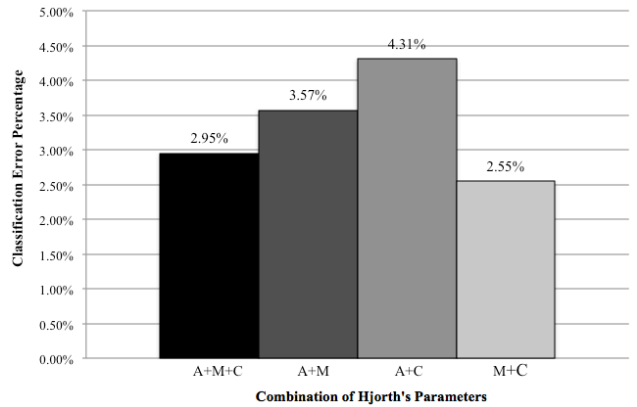


Figure 4. Mean classification error percentage obtained by using different combinations of Hjorth's parameters as features for classification.

C. Comparison in Classification Accuracy of the Transient and Steady EMG States

Previous studies such as [5], have reported higher classification accuracy when using the steady state of the EMG signal. Therefore, the proposed method was evaluated for both EMG states. The mean classification percentages obtained for each of the subjects are presented in Table IV. The comparison in mean classification accuracy per movement type is illustrated in Fig. 5.

TABLE IV. TABLE TYPE STYLES

Subject	EMG State	
	Transient	Steady
1	97.38%	97.62%
2	99.05%	99.29%
3	97.62%	97.14%
4	95.71%	96.67%
5	97.86%	99.76%
6	96.67%	97.14%
7	98.33%	99.05%
8	96.19%	96.67%
9	96.90%	98.10%
10	98.81%	97.86%
<i>Mean ± SD</i>	97.45±1.10%	97.93±1.11%

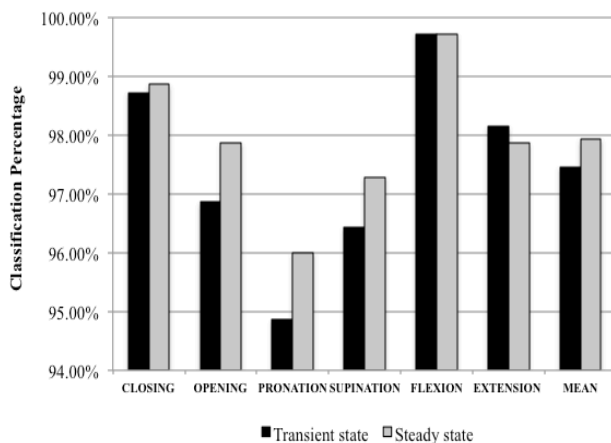


Figure 5. Mean classification percentage per movement type for the transient and steady EMG states.

V. DISCUSSION

The proposed method departs from the use of features originally intended for EEG description. The EEG signal is formed by the superposition of characteristic responses; in a similar way, the EMG signal is the superposition of MUAPs, which seems to make Hjorth's parameters also suitable for their analysis due to the nature of myoelectric sources.

The parameters' values, except for activity, referring to a single response, are also valid for a superposition of responses [22], which can justify that classification error increases when including this parameter, as shown in Fig. 4.

The mean classification percentage obtained from the steady EMG signals was just slightly higher than the one reported for the transient state (refer to Fig. 5). This suggests that similar classification accuracy can be obtained from both EMG states using Hjorth's parameters as compared to previous reported methods.

Classification accuracy did not suffer a significant decrease when using a window length of 128 ms as compared to one of 256 ms, which could allow obtaining a faster response for control purposes and would make it more suitable for on-line applications.

VI. CONCLUSIONS

It has been widely discussed whether or not the transient state of the muscle contraction contains enough relevant information as to accurately discriminate between different types of motions; however, Hjorth's parameters seem to adapt well enough to the transient MES as to extract highly representative information from it. Using the transient EMG state for myoelectric control would allow generating a control signal since the beginning of the muscle contraction, which would also reflect in a more natural control of the device.

Although Hjorth's parameters are based on spectral moments, they are also calculated by time variances where the computational cost is more affordable than other methods based on frequency-domain analysis that normally imply complex transformations. However, due to their mathematical significance, Hjorth's parameters allow characterizing the signal in both the time and frequency domains.

ACKNOWLEDGMENT

The authors would like to acknowledge the master scholarship granted to Michele Pla by CONACYT.

REFERENCES

- [1] M. Zecca, S. Micera, M. C. Carrozza, and P. Dario, "Control of multifunctional prosthetic hands by processing the electromyographic signal," *Critical Reviews in Biomedical Engineering*, vol. 30, no. 4-6, 2002, pp. 459-485, doi:10.1615/CritRevBiomedEng.v30.i456.80.
- [2] D. Desmond and M. MacLachlan, "Psychological issues in prosthetic and orthotic practice: a 25 year review of psychology in Prosthetics and Orthotics International," *Prosthetics and Orthotics International*, vol. 26, no. 3, Dec. 2002, pp. 182-188, doi:10.1080/03093640208726646.
- [3] K. Englehart and B. Hudgins, "A robust, real-time control scheme for multifunction myoelectric control," *IEEE Trans. Biomed. Eng.*, vol. 50, no. 7, July 2003, pp. 848-854, doi:10.1109/TBME.2003.813539.
- [4] B. Hudgins, P. Parker, and R. N. Scott, "A new strategy for multifunction myoelectric control," *IEEE Trans. Biomed. Eng.*, vol. 40, no. 1, Jan. 1993, pp. 82-94, doi:10.1109/10.204774.
- [5] K. Englehart, B. Hudgins, and P. A. Parker, "A wavelet based continuous classification scheme for multifunction myoelectric control," *IEEE Trans. Biomed. Eng.*, vol. 48, 2001, pp. 302-311.
- [6] P. Padmanabhan and S. Puthusserypady, "Nonlinear analysis of EMG signals – a chaotic approach," *Proc. IEEE Eng. Med. Biol. Soc. (IEMBS '04)*, IEEE Press, vol. 1, Sept. 2004, pp. 608-611, doi:10.1109/IEMBS.2004.1403231.
- [7] J. Rafiee, M. A. Rafiee, F. Yavari, and M. P. Schoen, "Feature extraction of forearm EMG signals for prosthetics," *Expert Systems with Applications*, vol. 38, 2011, pp. 4058-4067, doi:10.1016/j.eswa.2010.09.068.

- [8] A. Merlo, D. Farina, and R. Merletti, "A fast and reliable technique for muscle activity detection from surface EMG signals," *IEEE Trans. Biomed. Eng.*, vol. 50, no. 3, March 2003, pp. 316-323, doi:10.1109/TBME.2003.808829.
- [9] H. A. Romo, J. C. Realpe, and P. E. Jojoa, "Surface EMG signal analysis and its applications in hand prosthesis control (Análisis de señales EMG superficiales y su aplicación en el control de prótesis de mano)," *Revista Avances en Sistemas e Informática*, vol. 4, no. 1, Jun. 2007, pp. 127-136.
- [10] T. W. Calvert and A. E. Chapman, "The relationship between the surface EMG and force transients in muscle: simulation and experimental studies," *Proceedings of the IEEE*, vol. 65, no.5, May 1977, pp.682-689, doi:10.1109/PROC.1977.10547.
- [11] U. Kuruganti, B. Hudgins, and R. N. Scott, "Two-channel enhancement of a multifunction control system," *IEEE Trans. Biomed. Eng.*, vol. 42, no. 1, Jan. 1995, pp. 109-111, doi:10.1109/10.362912.
- [12] K. Englehart, B. Hudgins, M. Stevenson, and P. A. Parker, "Classification of myoelectric signal burst patterns using a dynamic neural network," *Proc. IEEE 21st Annual Northeast Bioengineering Conference (NEBC)*, May 1995, pp. 63-64, doi:10.1109/NEBC.1995.513734.
- [13] K. Englehart, B. Hudgins, M. Stevenson, and P. A. Parker, "A dynamic feedforward neural network for subset classification of myoelectric signal patterns," *Proc. IEEE 17th Annual Conference, Engineering in Medicine and Biology Society (IEMBS)*, vol. 1, Sept. 1995, pp. 819-820, doi:10.1109/IEMBS.1995.575359.
- [14] S. Karlsson, J. Yu, and M. Akay, "Time-frequency analysis of myoelectric signals during dynamic contractions: a comparative study," *IEEE Trans. Biomed. Eng.*, vol. 47, no. 2, pp. 228-238, Feb. 2000.
- [15] L. Hangrove, Y. Losier, B. Lock, K. Englehart, and B. Hudgins, "A real-time pattern recognition based myoelectric usability study implemented in a virtual environment," *Proc. IEEE 29th Annual International Conference of the Engineering in Medicine and Biology Society (EMBS 2007)*, IEEE Press, Aug. 2007, pp. 4842-4845, doi:10.1109/IEMBS.2007.4353424.
- [16] D. Staudenmann, I. Kingma, D. F. Stegeman, and J. H. van Dieën, "Towards optimal multi-channel EMG electrode configurations in muscle force estimation: a high density EMG study," *Journal of Electromyography and Kinesiology*, vol. 5, 2005, pp. 1-11, doi:10.1016/j.jelekin.2006.08.006.
- [17] M. F. Lucas, A. Gaufriau, S. Pascual, C. Doncarli, and D. Farina, "Multi-channel surface EMG classification using support vector machines and signal-based wavelet optimization," *Biomedical Signal Processing and Control*, vol. 3, no. 2, Apr. 2008, pp. 169-174, doi:10.1016/j.bspc.2007.09.002.
- [18] E. A. Clancy and N. Hogan, "Multiple site electromyograph amplitude estimation," *IEEE Trans. Biomed. Eng.*, vol. 42, no. 2, Feb. 1995, pp. 203-211, doi:10.1109/10.341833.
- [19] K. Davidge, "Multifunction myoelectric control using a linear electrode array," M.Sc. dissertation, Electronics and Electrical Engineering, University of New Brunswick, Canada, 2005.
- [20] B. Karlik, M. O. Tokhi, and M. Alci, "A novel technique for classification of myoelectric signals for prosthesis," *CD-ROM Proc. of the 15th Triennial World Congress of the International Federation of Automatic Control (IFAC)*, vol. 2, 2002.
- [21] P. P. Balestrassi, A. P. Paiva, A. C. Zambroni de Souza, J. B. Turrioni, and E. Popova, "A multivariate descriptor method for change-point detection in nonlinear time series," *Journal of Applied Statistics*, vol. 38, no. 2, Feb. 2011, pp. 327-342, doi:10.1080/02664760903406496.
- [22] B. Hjorth, "EEG analysis based on time domain properties," *Electroencephalography and Clinical Neurophysiology*, vol. 29, no. 3, Sept. 1970, pp. 306-310, doi:10.1016/0013-4694(70)90143-4.
- [23] B. Hjorth, "The physical significance of time domain descriptors in EEG analysis," *Electroencephalography and Clinical Neurophysiology*, vol. 34, 1973, pp. 321-325, doi:10.1016/0013-4694(73)90260-5.
- [24] T. Cecchin, R. Ranta, L. Koessler, O. Caspary, H. Vespignani, and L. Maillard, "Seizure lateralization in scalp EEG using Hjorth parameters," *Clinical Neurophysiology*, vol.121, 2010, pp. 290-300, doi:10.1016/j.clinph.2009.10.033.
- [25] O. Kanno and P. Clarenbach, "Effect of clonidine and yohimbine on sleep in man: polygraphic study and EEG analysis by normalized slope descriptors," *Electroencephalography and Clinical Neurophysiology*, vol. 60, 1985, pp. 478-484, doi:10.1016/0013-4694(85)91107-1.
- [26] H. Depoortere, D. Francon, P. Granger, and M. G. Terzano, "Evaluation of the stability and quality of sleep using Hjorth's descriptors," *Physiology & Behavior*, vol. 45, 1993, pp. 785-793, doi:10.1016/0031-9384(93)90093-U
- [27] M. Ziller, K. Frick, W. M. Hermann, S. Kubicki, I. Spieweg, and G. Winterer, "Bivariate global frequency analysis versus chaos theory," *Neuropsychobiology*, vol. 32, no. 1, 1995, pp. 45-51, doi:10.1159/000119211.
- [28] W. Spehr and G. Stemmler, "Postalcoholic diseases: diagnostic relevance of computerized EEG," *Electroencephalography and Clinical Neurophysiology*, vol. 60, 1985, pp. 106-114, doi:10.1016/0013-4694(85)90016-1.
- [29] S. Pourzare, O. Aydemir, and T. Kayikcioglu, "Classification of various facial movement artifacts in EEG signals," *Proc. 35th International Conference on Telecommunications and Signal Processing (TSP)*, IEEE Press, July 2012, pp. 529-533, doi:10.1109/TSP.2012.6256351.
- [30] W. Spehr, H. Sartorius, K. Berglund, B. Hjorth, C. Kablitz, U. Plog, P. H. Wiedemann, and K. Zapf, "EEG and haemodialysis. A structural survey of EEG spectral analysis, Hjorth's EEG descriptors, blood variables and psychological data," *Electroencephalography and Clinical Neurophysiology*, vol. 43, 1977, pp. 787-797, doi:10.1016/0013-4694(77)90001-3.
- [31] A. Persson and B. Hjorth, "EEG topogram - An aid in describing EEG to the clinician," *Electroencephalography and Clinical Neurophysiology*, vol. 56, 1983, pp. 399-405, doi:10.1016/0013-4694(83)90221-3.
- [32] K. Ansari-Asl, G. Chanel, and T. Pun, "A channel selection method for EEG classification in emotion assessment based on synchronization likelihood," *Proc. 15th European Signal Processing Conference (EUSIPCO 2007)*, EURASIP, Sept. 2007, pp. 1241-1245.
- [33] M. Mouzé-Amady and F. Horwat, "Evaluation of Hjorth parameters in forearm surface EMG analysis during an occupational repetitive task," *Electroencephalography and Clinical Neurophysiology*, vol. 101, 1996, pp. 181-183, doi:10.1016/0924-980X(96)00316-5.
- [34] M. León Ponce, "Classification of myoelectric patterns for the operation of an antropomorphic device (Clasificación de patrones mioeléctricos para la operación de un dispositivo antropomórfico)," Ph.D. dissertation, Bioelectronics Program, Electrical Engineering Department, CINVESTAV, Mexico City, Mexico, Dec. 2012.